

954468

**N78-24278**

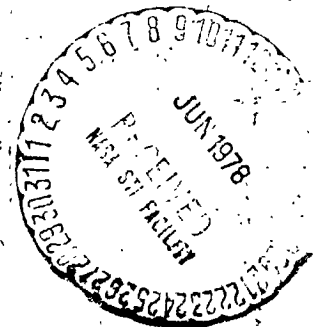
Unclas  
20686

G3/20

PHASE I  
FINAL REPORT  
Contract No. 954468

THE MARQUARDT COMPANY  
16555 SATICOY STREET  
VAN NUYS, CALIFORNIA 91409

CALIFORNIA INSTITUTE OF TECHNOLOGY  
JET PROPULSION LABORATORY  
4800 OAK GROVE DRIVE  
PASADENA, CALIFORNIA 91103



# EVALUATION OF THE SSRCS ENGINE WITH HYDRAZINE AS A FUEL

PHASE I  
FINAL REPORT  
Contract No. 954468

JANUARY 1978


THE MARQUARDT COMPANY  
16555 SATICOY STREET  
VAN NUYS, CALIFORNIA 91409

PREPARED BY:



S.J. Minton  
Marquardt Program Manager

APPROVED BY:



T. Linton  
Director, Rocket Systems

## ABSTRACT

The objective of this investigation is to predict the performance parameters for the Space Shuttle Reaction Control Thruster (SSRCT) when the fuel is changed from monomethylhydrazine to hydrazine. Potential problems are higher chamber wall temperature during steady state operation and explosive events during pulse mode operation. Solutions to the problems are suggested.

To conduct the analysis, a more realistic film cooling model was devised which considers that hydrazine based fuels are reactive when used as a film coolant on the walls of the combustion chamber. Hydrazine based fuels can decompose exothermally as a monopropellant and also enter into bipropellant reactions with any excess oxidizer in the combustion chamber. Prior studies treated the coolant as an inert fluid.

The study concludes that the conversion of the thruster from MMH to hydrazine fuel is feasible but that a number of changes would be required to achieve the same safety margins as the monomethylhydrazine-fueled thruster.

## TABLE OF CONTENTS

<u>Section</u>	<u>Title</u>	<u>Page</u>
I.	INTRODUCTION	1
	Technical Problem	1
	Some Experimental Data Related to the Feasibility Study	4
II.	DEFINITION OF SHUTTLE DESIGN CONSTRAINTS	6
	Pressure Schedules	6
	Feed System/Combustor Instability	7
	Chamber Temperatures	7
	Re-entry Heat Loads	10
	Thermal Conditioning of the Injector and Chamber	10
	Dimensional Considerations	14
	Other Space Shuttle Constraints	14
III.	ROCKET PERFORMANCE	16
	Rocket Performance Calculations	16
	Refinements in Performance Predictions	16
IV.	FILM COOLING ANALYSIS	20
	Cooling With Reactive Liquids	20
	Decomposition Model for Coolant	22
V.	RESULTS OF THE ANALYTICAL PROCEDURES	24
	Evaporation Model	24
	Thermal Decomposition Model	24
	Film Cooling Nonuniformity	28
	Sensitivity of Predicted Temperature to Analysis Assumptions	32
	Predicted Hydrazine Thruster Throat Temperature	32
VI.	PERFORMANCE TRADEOFFS	35
	Performance Tradeoffs	35
	Concept of Development Risk	35
	Effect of Chamber Length	36
	Effect of Injector Double Offset	36
	Interactions Between Film Cooling and Performance	39
	Nozzle Performance	42
	Optimizing the Injector	42
	MMH Thruster	44
	Hydrazine Thruster	46

TABLE OF CONTENTS  
(Continued)

<u>Section</u>	<u>Title</u>	<u>Page</u>
VII.	PULSE MODE OPERATION AND COMBUSTION STABILITY CONSIDERATIONS	50
	Vapor Phase Detonations	51
	Condensed Phase Explosions	53
	ZOTS	56
	Transducer Cavity Explosions	61
	Combustion Instability	62
	Feed System Stability	65
VIII.	WEIGHT AND COST	66
IX.	CONCLUSIONS	68
	REFERENCES	69
	APPENDIX A - Tankage Considerations for Constant Takeoff Weight	A-1
	APPENDIX B - Rocket Performance Calculations	B-1
	APPENDIX C - Film Cooling Analysis Technique	C-1

# LIST OF ILLUSTRATIONS

<u>Figure</u>	<u>Title</u>	<u>Page</u>
1	Aft Module Thruster Envelope	2
2	Core Temperature	3
3	TMC R-4D, 100-Pound Thrust Engine	5
4	Primary Thruster Operating Envelope	8
5	Oxidation-Protective Coating Life	9
6	Thruster No. 5 Wall Temperature Uninsulated Bolted Chamber	11
7	Thruster 5 Throat Temperature vs O/F Propellant Temperature	12
8	Predicted Thruster Re-entry Temperatures with Long Scarf	13
9	Aft Yaw Thruster 5 Heater Power	15
10	Three Zone Model	17
11	Predicted Specific Impulse	18
12	Photographs of Burning Droplets	21
13	Two-Flame Model for Reactive Liquid Film Cooling	23
14	Liquid Film Lengths Evaporation Model	25
15	Film Cooling Analysis	26
16	Film Cooling Analysis	27
17	Radiation Cooled Thruster Comparison of Experimental and Calculated Wall Temperatures	29
18	Film Cooling Analysis	30
19	Pattern View of Film-Cooled Section	31
20	Film Cooling Analysis	33
21	Film Cooling Analysis	
22	Effect of Chamber Length Upon Specific Impulse	37
23	Effect of Doublet Offset	38
24	Predicted Effect of Film Cooling for Different Amounts of Mixing with the Core Flow	40
25	Effect of Film Cooling and Its Mixing with the Core Flow	41
26	Optimized Hydrazine Injector	43

LIST OF ILLUSTRATIONS  
(continued)

<u>Figure</u>	<u>Title</u>	<u>Page</u>
27	SSRCS Thruster - Performance and Temperature Tradeoffs	45
28	Performance-Temperature Tradeoff for Chamber Length and Film Cooling	47
29	Hydrazine Thruster - Configuration B Performance and Temperature Tradeoffs	49
30	Ignition Overpressure Summary	52
31	Aft X and Fwd Z Cold Soak Temperature	55
32	ZOT Plot	57
33	ZOT Plot	59
34	Frequency and Magnitude of ZOTs	60
35	Stability Map - Transverse Modes	63
B-1	Three-Zone Model	B-1
B-2	Effect of Zone Mixture Ratio Upon Specific Impulse	B-4
B-3	Mixture Uniformity Parameters	B-5
B-6	Effect of Rupe Number Upon Specific Impulse	B-8
B-7	Effect of Contact Time Upon Specific Impulse	B-9
B-8	Effect of Momentum Angle Upon Isp	B-10
C-1	Splash Pattern Losses	C-2
C-2	Film Stability Effectiveness	C-4
C-3	Decomposition Temperature	C-10

## I. INTRODUCTION

The Space Shuttle Reaction Control Thruster presently uses monomethylhydrazine (MMH) as a fuel ( $N_2O_4$  oxidizer) to provide 870 pounds of vacuum thrust and a specific impulse of 281 seconds (Figure 1). Given the performance data for this thruster, with MMH as a fuel, can we analytically predict what happens when hydrazine is used instead of MMH?

### Technical Problem

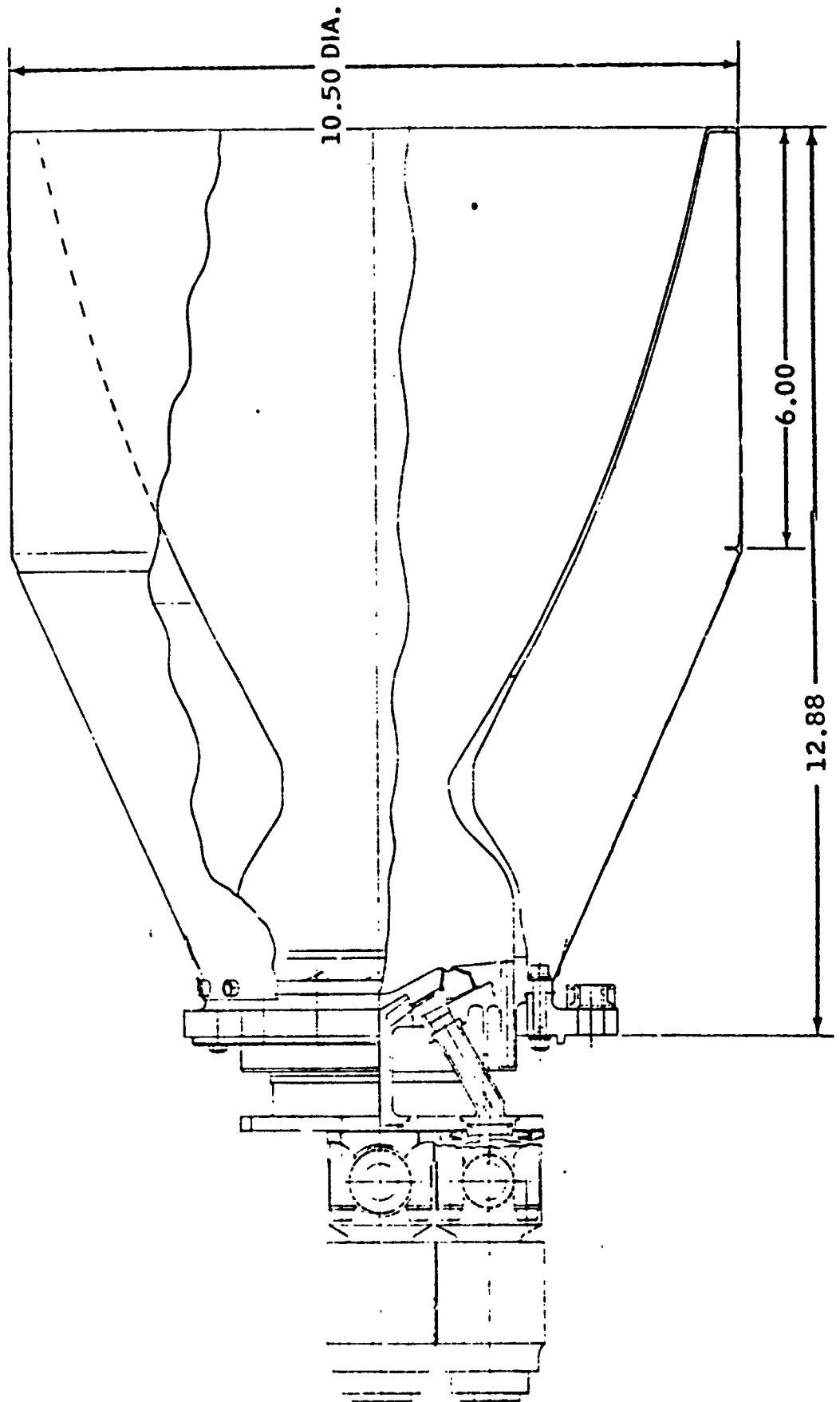
Already known, from experiments and analysis, is that hydrazine is of the same family of hypergolic fuels as MMH; therefore, no major differences in combustion performance can be foreseen when one fuel is interchanged with the other. To illustrate this point, ideal performance capabilities of the two fuels with  $N_2O_4$  as the oxidizer are shown in Figure 2. The specific impulse,  $I_{sp}$ , with  $N_2H_4$ , is seen to be lower than for the MMH fueled thruster at a mixture ratio, O/F, of 1.6, which is the present equal volumetric flow ratio for MMH. However, at an O/F = 1.4, the equal volumetric flow ratio for hydrazine, the specific impulse with hydrazine is the same as that with MMH at O/F = 1.6. Figure 2 also presents the theoretical gas temperatures for the two fuels and shows that the gas temperature of hydrazine at O/F = 1.4 is about 200°F higher compared with MMH at O/F = 1.6.

The major problem foreseen, when hydrazine is used as the fuel, is the effectiveness of hydrazine as a film coolant. The problem lies in the large release of thermal energy from hydrazine when it thermally decomposes. The exothermic decomposition of hydrazine occurs at about 550°F and gas temperatures of 2500°F can theoretically be produced if no ammonia decomposition occurs. However, at high temperature, the ammonia generated in the reaction rapidly begins to thermally decompose and absorb energy. As a result, the maximum gas temperature drops to the neighborhood of 2200°F at 25% ammonia decomposition for stay times characteristic of rocket chambers (Appendix C). Since the design goal for throat temperature of the SSRCT thruster is 2100°F, one can foresee some difficulties in obtaining this temperature if the coolant stream temperature may locally reach 2200°F just from its own thermal decomposition processes.

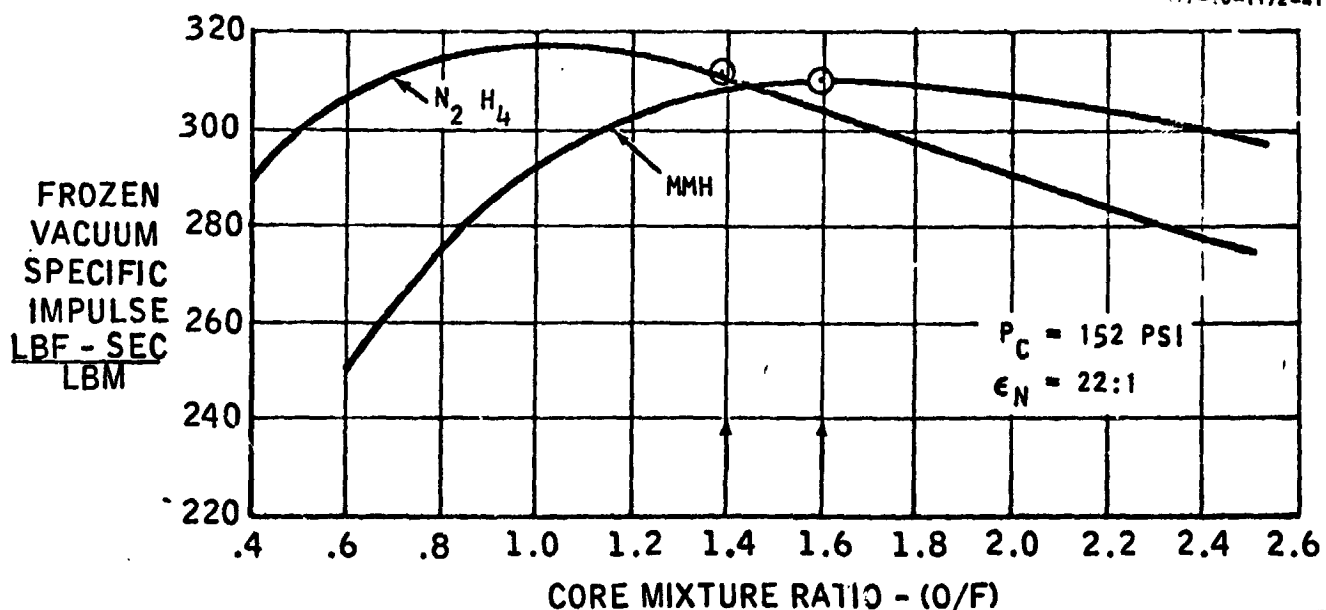
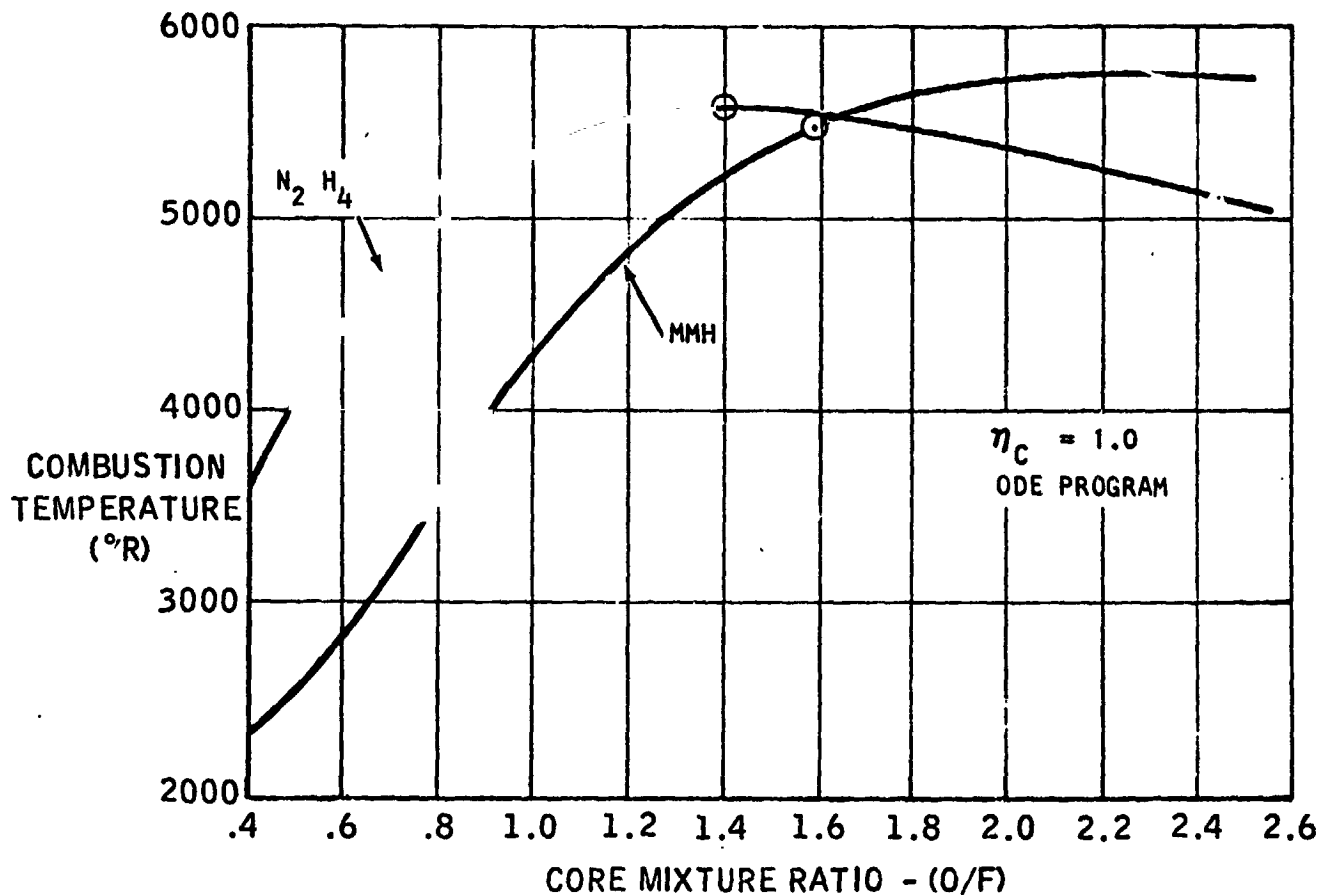
A second potential problem arising from the fuel change is the increased possibility of chamber and manifold explosions (spikes and ZOTs) during pulsing operations. Hydrazine, with its different vapor pressure and condensation temperatures, has a greater tendency to deposit residual propellant or detonable materials everywhere in the thruster after each pulse. These residues may detonate upon reignition and damage the valves, combustion chamber, and pressure transducer. The Space Shuttle Reaction Control Rocket is already designed to minimize the causes and the effects of the detonations by minimizing dribble (manifold) volumes, by thermal management which maintains adequate oxidizer cavity and chamber temperatures, and by designing all cavities and the chamber to withstand the worst pressure spike previously experienced. Due to these inherent design features, the occurrence of spikes or ZOTs are not expected to be a major problem, provided the same thermal management criteria are applied to the hydrazine fueled rocket.



**AFT MODULE THRUSTER ENVELOPE**  
(-0001 ± Z)



# CORE TEMPERATURE



ORIGINAL PAGE IS  
OF POOR QUALITY

One reason for considering the substitution of hydrazine is the potential future cost savings for second generation Space Shuttle vehicles. The lower cost of hydrazine, compared with MMH, is the economic incentive.

#### Some Experimental Data Related to the Feasibility Study

The theoretical performance computations presented in Figure 2 show no difference in specific impulse at the respective equal volumetric flow ratios. These numbers apply to a 100% efficient combustor with no film cooling. What happens when a real thruster, designed to maximize performance at one mixture ratio (with monomethylhydrazine), is made to operate at a different mixture ratio (with hydrazine), has been experimentally explored previously at Marquardt.

Experimental data have been obtained at Marquardt on two prior rocket engines when hydrazine was substituted for MMH without changing the injector or the combustion chamber. The Marquardt R-4D 100-pound force rocket engine was tested unmodified with  $N_2H_4$ . Figure 3a shows the  $I_{sp}$  comparisons for  $N_2H_4$  and MMH. As suggested by the analytical predictions, peak performance was higher for the hydrazine-fueled rocket, but the mixture ratio (O/F) at peak performance shifted from 1.55 for MMH to 1.1 for hydrazine. Significantly higher performance was measured for hydrazine at an O/F of 1.4 compared with MMH at an O/F of 1.6.

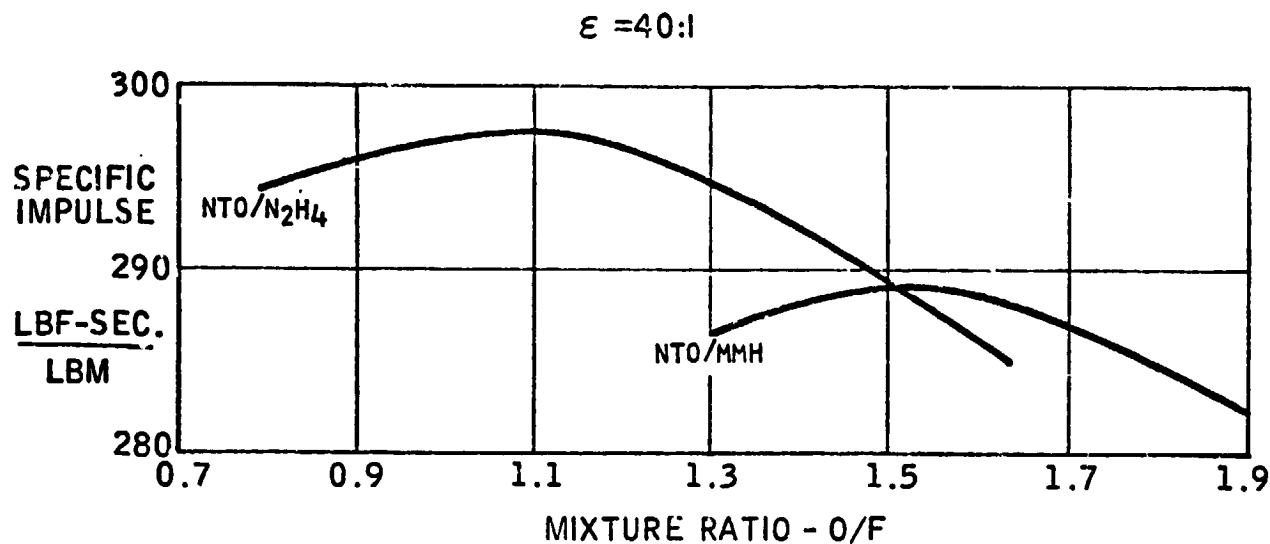
The chamber throat temperatures were also measured, and the steady state throat temperature of the hydrazine-fueled rocket was 2520°F at O/F = 1.1, compared with 1947°F at an O/F = 1.6 for the MMH-fueled rocket.

Similar test results were obtained for the Marquardt Model R-24B rocket, an experimental rocket designed for 300 pounds vacuum thrust. This engine was tested with three propellant combinations: MMH/ $N_2O_4$ ,  $N_2H_4$ / $N_2O_4$ , and 50% UDMH-50%  $N_2H_4$ / $N_2O_4$ . Figure 3b shows the performance of the rocket with the three fuels. For this rocket, the performance at the respective equal volumetric flow ratios is about the same. Peak performance of the hydrazine-fueled engine is higher than the MMH-fueled rocket.

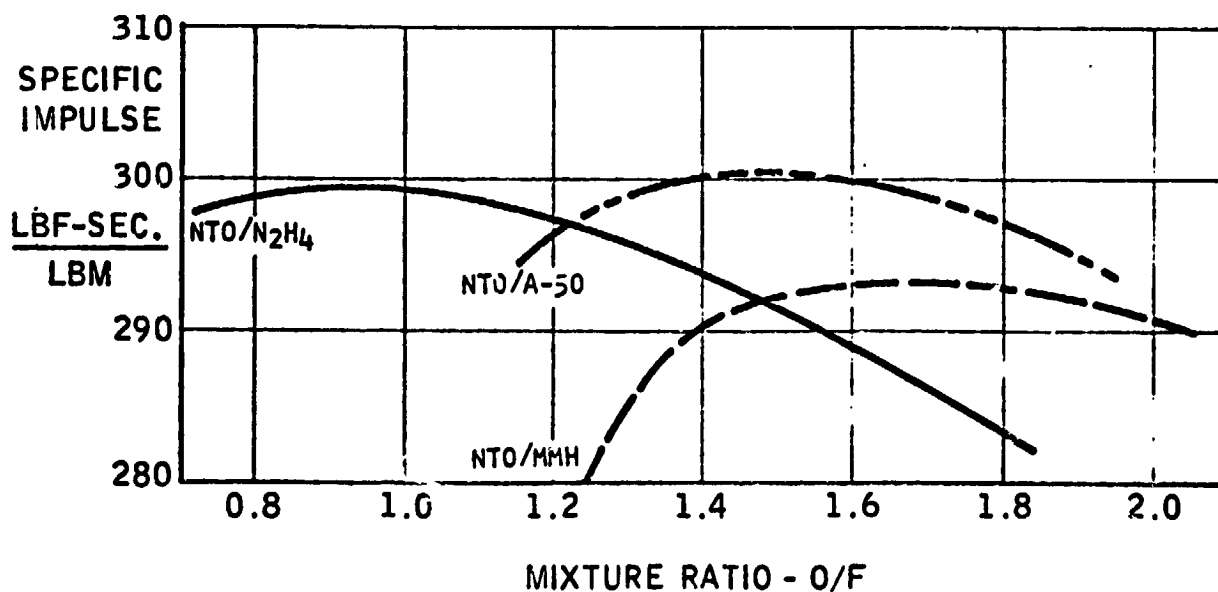
Temperature measurements once again indicated that the hydrazine-fueled rocket produced higher maximum throat temperatures (2240°F) than MMH (1900°F). The film coolant flow was in the neighborhood of 25-27% of the total fuel flow for both thrusters.

These experimental data on smaller thrusters provide evidence that the specific impulse requirements can be met at the equal volumetric mixture ratios but that chamber throat temperatures can be significantly higher. The objective of this program is to evaluate whether both quantities, specific impulse and throat temperatures, can be kept at design values when hydrazine is substituted for MMH. Since prior experimental data indicate that some change in engine design may be necessary to reduce throat temperatures, the study investigates two thruster configurations. Configuration A is the present shuttle thruster and the analysis attempts to define its behavior with hydrazine as a fuel. Configuration B is a "modified" shuttle thruster, where the modifications are chosen to better meet the throat temperature and specific impulse specifications for the thruster.

(a) TMC R-4D, 100 POUND THRUST ENGINE  
 Performance Test With  $N_2H_4$  & MMH Propellants



(b) TMC R-23, 300 POUND THRUST ENGINE  
 Calculated Specific Impulse (From  $C^*$ )  
 $C_f = 1.798$  (Assumed)  $\epsilon = 40:1$



## II. DEFINITION OF SHUTTLE DESIGN CONSTRAINTS

The Shuttle uses equal volume tankage for the MMH and the nitrogen tetroxide. To effectively utilize the propellants, the thrusters must operate at equal volumetric flow rates for the fuel and oxidizer. With a specific gravity of 0.876 for MMH and 1.446 for nitrogen tetroxide, the theoretical equal volumetric flow mixture ratio (O/F) is 1.65. However, the flight system requires a larger ullage volume in the oxidizer tank than in the fuel tank, and, therefore, the specification calls for an  $O/F = 1.6$ .

The theoretical equal volumetric flow mixture ratio for the hydrazine  $N_2/O_4$  thruster is 1.43, but when corrected for the tank ullage volume differences, the effective equal volumetric flow mixture ratio becomes 1.4 (1.39). Both 1.4 and 1.6 will henceforth be called the equal volumetric flow mixture ratios. Hydrazine is denser (S.G. = 1.008) than MMH. Therefore, when the present tankage is loaded with the same total weight of propellants, it can be shown that both tanks are loaded to only 95% of their previous capacity (volume) when hydrazine is used as the fuel.

As indicated by the previous experimental data and as predicted later in this report, the specific impulse of the hydrazine thruster improves at mixture ratios less than 1.4. Therefore, either increased range for the same takeoff weight or reduced takeoff weight for the same total impulse could be achieved if the thruster could be operated at a lower mixture ratio. Appendix A indicates that for the shuttle tankage the minimum operating mixture ratio could be  $O/F = 1.29$  if the fuel tank is loaded to its full capacity while the oxidizer is off-loaded to 91% capacity.

While this reduction of mixture ratio at constant propellant weight offers a potential means for further improvement of the hydrazine thruster performance, it is only mentioned as a point of interest. The study uses the equal volumetric flow ratio of 1.4 as the reference or operating condition.

### Pressure Schedules

The function of the injector is to distribute, mix and control the combustion of propellants in a manner which optimizes the performance of the thruster. As will be discussed later, the shuttle injector uniquely produces two combustion zones, each with a specific mixture ratio. It delivers the propellants at velocities and momentum angles which maximize the mixing and combustion of the propellants. To achieve this function, certain minimum pressure drops are required from the fuel and oxidizer distribution manifolds. For the shuttle application, the available pressure drop across the valves and injector is 53 psi. The nominal supply pressure for both propellants is 250 psi and the chamber pressure 152 psi.

A separate pressure regulator is used for each propellant delivery system to regulate the propellant supply pressure. Pressure regulator malfunction is possible. The specification requires that the thruster must operate with one regulator at a maximum pressure of 350

psia and the other at minimum pressure of 175 psia or with both regulators locked at high or low pressure. These combinations and permutations cause changes in operating mixture ratio and thrust level.

Figure 4 shows the resultant operating envelope for the MMH fueled Shuttle Thruster. The solid lines define the normal operational envelope. The lower thrust limit at 700 pounds thrust corresponds to the operation at the low regulator limits. The low thrust limit is also approached during multiengine firing where the pressure losses in the propellant supply lines increase due to the increased propellant flow. The dashed lines indicate the operating regions when either the fuel tank pressure regulator, the oxidizer tank pressure regulator, or both, malfunction at the high limit. In the solid region, the thruster must perform to specification. In the dashed regions, it must only operate safely. The operating zones for the hydrazine fuel thruster can be approximated by moving the ordinate scale to the right by 0.2 mixture ratio units (i. e., the nominal O/F ratio is 1.4 rather than 1.6).

### Feed System/Combustor Instability

Two kinds of instability are common in rocket systems. One is a feed system - combustion instability in which pulsations occur due to an undamped interaction between the propellant supply systems and the combustion process. The second kind is an undamped acoustic resonance set by a coupling between the combustion process and certain acoustic resonances within the combustion chamber.

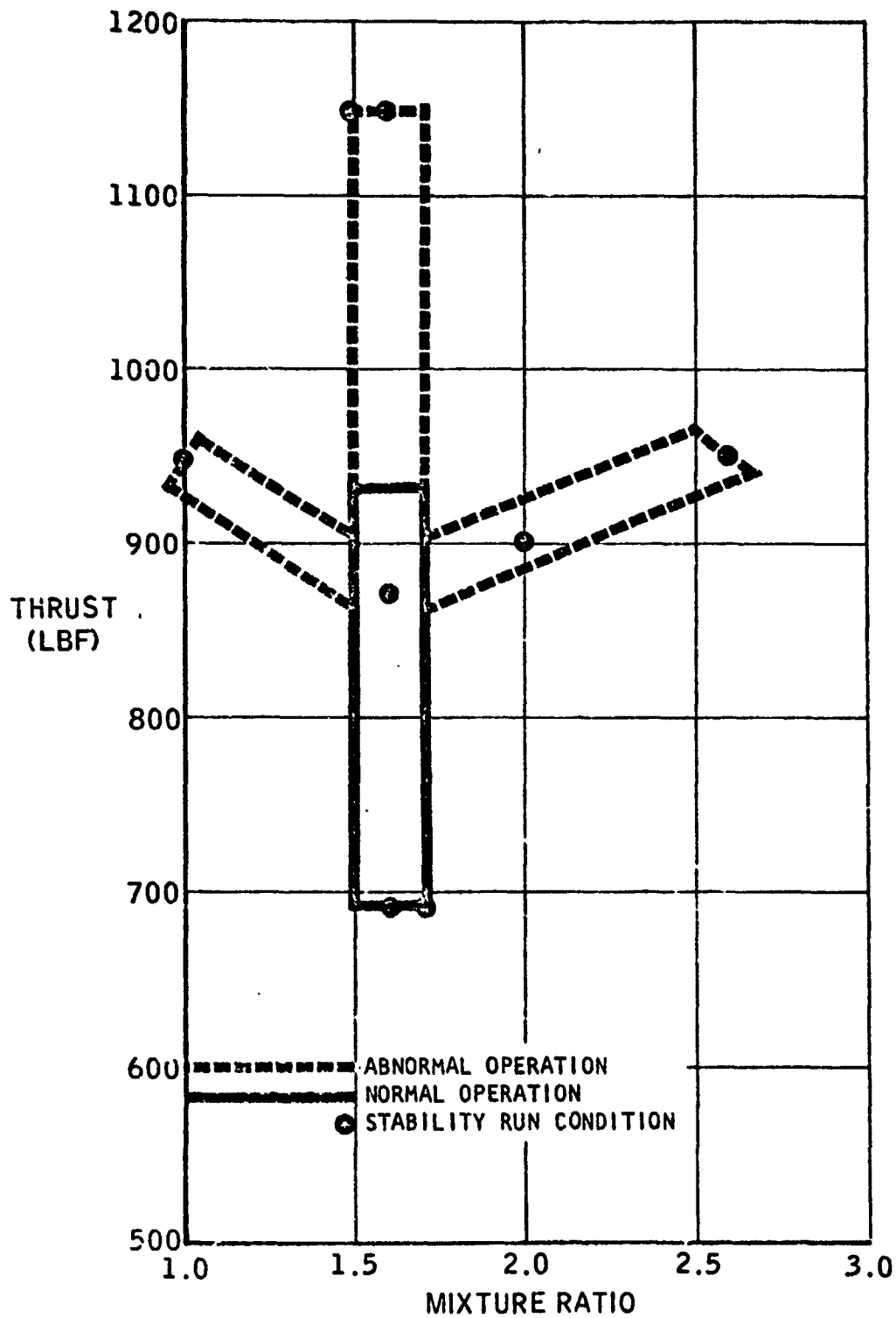
The Shuttle Thruster has demonstrated feed system stability over the entire range of thruster operating conditions shown in Figure 4.

Combustor stability relative to damping any acoustical resonances within the combustion chamber is achieved through the use of tuned acoustical cavities located around the outer rim of the injector. Figure 4 indicates the test conditions at which the combustion stability and feed system stability have been demonstrated.

### Chamber Temperatures

The shuttle thruster chamber is C-103 Columbium coated with R512A oxidation-resistant disilicide coating. The original throat temperature target at design operating conditions was 2100°F. Very large margins of safety exist with the Shuttle disilicide coated columbium chamber at this temperature. Figure 5 summarizes and compares the experimental data for coated columbium to the Shuttle mission requirements as a function of wall temperature. (Ref. 1). At the maximum design operating temperature of 2100°F, the measured coating life is almost 100 times the entire mission operating time. Even if the engine malfunctioned in such a way to continually produce wall temperatures of 2900°F, the engine could operate at this temperature for the required 100 missions. At 3000°F, 1.5 hours of life are available. These data were obtained from torch impingements experiments in oxidizing atmospheres (Ref. 1). Both the fuel film cooling and the fuel-rich O/F profiles near the walls provide a fuel-rich environment over the walls for the Shuttle thruster. This would contribute to even greater life than predicted by the data.

# PRIMARY THRUSTER OPERATING ENVELOPE



# OXIDATION-PROTECTIVE COATING LIFE COLUMBIUM ALLOY (C-103) WITH R512A COATING

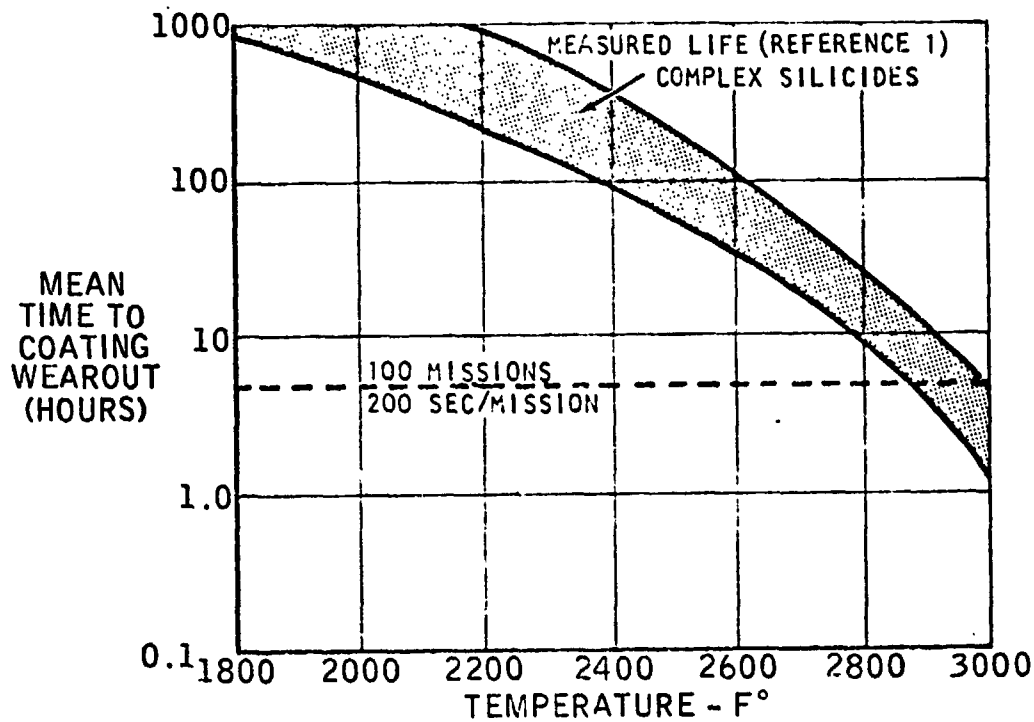




Figure 6 presents experimental temperatures measured on a prototype Shuttle thruster with MMH fuel. The maximum and minimum temperatures for an uninsulated thruster are shown. The variation of temperature at the nozzle throat station (1250-1550°F) suggests that the cooling film is not uniform due to the discrete number of film cooling injection points and to random variations of flow from each orifice. Test data with the insulated chamber indicate that throat wall temperatures are about 150°F warmer than the radiation cooled version (i.e.; the uninsulated thruster). The MMH fueled Shuttle thruster, therefore, is seen to be operating substantially below the target temperatures. At the design operating point, the maximum temperature measured for the insulated thruster is about 1850°F and is downstream of the nozzle throat in the supersonic flow region.

Figure 4 is a reminder that there are a wide range of off-design operating conditions at which the thruster must safely operate. The results of Thermal Tests conducted over the entire operating region are shown in Figure 7. The throat temperatures begin rising rapidly when the mixture ratio exceeds 2.0 and reach the maximum design temperature of 2100°F at a mixture ratio of 2.56. As will be discussed later, this rise in temperature appears to be related to an injector design parameter.

#### Re-entry Heat Loads

Analysis of re-entry heating indicated that the maximum chamber and flange temperatures are not caused by the hot combustion gases during firing of the thruster but by the re-entry heating when the thruster is not being fired.

During re-entry of the vehicle into the atmosphere, the high stagnation temperature of the air produces significantly higher chamber and wall temperatures than are produced by the rocket combustion. Figure 8 presents the calculated thruster wall temperatures during re-entry. The maximum re-entry wall temperature of 2250°F is greater than those presented in Figures 6 and 7 for a firing thruster. Furthermore, the re-entry temperatures occur in the presence of more corrosive oxidizing atmosphere rather than the fuel-rich environment when the rocket is firing.

The more severe nonfiring condition should therefore be used to specify the maximum allowable chamber temperatures. In terms of the objectives of this analysis program, if the hydrazine thruster produces temperatures the same as or less than the 2250°F (with a fuel-rich environment), little or no significant effect upon the life and thermal margins of the thruster material system is expected. The re-entry heating, thereby, allows the maximum thruster firing temperature target for hydrazine to be realistically raised to this higher value.

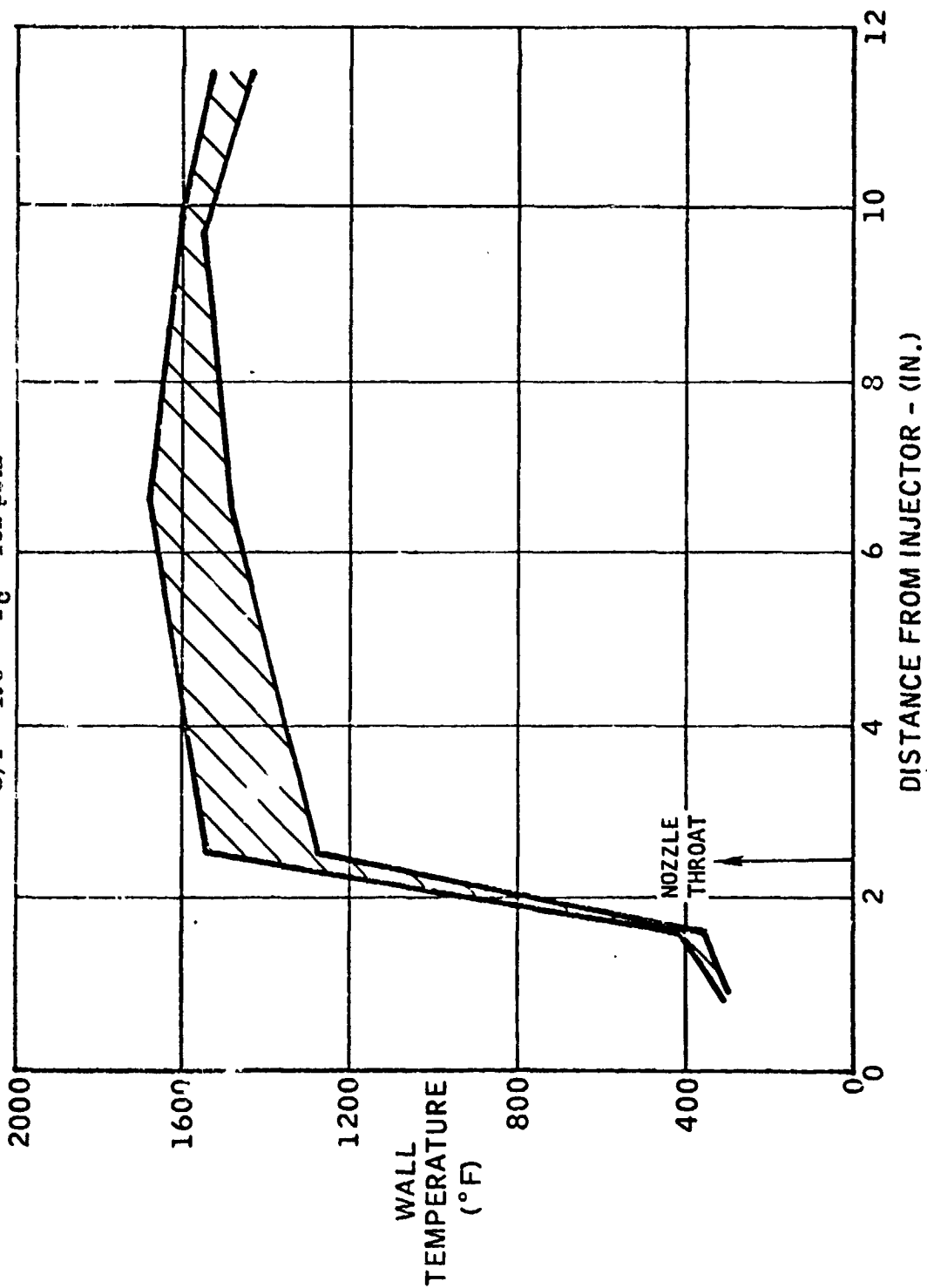
#### Thermal Conditioning of the Injector and Chamber

The SSRCS thruster uses an electric heater located on the injector head to prevent the injector head, valve, and combustion chamber temperatures from falling below the freezing points of the fuel (-62.5°F) and oxidizer (11.5°F). As discussed in more detail in the section on Vacuum Ignition, Spike, and Stability Analysis, the thermal conditioning

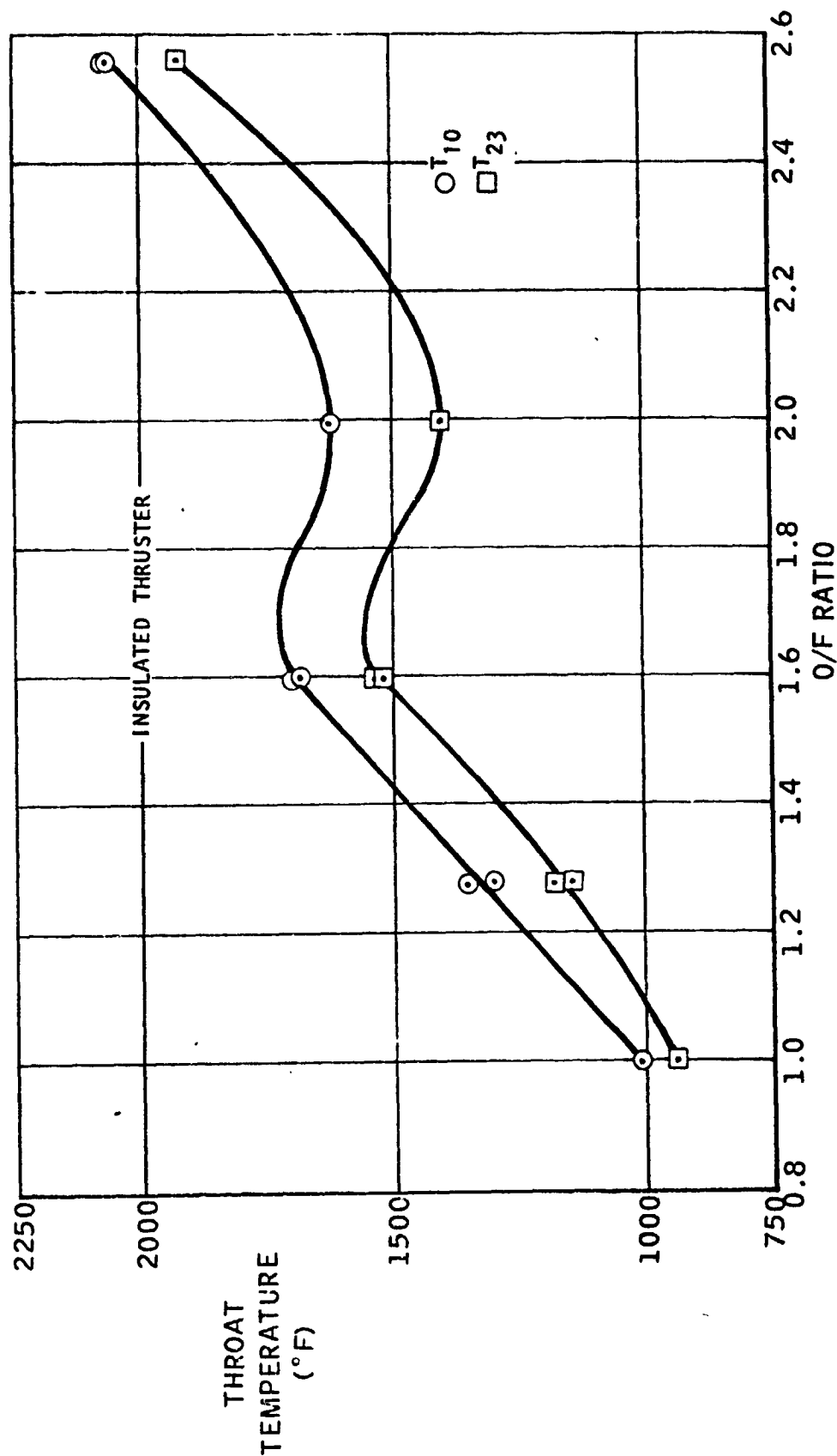
ORIGINAL PAGE IS  
OF POOR QUALITY

THRUSTER NO. 5 WALL TEMPERATURE  
UNINSULATED BOLTED CHAMBER

O/F = 1.6  $P_c = 152$  psia

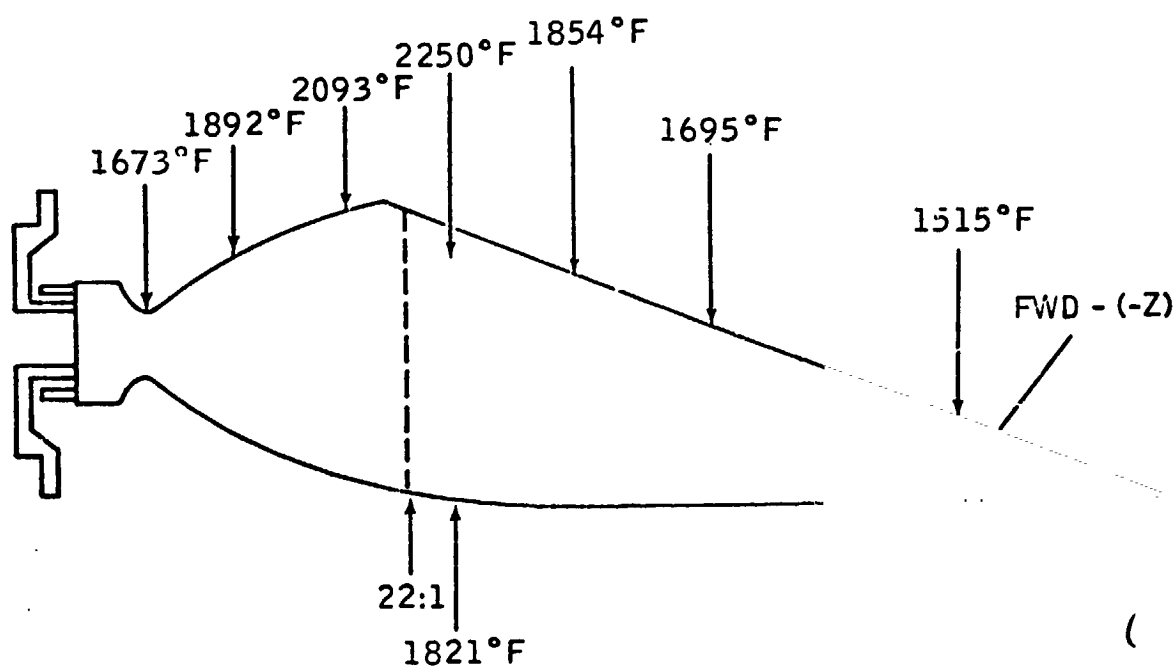


THRUSTER 5 THROAT TEMPERATURE VS O/F  
PROPELLANT TEMPERATURE = 70°F  
THRUST 870-960 lbs.



# PREDICTED THRUSTER RE-ENTRY TEMPERATURES WITH LONG SCARF

2.5" CHAMBER - INSULATED



ORIGINAL PAGE IS  
OF POOR QUALITY

affects the incidence of damaging explosive events due to condensation of fuel on chamber surfaces. The heater, therefore, insures that the start transient is rapid, reproducible, and smooth and that explosive events which could damage the valve or chamber are minimized.

When the thruster is not firing, the heater must compensate for conduction to the vehicle and radiation losses to space. The results of an analysis of the steady state power requirements for the heater are shown in Figure 9. To keep the head temperatures above the specified 50°F, approximately 10 watts of power must be supplied by the heater. To provide a margin of safety which covers the uncertainties in defining and analyzing the steady state and any transient environment, the heater is designed with a safety factor of two (i.e., delivers 20 watts). Another way of looking at this safety factor is that the heater must be ON 50% of the time to compensate for the anticipated heat losses.

The freezing point of hydrazine is 34.7°F and this is appreciably higher than for MMH or the nitrogen tetroxide. Therefore, it is anticipated that significant increases in heater power will be required to maintain the same thermal conditioning margins as for MMH. As will be discussed later in the report, doubling the heater power will provide adequate but not equivalent thermal conditioning.

#### Dimensional Considerations

The thruster is required to fit into closely controlled dimensional boundaries on the space shuttle vehicle. Therefore, for this study, the thruster length and outside overall dimensions are not allowed to vary. However, internal dimensions such as injector and film cooling orifice diameters, injection angles, and the propellant flow splits between inner and outer combustion zones may be allowed to vary. Small changes can be made to the combustion chamber length provided compensating changes are made to the nozzle length to assure that the overall length and maximum diameter remain constant and that performance is maintained or exceeded. For other applications this constraint does not exist, and overall dimensions can be changed.

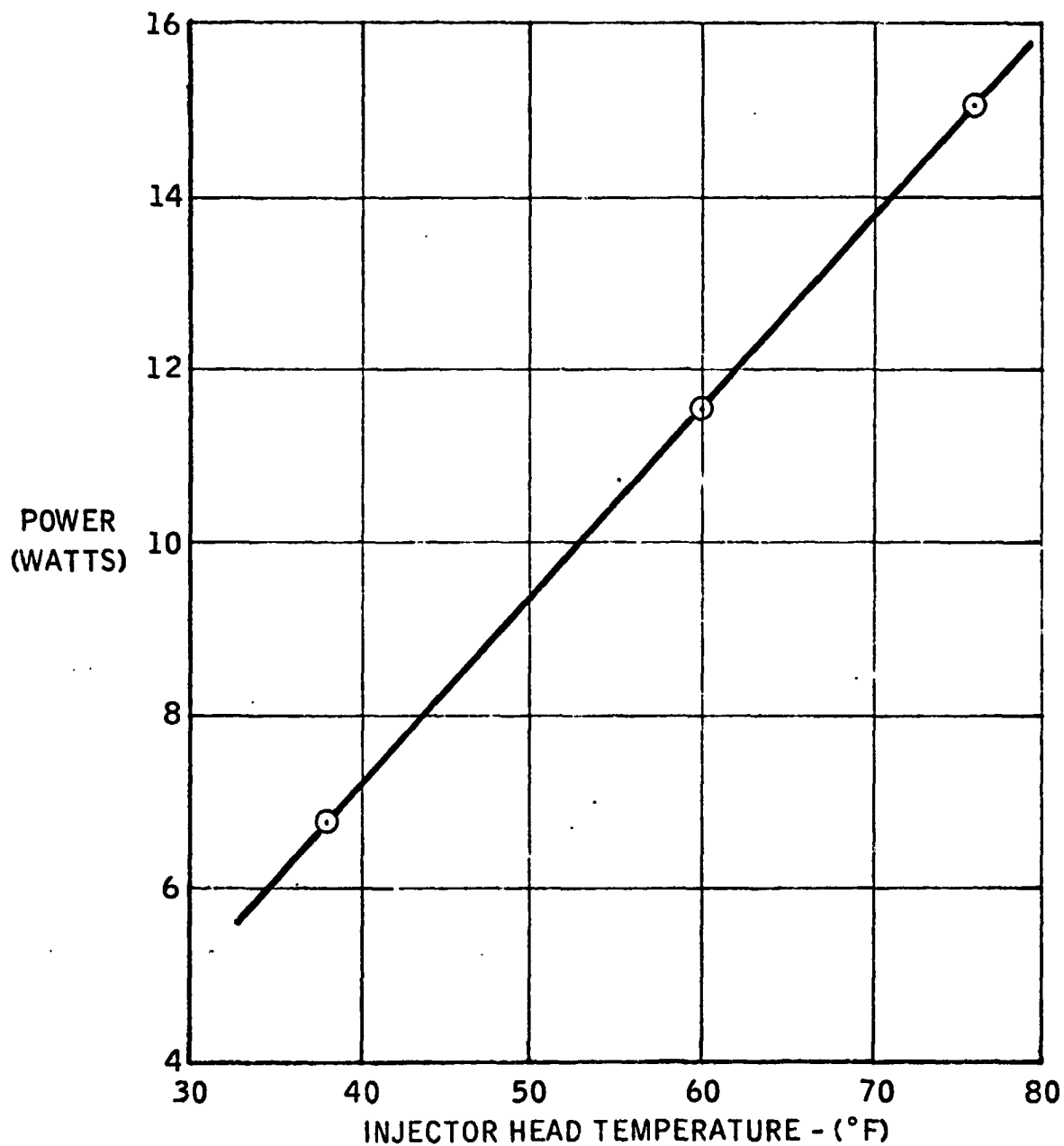
The study looks at two configurations for the hydrazine-fueled thruster. One is the unmodified shuttle thruster. Here, with the exception of a change of heater power consumption and a possible change of injector orifice or cavity dimensions, no modifications are made which require a change in tooling. The second configuration, Configuration B, is one which is modified to meet the present temperature and performance targets. Modifications which might require tooling changes are allowed for Configuration B.

#### Other Space Shuttle Constraints

The thruster specification (Ref. 2) lists many other requirements that the thruster must meet. The potential problems discussed in this report are those which are expected to affect the safety and integrity of the thruster.

In addition to the thruster specification, there may be other shuttle vehicle-related constraints which can only be evaluated by the System Manager (Rockwell/SD and the customer, NASA). No attempt is made to evaluate the feasibility of the conversion to hydrazine from the viewpoint of system operation, vehicle safety, logistics, or maintenance.

# AFT YAW THRUSTER 5 HEATER POWER



### III. ROCKET PERFORMANCE

The One-Dimensional Equilibrium (ODE) performance analysis program (Ref. 3) was used to predict the theoretical core gas temperatures and specific impulse for the shuttle thruster. "Frozen" nozzle flow was assumed downstream of the throat for the specific impulse calculations. Experience with small thrusters having short exhaust nozzles indicates that chemical equilibrium freezes very close to the throat. Figure 1 presented specific impulse and core temperatures for 100% combustion efficiency as a function of core mixture ratio. These predictions must be corrected to account for the losses in performance due to: (1) the use of the fuel as a coolant and (2) the less than perfect combustion that exists in the combustion chamber. An analysis procedure was developed for predicting these losses for the shuttle thruster. This method was modified to account for the different physical and chemical properties of hydrazine and is discussed in Appendix B.

The performance analysis considers that the propellants occupy three specific zones whose configuration is dictated by the shuttle injector pattern - a film cooling zone covering the interior chamber walls and two core combustion zones (Figure 10). The analysis procedure for the core zones accounts for variations of doublet mixing efficiency as the doublet Rupe number and contact time (or blowapart) parameters are changed. It also considers the effects of the mixture ratios in each combustion zone and the effects of changes in resultant momentum angle of the two propellants in each zone. The remaining combustion efficiency terms, due primarily to secondary mixing within each zone and between zones, are derived empirically from experimental data. These data correlated best with chamber length. Finally, the performance increment due to the film cooling zone is included using the assumption that the cooling zone gas temperature is a fixed value. Appendix B describes the performance assumptions in more detail.

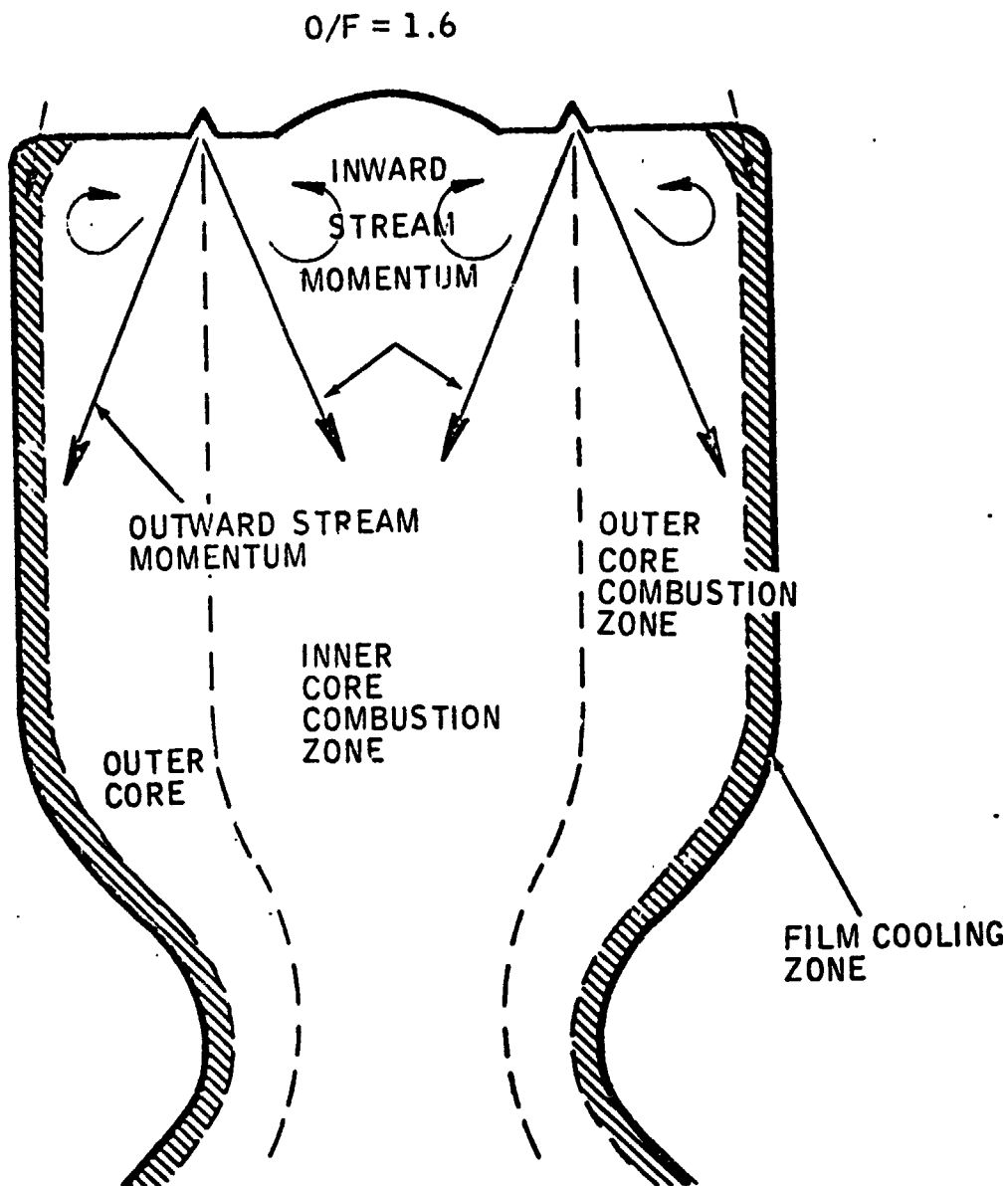
#### Rocket Performance Calculations

The functional relationships discussed in Appendix B were combined into a computer program which calculates the changes in specific impulse as the thruster design parameters are varied. Figure 11 compares the predicted  $I_{sp}$  of the MMH and hydrazine fueled thrusters using the three-zone model and incorporating the effects of Rupe number, contact time, zone mixture ratio, momentum angle, and film cooling. The hydrazine thruster performance is predicted to peak at an O/F of 1.2. Performance at the equal volumetric flow mixture ratio of 1.4 is only slightly less than that of the MMH thruster at an O/F of 1.6.

#### Refinements in Performance Predictions

The film cooling study, discussed later in this report, was conducted subsequent to the performance calculations. It indicates that the liquid film for hydrazine persists for only 0.85 inch along the chamber wall as compared to 2.3 inches for MMH and that the film temperatures are higher than for MMH. This finding suggests that the performance of the

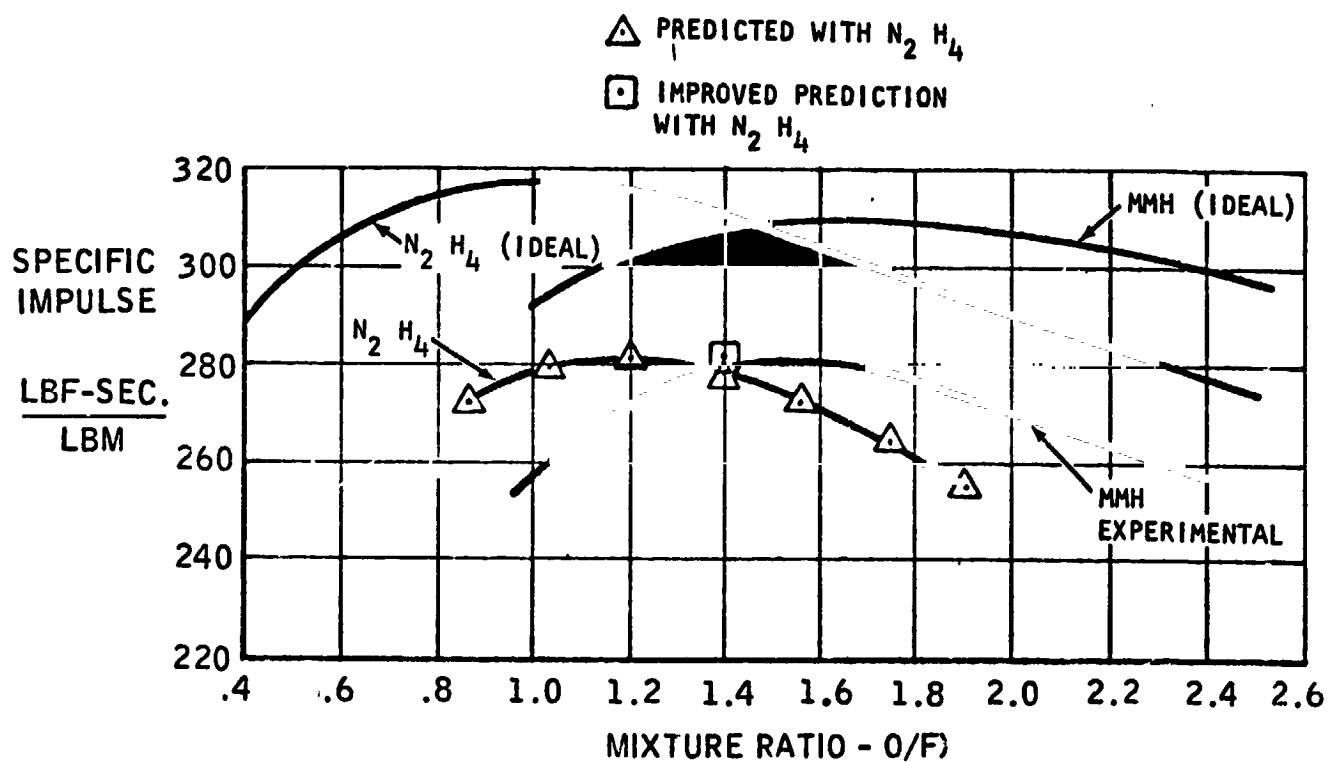
## THREE ZONE MODEL



ORIGINAL PAGE IS  
OF POOR QUALITY



# PREDICTED SPECIFIC IMPULSE HYDRAZINE THRUSTER



hydrazine thruster will be higher than originally predicted due to a greater amount of mixing between the cooling and outer core flow and also due to the higher specific impulse derived from that portion of the cooling flow which remains unmixed. The additional specific impulse estimated due to these two effects brings the  $I_{sp}$  to 281.4 at  $O/F = 1.4$ . This correction to the original prediction is also shown in Figure 11 by the square symbol. The specific impulse of the hydrazine thruster is predicted to be only slightly better than the MMH thruster at their equal volumetric flow ratios. Corrections were not made at other than design mixture ratio since the thermal and mixing analysis were only conducted at  $O/F = 1.4$ .

#### IV. FILM COOLING ANALYSIS

Extensive literature is available regarding the analysis of film cooling in combustion or other systems. From this, it is clear that the analysis procedure are complicated by the large number of parameters affecting the transfer of heat from the hot gas core to the liquid or gas coolant layers. These parameters include the physical properties of the liquid and/or gaseous coolants (i.e., their density, viscosity, surface tension, heat capacity, vapor pressure), the film coolant injection velocities, method of injection, Reynolds number, Weber number, and temperatures. The conditions in the hot gaseous core such as its turbulence level, the relative velocity between it and the coolant flow, the core temperature and core physical properties also contribute to heat and mass transfer. Research to better define, simplify, and correlate the relationships between these properties is continuing; but disagreements still exist on which of these parameters are most important for predicting the effectiveness of film cooling.

Despite these difficulties, reasonable estimates of film coolant effectiveness have been accomplished in the past, in those applications where some experimental data were available. The experimental data permit the calculation of an empirical factor which accounts for many of the unknown or poorly defined parameters. Most importantly, this empirical factor permits the prediction of the effect of changes of the film cooling parameters provided that large deviations are not made from the original experimental points.

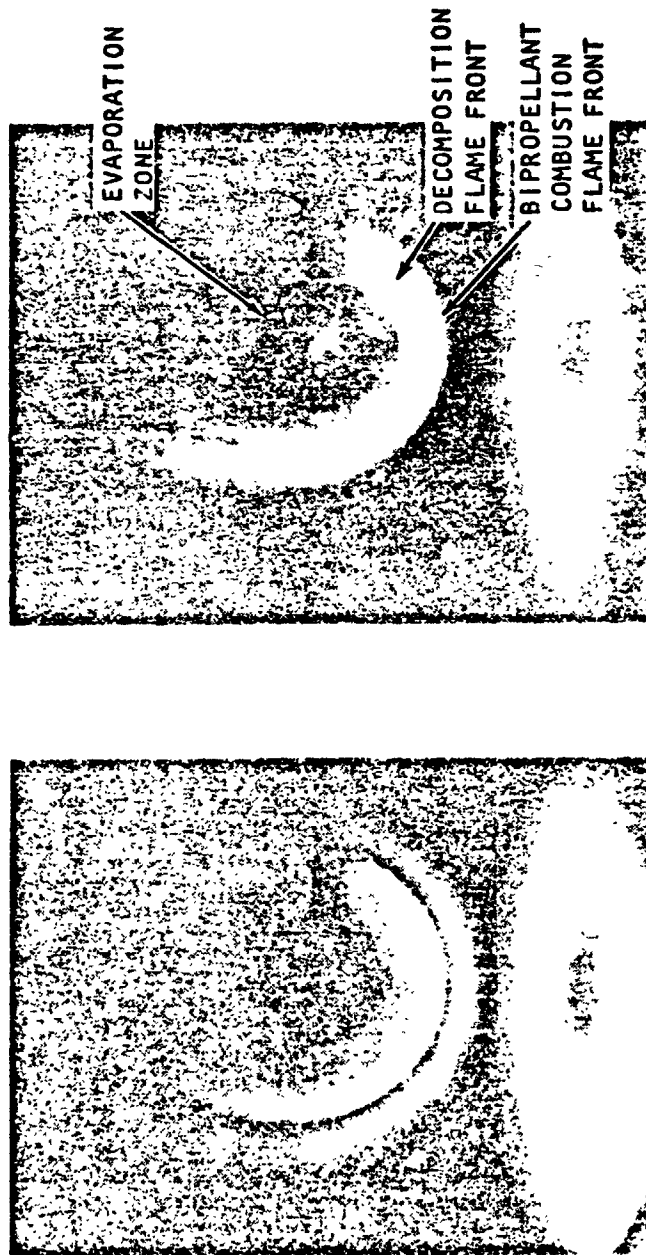
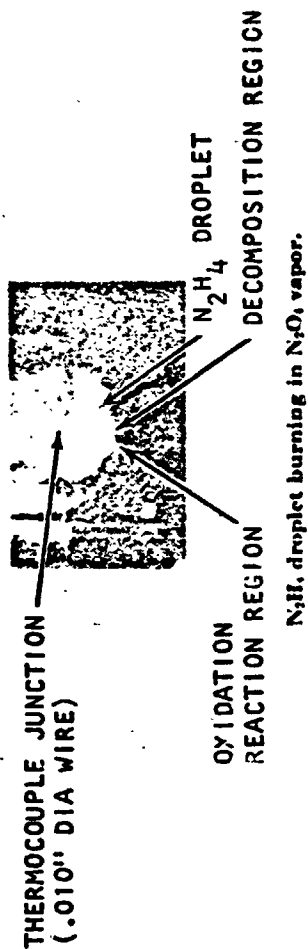
##### Cooling with Reactive Liquids

One of the areas where the least amount of film cooling research has been conducted is in the use of reactive liquids as a film coolant. A reactive liquid is one which chemically reacts with the hot core flow and thereby produces or absorbs thermal energy or one which decomposes at the temperatures generated by the hot core and once again produces or absorbs thermal energy. This is not to imply that combustible film coolant materials such as JP-4, RP-1, methanol, butanol, or others have not been used in film cooling investigations. When they are used, the tests are specifically designed to investigate the differing physical properties of these liquids and to avoid the chemical reactions.

Hydrazine and hydrazine derivatives such as monomethylhydrazine are fluids which are capable of both decomposition and combustion reactions when nitrogen tetroxide is used as the oxidant in the core flow. A significant body of literature directly concerned with hydrazine droplet decomposition and burning exists which documents that the droplets of hydrazine (and its derivatives) are surrounded by clearly visible monopropellant and bi-propellant flames in the chamber combustion environment. Figure 12 shows pictures obtained by Lawver (Ref. 4) and also Allison (Ref. 5) which illustrate the dual sheath of flame encircling the droplet.

ORIGINAL PAGE IS  
OF POOR QUALITY

# PHOTOGRAPHS OF BURNING DROPLETS



$N_2H_4$ ,  $d_d = 1.27$  cm,  $T_{\infty} = 2530$  K,  $Y_{O_2} = 0.418$  UDMH,  $d_d = 1.27$  cm,  $T_{\infty} = 2530$  K,  $Y_{O_2} = 0.418$

ORIGINAL PAGE IS  
OF POOR QUALITY

Three vapor zones exist around the drop in these figures. First, the liquid hydrazine is vaporized by the thermal flux from the surroundings. When the vapor reaches the decomposition temperature, it exothermically decomposes, producing the inner flame front quite close to the drop. The decomposed gases (the second zone) move outward where they mix with the inwardly diffusing oxidizer. When an ignitable fuel-oxidizer ratio is reached, combustion occurs. The resultant hot combustion gases (the third zone) generated by the second flame front move outward and mix further with the ambient oxidizer rich gases of the experiments.

The same concept of decomposition and possible combustion can be extended to the two-dimensional hydrazine coolant film on the walls of the combustion chamber. Referring to Figure 10, the liquid film coolant along the wall is exposed to the 5000° F gas temperatures of the combustion core. This heat flux causes evaporation of the coolant and produces a vapor layer above the liquid. As the vapor moves radially inward toward the core flow (and is carried toward the nozzle), its temperature rises to the decomposition point and the hydrazine begins decomposing quite close to the liquid film and forming a decomposition flame front over the coolant layer. As the decomposed products move away from the wall, they mix with the core flow. Combustion may or may not occur, depending upon the amount of oxidizer in the hot gases. Figure 13 illustrates these many possible zones in the film cooled layer. Since decomposition and possible combustion of the vaporized coolant seems sure to occur, one can visualize that a reactive liquid film cooling layer is covered with one or two sheets of flame due to its decomposition and possible bipropellant combustion flames when exposed to the very hot core gases. This is much more complex than the conventional concept of a coolant layer. This chemical reactivity is believed to explain the relatively poor cooling properties of such fluids as hydrazine and MMH as compared to more inert fluids such as water.

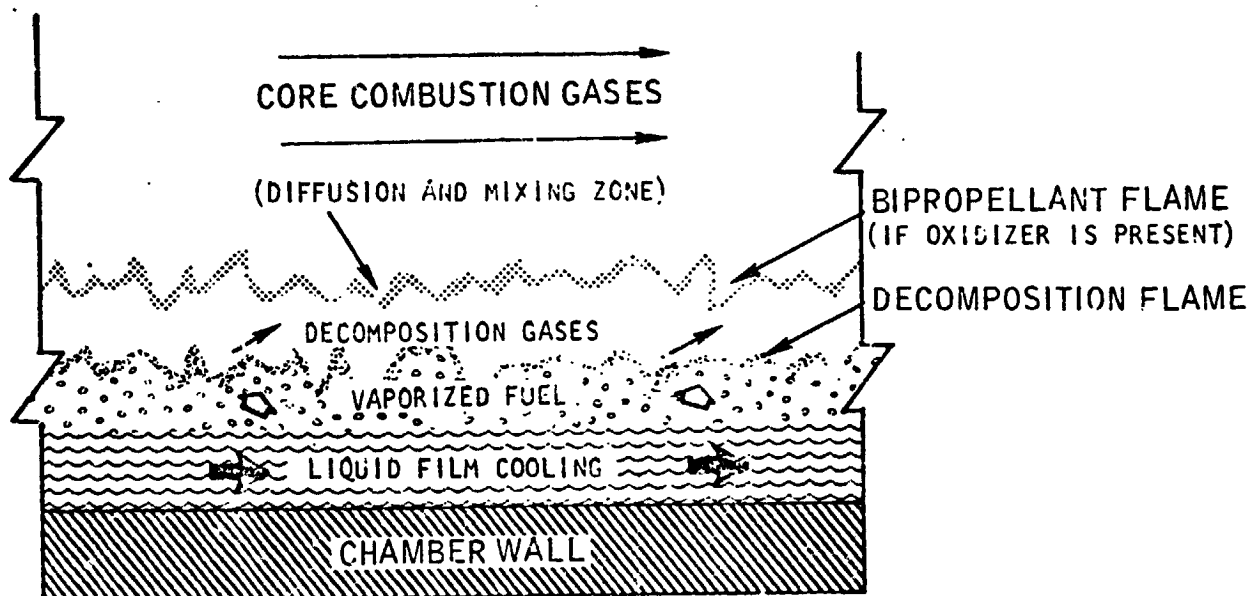
#### Decomposition Model for Coolant

In this study, an approach was formulated to account for the effects of the decomposition flame above the coolant layer. This model fits the experimental data better than non-reactive film cooling theory. No bipropellant reaction was considered for the thruster, since the outer combustion zone normally operates fuel rich, and little or no bipropellant reactions are expected.

Some simplifying results arise from the decomposition model. The evaporation rate of the liquid hydrazine (or hydrazine derivative) is predicted to be independent of the core temperature or oxidizer content of the hot core gases. It is rather primarily a function of the laminar flame speed for the decomposition reaction. In addition, as a result of the decomposition reaction, the gaseous coolant film temperature beyond the liquid layer rises rapidly to the decomposition temperature of the fuel. Therefore, minimum temperatures of the coolant gas is on the order of 1600-1800°F.

Appendix C presents the assumptions and calculation procedures used for both the evaporative and decomposition film cooling analysis.

## TWO FLAME MODEL FOR REACTIVE LIQUID FILM COOLING



## V. RESULTS OF THE ANALYTICAL PROCEDURES

### Evaporation Model

To provide a perspective on the differences between the simple evaporation film cooling model and the thermal decomposition model, calculations of the coolant evaporation rate were first made assuming no decomposition. Evaporation is produced only by the heat flux from the core combustion where the heat transfer coefficient is based upon Bartz's turbulent combustion model. Figure 14 shows the calculated liquid film lengths as a function of film effectiveness for both hydrazine and MMH. Film effectiveness is the percent of the original coolant flow that remains on the wall for cooling. The effectiveness factor considers liquid coolant losses due to splashing at the injection point and due to film instability. Appendix C discusses the factors affecting the amount of liquid lost. As indicated in the figure, only 48% of the liquid injected is calculated to be effective for cooling with hydrazine and 44% is effective with MMH.

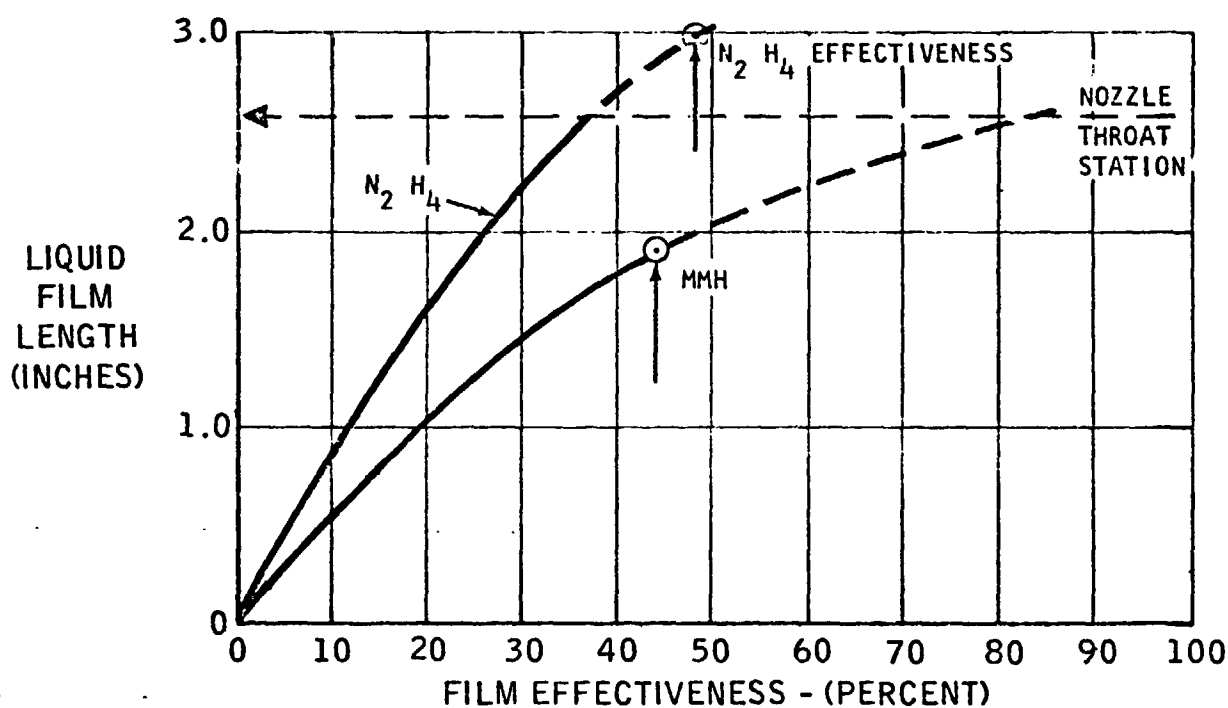
The important observation made from Figure 14 is that the evaporation model predicts that the hydrazine liquid length is greater than that for MMH, and this contradicts experimental data. The hydrazine liquid film is predicted to extend beyond the nozzle throat station, while the MMH liquid film does not reach the throat. The evaporation model predicts a longer hydrazine liquid length because the heat of vaporization of hydrazine is greater than that of MMH and it therefore takes longer to evaporate for the same heat flux. The liquid film for hydrazine infers that the throat is at boiling liquid film temperature for hydrazine (400°F at a chamber pressure of 150 psia). This is contrary to Marquardt's experimental data on prior thrusters. As discussed earlier, measured throat and wall temperatures with hydrazine have always been higher than with MMH (2200-2540°F versus 1800 to 1900°F).

The analysis was carried one step further. The coolant gas temperatures were calculated for MMH beyond the liquid film. Figure 15 shows the predicted coolant film temperatures as a function of coolant effectiveness for MMH. For the 44% effective MMH film, the gas recovery temperature at the throat is calculated to be 850°F. This evaporation model prediction will be compared to the decomposition model in the next section.

### Thermal Decomposition Model

The liquid film lengths and gas temperatures were calculated using the laminar burning velocity and decomposition temperature discussed in Appendix C. Figure 16 presents the calculated film temperatures for the decomposition model as a function of film effectiveness for MMH. The liquid film is assumed to be at the temperature corresponding to the boiling point associated with the chamber pressure. When the liquid film ends, the temperature of the gaseous coolant is assumed to rise to the 1600°F decomposition temperature in the short distance of 0.2 inch. Thereafter, heat transfer to the decomposed coolant gas from the core gases causes an additional temperature rise. For the MMH thruster with the estimated 44% cooling effectiveness, the recovery film temperature is predicted to be 1620°F. The liquid film length is 2.3 inches.

# LIQUID FILM LENGTHS EVAPORATION MODEL



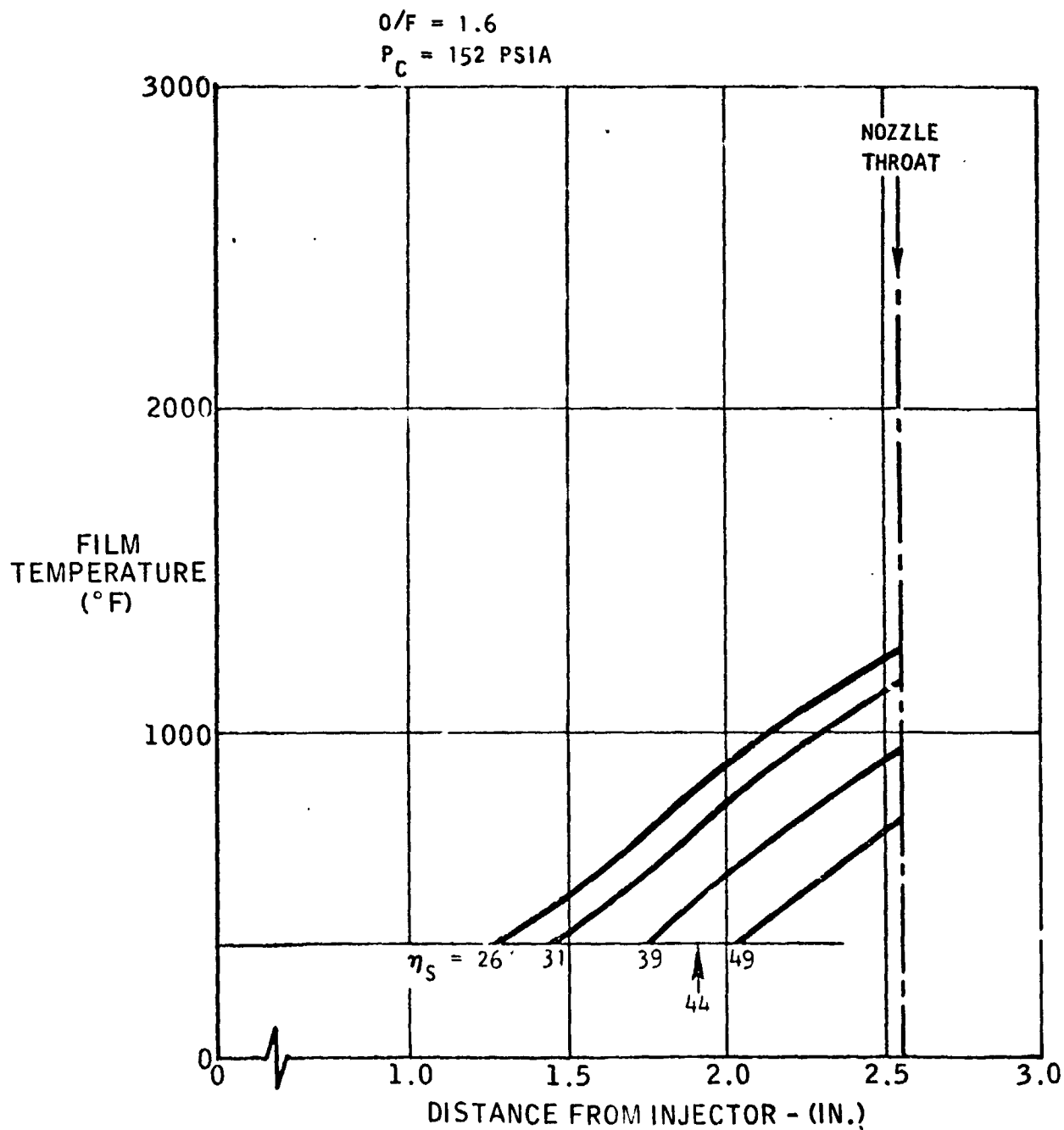
ORIGINAL PAGE IS  
OF POOR QUALITY



# FILM COOLING ANALYSIS

## EVAPORATION MODEL

### MMH/N<sub>2</sub>O<sub>4</sub>



# FILM COOLING ANALYSIS

MMH/N<sub>2</sub>O<sub>4</sub>

O/F = 1.6

DECOMPOSITION TEMP. = 1600°F

FILM COOLING = 24°

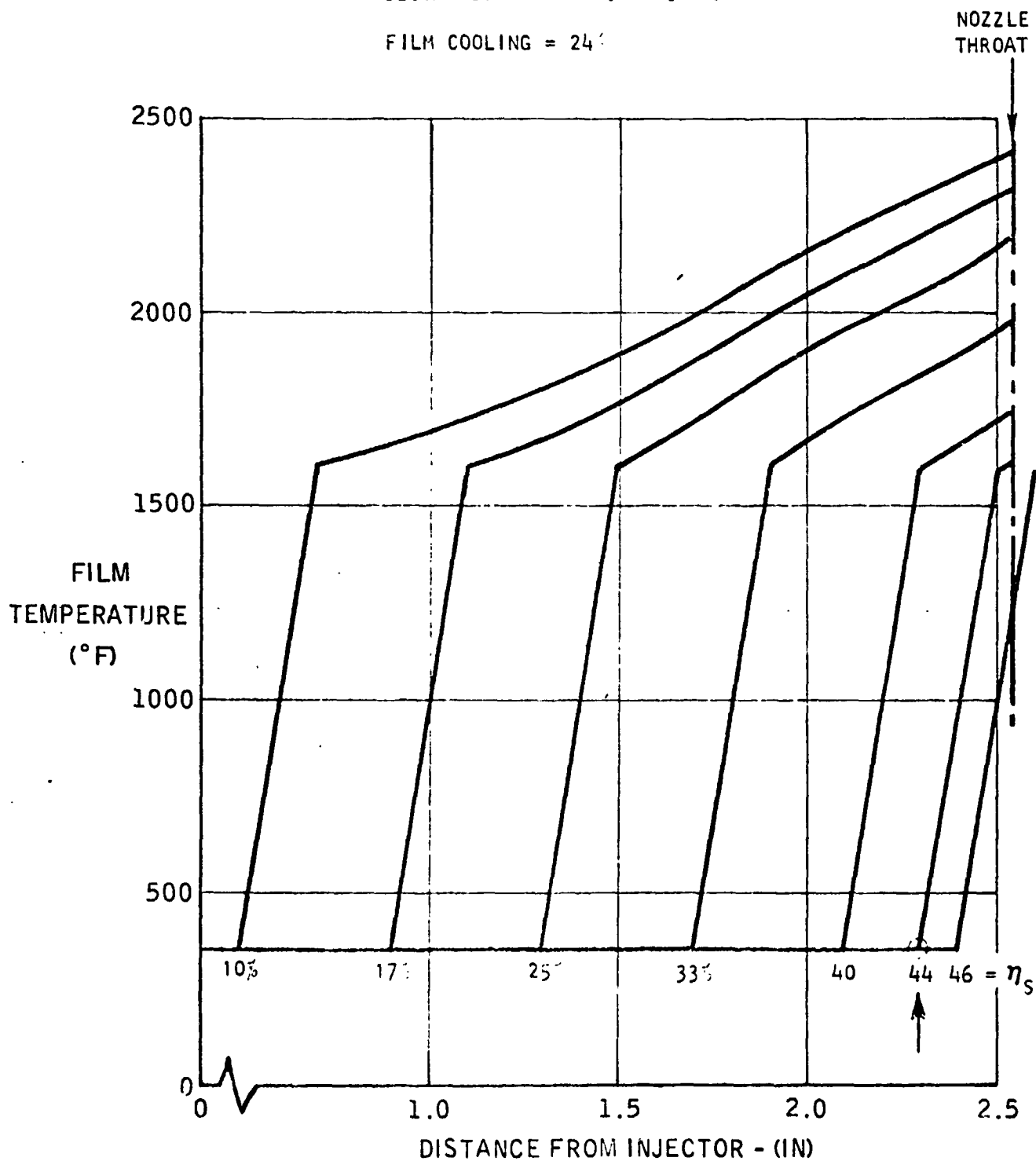


FIGURE 16

The two prediction models can be compared to experimental data obtained on the Shuttle thruster in Figure 17. The predicted film recovery temperatures for the evaporation and decomposition models and the measured outside wall temperatures on the chamber are shown. The predicted temperatures have been corrected for the 150° F difference in temperature between the insulated and uninsulated chambers. Separate computations conducted for the Shuttle program indicate that film recovery temperature and throat temperature are almost identical at the throat station for an insulated thruster. The decomposition model appears to provide significantly better correlation with respect to both the magnitude of the throat temperature and the sharp rise of wall temperature due to the rapid decomposition reaction.

Figure 18 presents the calculated film recovery temperatures for film cooling with hydrazine. For the estimated 48% hydrazine film effectiveness, the predicted gas temperature is 2380° F. Also observe that the liquid film length is only .85" due to the 3 times higher mass burning rate (evaporation rate) of hydrazine compared to MMH (Appendix C). The predicted film temperature is now in the neighborhood of the experimental temperatures measured on the other Marquardt thrusters using hydrazine.

#### Film Cooling Nonuniformity

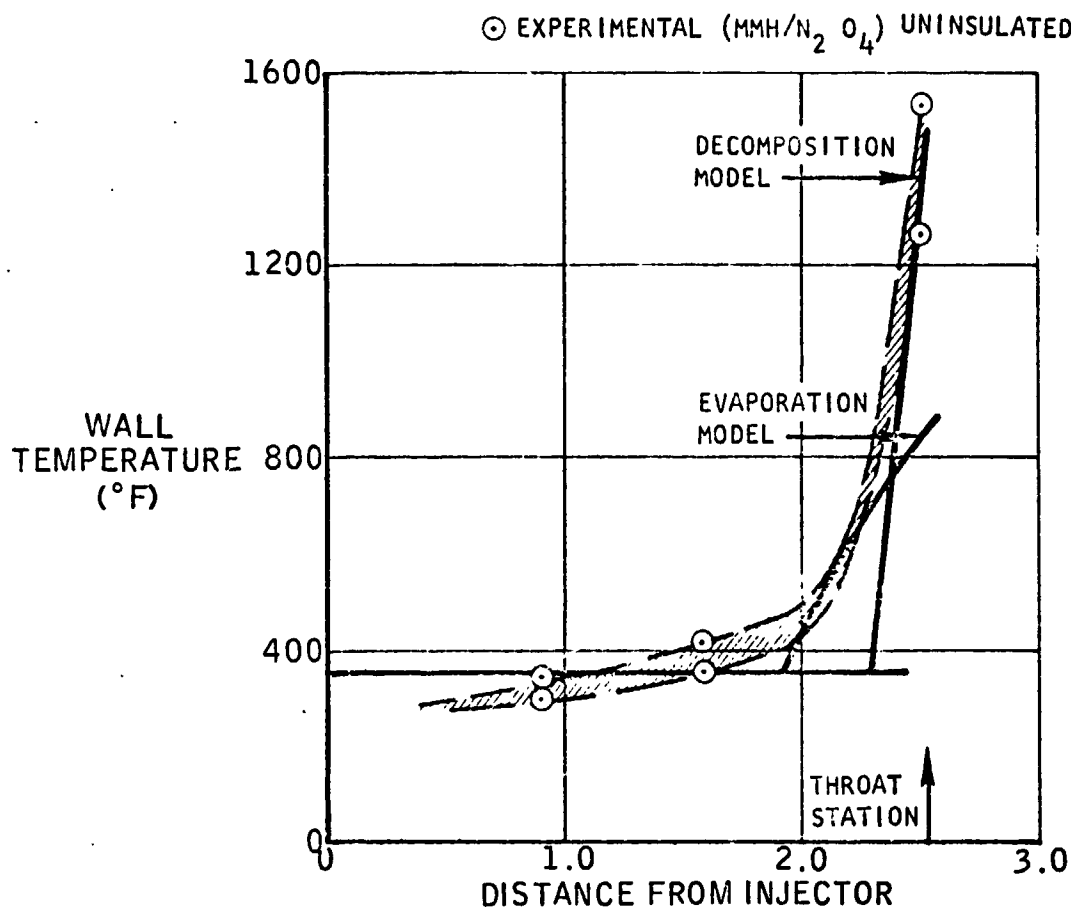
Due to orifice manufacturing tolerances and the discrete number of injection ports, the film coolant cannot always be laid down absolutely uniformly on the wall. Figure 19 illustrates the concept that liquid coolant length varies around the circumference of the thruster.

The experimental data obtained on the present Shuttle thruster in conjunction with the decomposition model can be used to estimate the degree of film nonuniformity. The decomposition model for MMH (Figure 16) predicts that a large variation of film temperature can occur near the throat of the thruster for small changes in film cooling. This occurs because the decomposition zone with its rapidly changing temperature is at the throat location. Assume that the minimum and maximum liquid film lengths are  $\pm 5\%$  of the average length. Entering Figure 16 at an average effectiveness of 44%, the film temperature is predicted to vary between 1150° F and 1680° F. The predicted film temperature difference of 530° F is somewhat larger than the experimental wall temperatures difference of 400° F. However, the influence of chamber metal conductivity is not included in the prediction and would act to provide better agreement.

The hydrazine thruster throat section will be much less sensitive to variations in film cooling pattern. From Figure 18, the liquid film is predicted to end less than an inch from the injector face. The same  $\pm 5\%$  variation in film length this far from the throat is predicted to produce less than  $\pm 25^\circ$  F variation in throat temperature. Of course, larger temperature gradients will still be produced upstream in the chamber where the liquid film ends.

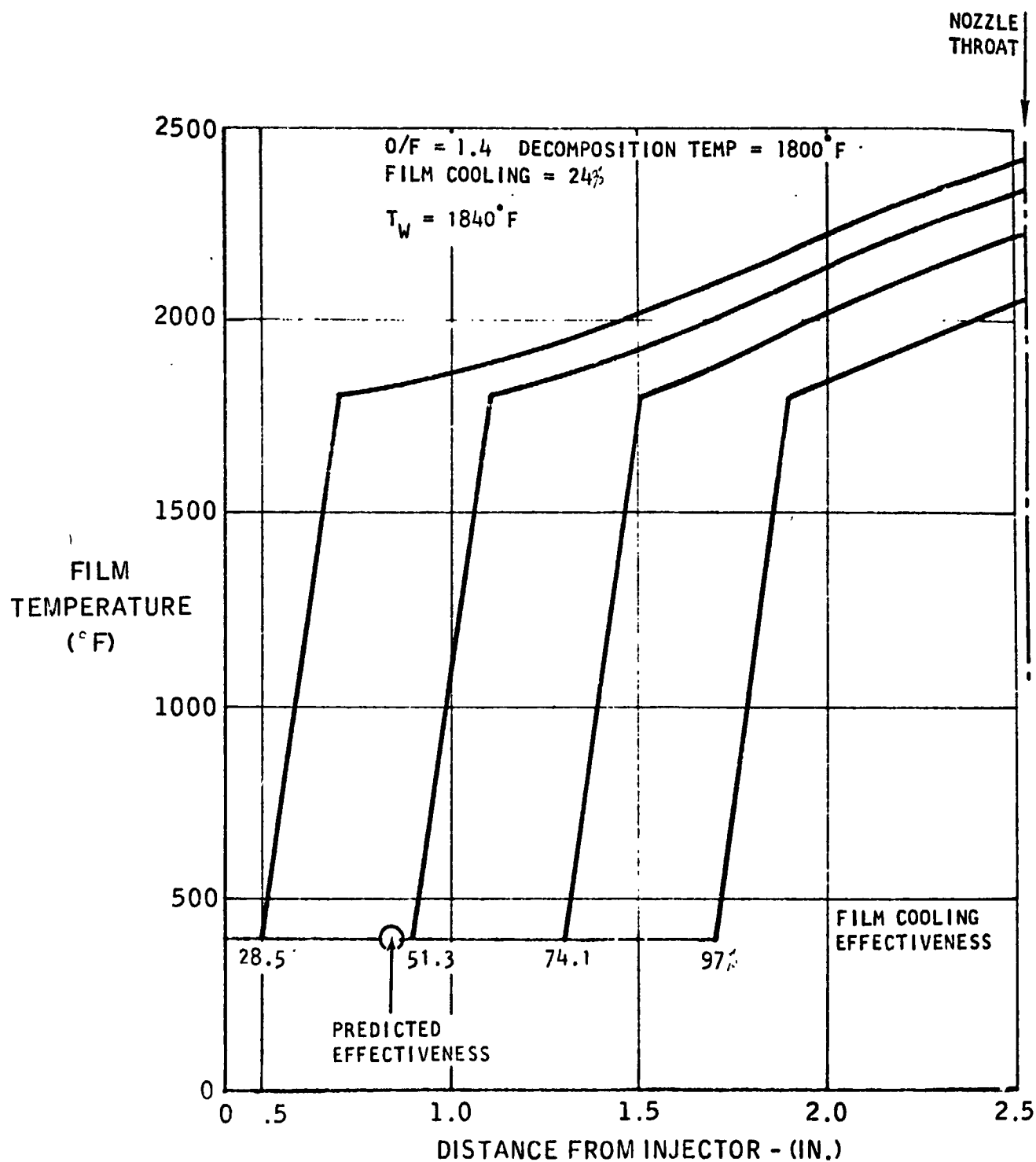
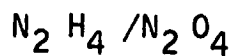
The MMH thruster temperature can vary widely at the throat for small changes of the film cooling effectiveness due to the rapid temperature gradients when the end of the liquid film approaches the throat. On the other hand, the hydrazine thruster requires strikingly

# RADIATION COOLED THRUSTER COMPARISON OF EXPERIMENTAL AND CALCULATED WALL TEMPERATURES



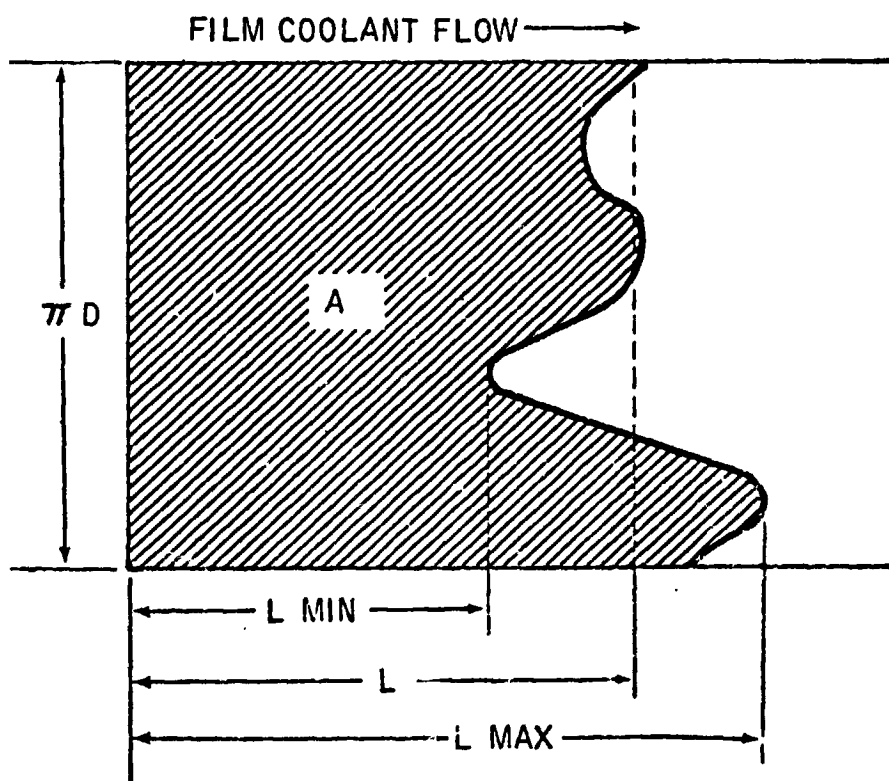
ORIGINAL PAGE IS  
OF POOR QUALITY

# FILM COOLING ANALYSIS



# PATTERN VIEW OF FILM-COOLED SECTION

FILM COOLANT  
INJECTION



ORIGINAL PAGE IS  
OF POOR QUALITY

large changes of film effectiveness to cause even small changes in the gas temperature at the throat.

### Sensitivity of Predicted Temperature to Analysis Assumptions

In view of the preliminary nature of some of the assumptions in the analysis, an attempt was made to investigate the variation in predicted temperature as the key elements of the analytical assumptions are changed. Figures 16 and 15 already permit evaluation of the effect of changing the liquid film cooling effectiveness.

Figure 20 illustrates the effect of decomposition temperature upon the throat gas temperature for the hydrazine thruster. A 200° F change in the decomposition temperature produces a 100° F change in throat temperature when liquid film length is near the predicted length.

Figure 21 illustrates the effect of core temperature upon gas film temperatures. A 400° F change in core combustion gas temperature produces about a 70° F change in throat temperature at predicted liquid film lengths.

### Predicted Hydrazine Thruster Throat Temperature

The previous analysis provides sensitivity coefficients which indicate how much the film temperature changes for a change of combustion gas temperature, a change in decomposition temperature, and a change in film cooling effectiveness. To calculate the throat temperature for the hydrazine thruster, the values of these three parameters must be defined. The film effectiveness for hydrazine was calculated to be 0.45, the decomposition temperature was assumed to be 1800° F, and the combustion temperature at real thruster combustion efficiencies was estimated to be 4660° F from the performance calculations. Figure 18 can be used first to find the predicted film temperature for a combustion gas temperature of 5010° F, and the above values of effectiveness and decomposition temperatures. The combustion sensitivity coefficient can then be used to correct the data of Figure 18 for the combustion temperature of 4660° F. Performing this calculation indicates that the predicted film temperature will be 2310° F. Therefore, for the insulated thruster the throat temperature will also be very close to 2310° F.

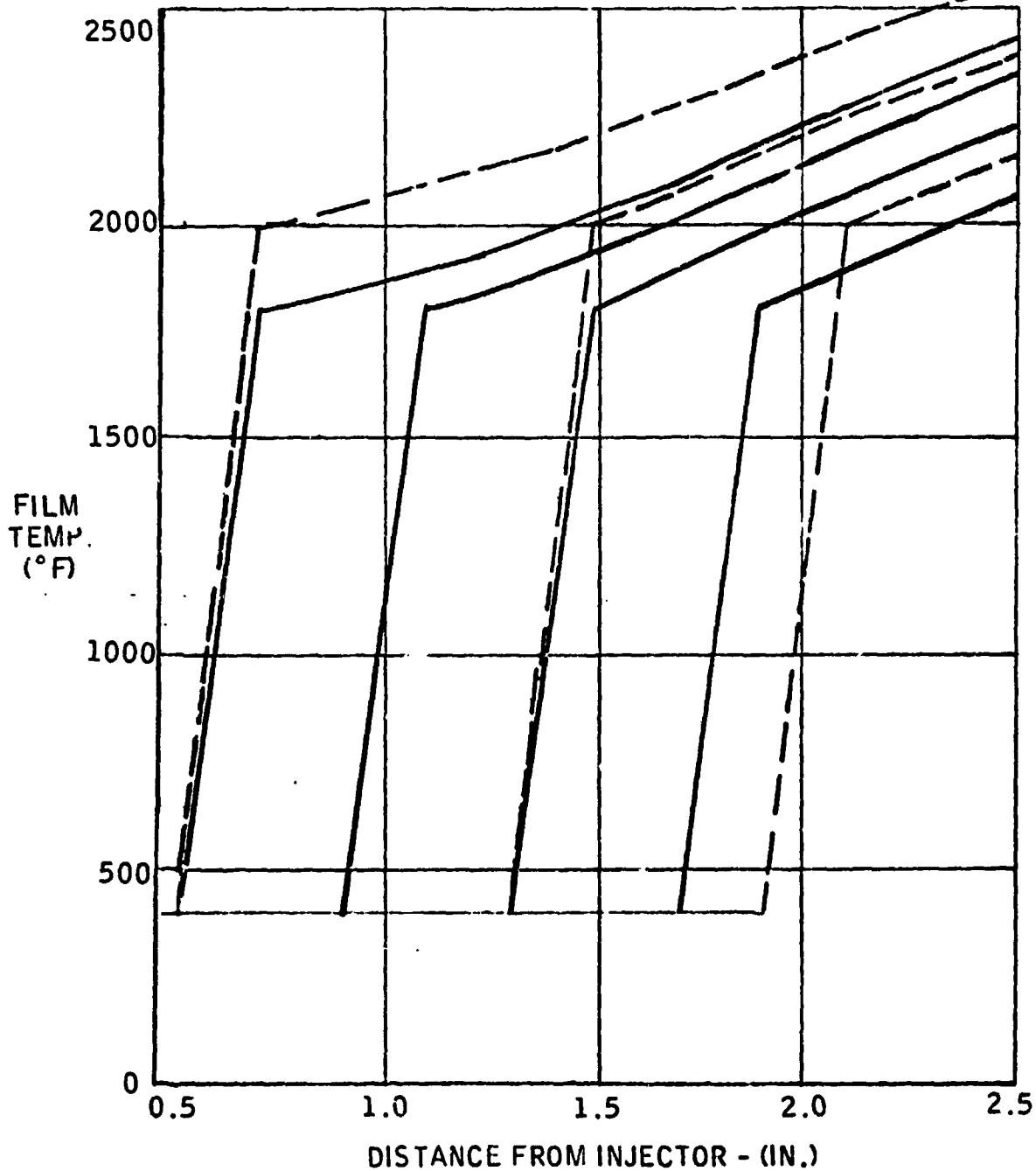
# FILM COOLING ANALYSIS EFFECT OF DECOMPOSITION TEMPERATURE

DECOMPOSITION TEMP  $N_2H_4$  1800°F ————— FILM COOLING = 24%

2000 °F ————  $T_w = 1840^\circ F$

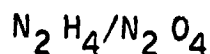
O/F = 1.4

$N_2H_4/N_2O_4$





# FILM COOLING ANALYSIS EFFECT OF COMBUSTION GAS TEMPERATURE

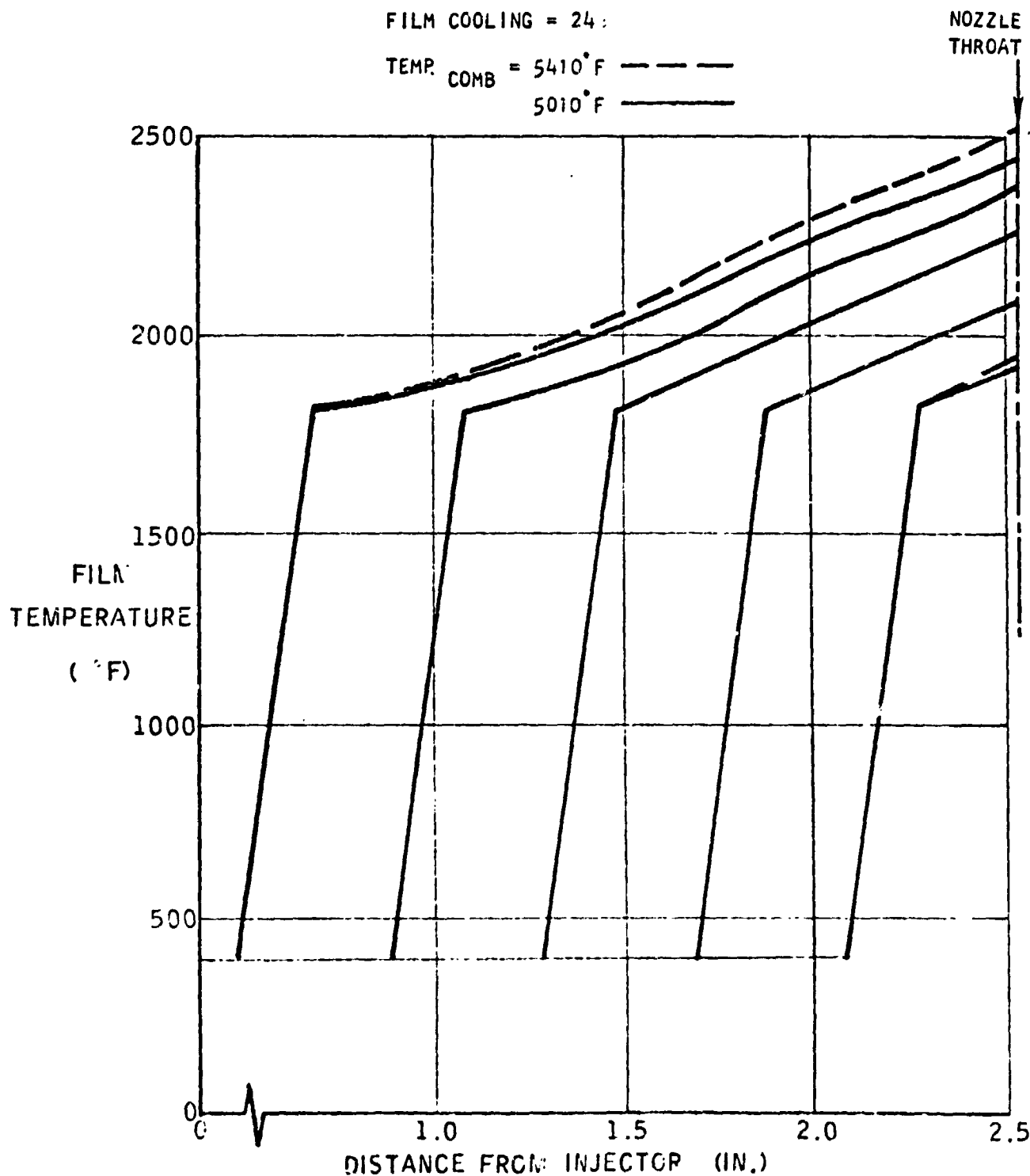


O/F = 1.4      DECOMPOSITION TEMP. = 1800°F

FILM COOLING = 24:

TEMP. COMB = 5410°F — — — —

5010°F — — — —



## VI. PERFORMANCE TRADEOFFS

One objective of this program was to predict the performance of the Space Shuttle Reaction Control System Thruster when hydrazine was used as the fuel. It was originally anticipated, on the basis of prior testing with other thrusters, that the specific impulse would be about the same at the equal volumetric flow mixture ratio but that chamber temperatures would be above the original shuttle thruster target of 2100°F. This expectation led to the concept of a "modified" configuration specifically tailored to hydrazine fuel. This thruster, Configuration B, would incorporate changes which would result in reduced chamber temperatures but which would not violate other significant space shuttle design constraints. In this section of the report we examine the effects of possible thruster modifications upon the specific impulse and throat temperature.

### Performance Tradeoffs

Specific impulse and nozzle throat temperature are used as the two primary tradeoff parameters. There are significant differences between the MMH and the hydrazine-fueled thrusters relative to these parameters, and since an examination of these differences leads to a better understanding of the tradeoffs, the performance with the two fuels will be compared. Since the throat temperature of the MMH-fueled thruster is low, any changes made to the thruster can be oriented solely to improving the specific impulse. The hydrazine thruster, on the other hand, will be operating at higher than the maximum target temperature. Therefore, modifications must first be made which reduce chamber temperature. Since this will penalize specific impulse, additional changes will be required to recover performance.

### Concept of Development Risk

In the following sections statements regarding "development risk" will appear. The concept of development risk will be based upon the following hypothesis: Virtually any solution to a problem, even a very difficult one, provided it is physically permissible, can be carried through to a physically realizable design if a sufficiently large amount of money is appropriated and an indefinite amount of development time is allowed. If the budget of time and money is limited, then whether or not the design is realizable becomes uncertain. The greater the limitation, the greater the uncertainty.

Experience with complex projects substantially supports this hypothesis. It is to be noted that the hypothesis does not state that it is proper, economical, or practical to allow excessive budgets for development.

Development risk thereby is related to the time and money required to achieve a physically realizable objective and the magnitude of the risk depends upon the amount of favorable (or unfavorable) evidence that exists at the present time. The amount of risk involved in making a change in the thruster for the purpose of changing the specific impulse and/or

ORIGINAL PAGE IS  
OF POOR QUALITY

chamber temperature will be assumed to be related to the amount of experimental data which documents or supports the analytical predictions for the change. If experimental data exist which document the effect of a specified change, then that approach is said to have a low risk for achieving the goal. If no experimental documentation exists for a given change or approach that approach is said to have undetermined but higher risk. Finally, if experimental data contradict the analytical predictions or disclose other detrimental effects for a specific thruster modification, that modification is said to have a high development risk.

The applicable experimental data which have been obtained at Marquardt can now be examined to provide both a qualitative insight into the risks and a quantitative measure of the effects of certain design variables upon performance.

#### Effect of Chamber Length

Figure 22 presents data obtained from tests of an early shuttle configuration where the chamber length could be easily changed. Additional experimental data obtained later in the development program when the chamber length was changed from the original 3-inch length to the 2.5-inch length substantiate the early data. The incremental change of specific impulse are shown as a function of length using the present chamber length of 2.5 inches as a zero reference. Specific impulse can be improved or degraded by six seconds for small changes in combustion chamber length. Also shown are measured throat temperatures as a function of chamber length.

#### Effect of Injector Double Offset

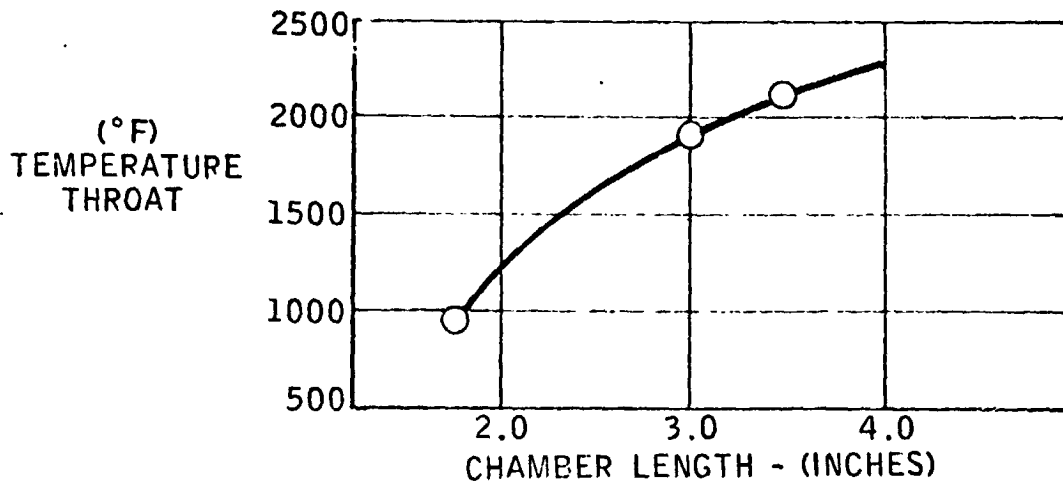
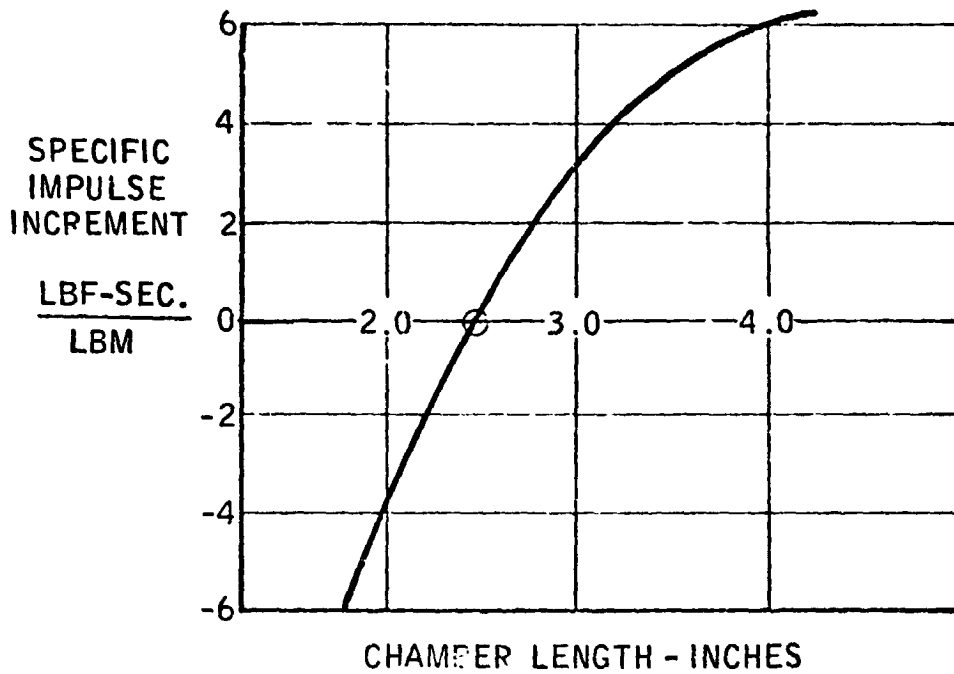
The shuttle thruster uses a single ring of unlike doublet elements (i.e., fuel jets impinge upon oxidizer jets). These doublet elements are closely spaced around the ring and considerable splashing and beneficial interaction occurs between adjacent doublets. For single doublets (without interference from other doublets), experimental investigations have revealed that the optimum mixing and performance is obtained when the centerlines of the two impinging liquid jets are exactly lined up with each other (i.e., intersect with each other). This is called zero offset of the doublet centerlines. When the centerline offset is made increasingly larger than zero, the performance of the single doublet injector slowly degrades (Ref. 6).

Experimental data obtained with the closely-spaced doublets on the shuttle thruster indicate that performance is improved when the doublets are offset sufficiently. Figure 23 shows that offset initially makes no change in performance. When the doublet offset exceeds 0.006 inch, the thruster performance begins to improve and continues to improve over a wide range of offset. This improvement can be attributed to a gradual tilting of the propellant fans. When the fans tilt beyond a certain angle, they begin to overlap each other in a manner which improves secondary mixing.

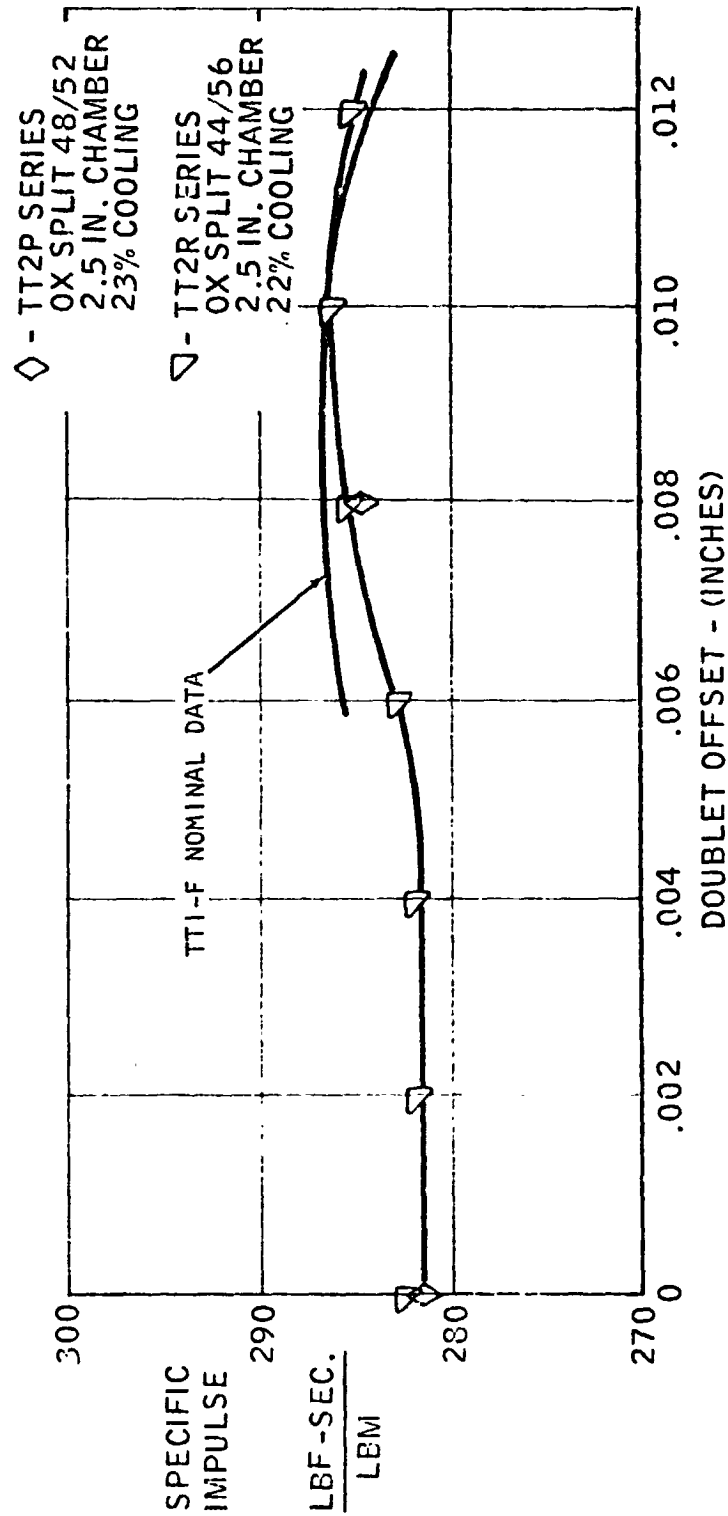
Specific impulse improvements between four to five seconds were achieved over a fairly wide range of offset for three slightly different test configurations during the program to optimize the shuttle injector. Little or no change of throat temperature was observed during these tests.

# EFFECT OF CHAMBER LENGTH UPON SPECIFIC IMPULSE

## SSRCS THRUSTER-MMH/ $N_2O_4$



# EFFECT OF DOUBLET OFFSET



### Interactions Between Film Cooling and Performance

Experimental data on the effect of film cooling upon specific impulse has been obtained only over a relatively narrow range of cooling percentages. The observed magnitude of the specific impulse change for a small film cooling change is close to the instrumentation accuracy and a relatively large data scatter was evident. As a result, reliance is placed primarily upon the analytical predictions rather than experimental data.

The film cooling model considers that a portion of the film cooling which splashes on the chamber wall moves back toward the face of the injector and, thereby, cools that region of the chamber. This was a specific design goal for the film cooling configuration. It also considers that additional liquid is lost from the film cooling which moves toward the throat. This latter loss is due to instabilities in the liquid film that cause waves to form. These waves break up into droplets that leave the liquid film. What happens to the liquid cooling flow that is "lost" from the cooling film? The SSRCS Thruster design, with its outward and inward momentum angles, induces re-circulation eddies within the thruster which encourage mixing of the "lost" coolant with the outer zone flow. In addition, a portion of the vaporized coolant can mix with the core flow but the amount of mixing depends upon the length of the mixing distance (i.e., how soon the liquid film is vaporized).

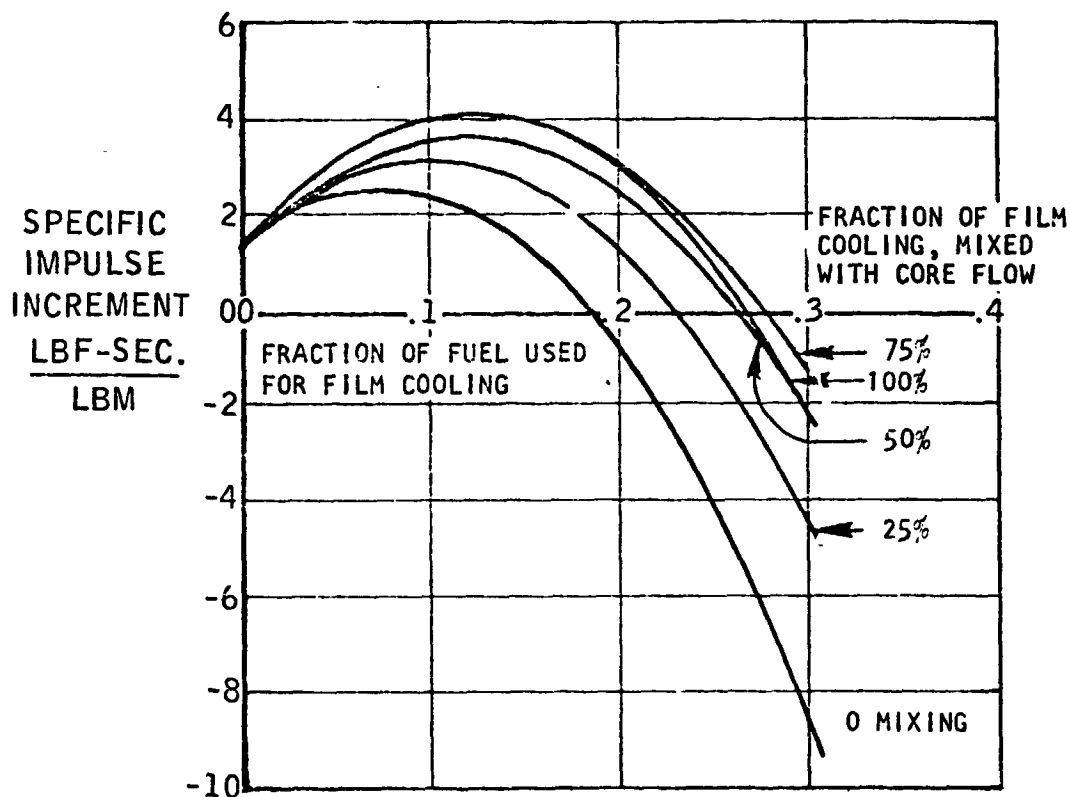
The MMH-fueled thruster with the liquid film extending to the throat of the nozzle (2.3-inch liquid length) is expected to have less vapor mixing than the hydrazine thruster, which is predicted in Section 4 to have a liquid length of only 0.85 inch. Therefore, hydrazine vapor and droplets which are generated at the beginning of the chamber have a greater chance of mixing with both the core flow and its recirculation eddies.

To evaluate the effect of mixing with the outer zone core flow, the thruster performance analysis equations were modified to include a mixing factor. As indicated by Figure 10, the original performance analysis procedure considered three completely independent zones - the inner combustion core, the outer combustion zone, and the film cooling zone - which did not mix with each other. For the revised analysis, the hypothesis is made that some mixing occurs between the film cooling zone and the outer combustion zone. The mixing factor is the fraction of the film cooling which mixes with the outer combustion zone. The fraction which mixes with the combustion zone increases the mass flow and reduces the mixture ratio (O/F) of that zone. The film cooling zone mass flow is reduced. The change in thruster specific impulse due to these changes in mass and mixture ratio distribution is calculated to define the effect of the coolant mixing.

The percentage of fuel used for film cooling affects the thruster performance, since the momentum angles, Rupe number, contact time ( $D/V$ ), and zone mixture ratios change as the film cooling percentage changes. Figures 24 and 25 show the predicted effect of mixing upon the specific impulse of the MMH and hydrazine thrusters. The independent variables are the amount of coolant flow and the degree of mixing. A number of observations can be made from the computed results. One unexpected result is that reduction of coolant flow below about 12% of the total flow does not result in increased thruster performance for this

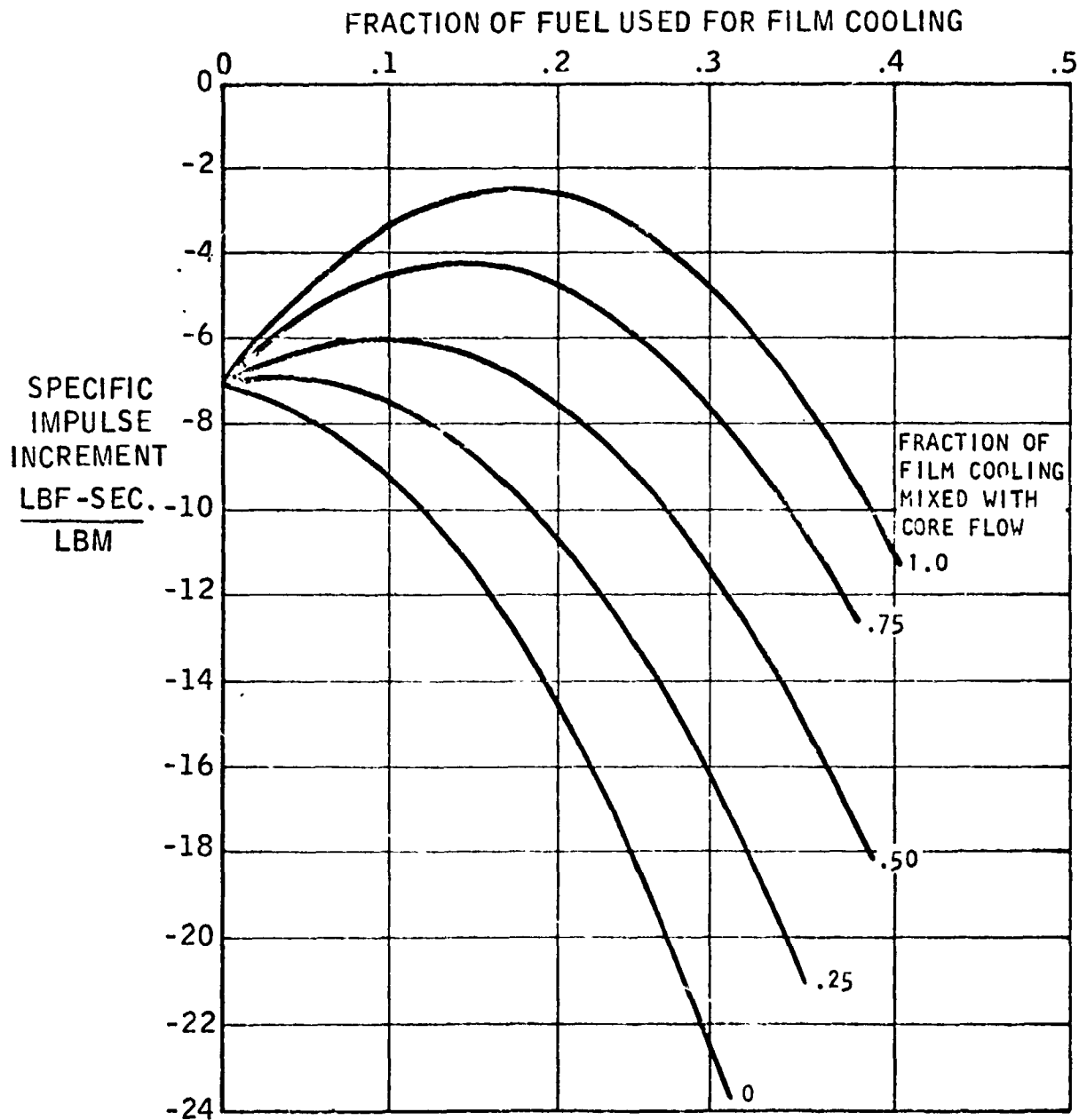
# PREDICTED EFFECT OF FILM COOLING FOR DIFFERENT AMOUNTS OF MIXING WITH THE CORE FLOW

MMH/N<sub>2</sub>O<sub>4</sub>



ORIGINAL PAGE IS  
OF POOR QUALITY

# EFFECT OF FILM COOLING AND ITS MIXING WITH THE CORE FLOW $N_2 H_4 / N_2 O_4$





injector design. Any further reduction of coolant flow adversely affects the outer and inner zone performance parameters of the doublets and, thereby, reduces performance more than the reduction of coolant flow improves it. A further observation for the MMH thruster is that improved mixing between the coolant zone and the outer combustion zone first acts to improve performance, but when mixing exceeds 50% no further improvement occurs.

Analytical predictions for the hydrazine thruster show some differences. The performance is more strongly affected by both the amount of film cooling and the degree of mixing with the outer zone flow. For this injector design, performance continues to increase as the mixing factor is increased.

The question of how much mixing between the coolant and combustion zones occurs in each thruster must still be answered. Limited experimental data, when the amount of film cooling was varied, indicates that 25% mixing curve matches the data for the MMH thrusters (i.e., the experimental change in specific impulse corresponds to that predicted for 25% mixing factor over the limited range of film coolant flow tested). Since increased mixing is expected in the hydrazine thruster due to its three times faster evaporation rate, a 50% mixing factor was arbitrarily assumed for it for the performance calculation.

### Nozzle Performance

The emphasis on the original Shuttle procurement was minimum weight and small envelope, along with reasonable good performance levels. Since high premium was put on the first two items, the 22:1 exhaust nozzle bell was made very short (65% of an optimum Rao nozzle contour). Experimental data indicated that increasing nozzle length by 1 or more inches will provide a positive specific impulse increment of two or more seconds. Throat temperatures remain unchanged.

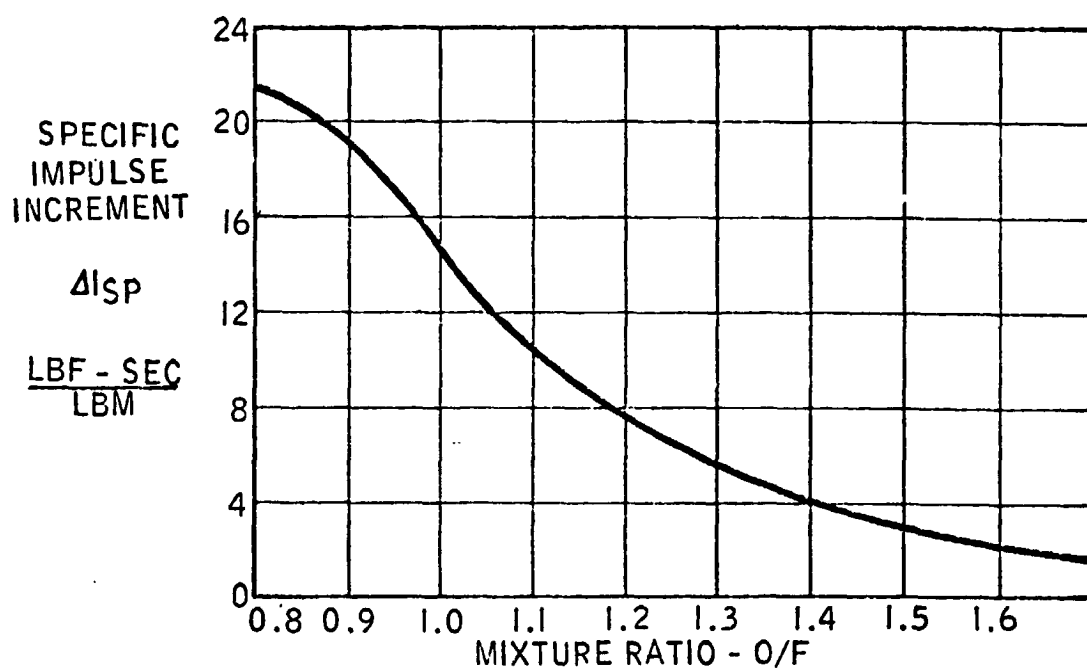
### Optimizing the Injector

According to the performance analysis model, the shuttle injector configuration is not the optimum configuration for MMH; that is to say, the Rupe number, the contact time, the local mixture ratios, and the momentum angle are not at their optimum values at the design operating point. An improvement of approximately four seconds of specific impulse is predicted if the injector were to be "optimized" (with a corresponding increase in throat temperature of 50°F).

For the hydrazine-fueled thruster, similar improvements can be obtained. Figure 26 shows the difference in performance between the present shuttle thruster (Configuration A) and a thruster with the injector optimized at each mixture ratio. At an O/F of 1.4, approximately four seconds' improvement is predicted. Significantly larger improvements are possible at lower mixture ratios. The achievement of these performance improvements requires modification of the propellant injection angles, orifice diameters, propellant velocities, and propellant distribution between inner and outer combustion zones. In particular, the changes of the momentum angles of both inner and outer zones provide the major portion of the performance improvement.

# OPTIMIZED HYDRAZINE INJECTOR

## Improvement Of Performance Relative To Configuration A



During the early phases of the Shuttle program, optimization experiments were made. At that point in time, the analytical performance analysis methods had not been completed and, therefore, the modifications were based upon existing knowledge and were limited by manufacturing and time constraints. Changes were made of doublet orifice diameters and of the inner combustion zone momentum angle. Over the range of orifice diameters tested, little or no significant change (relative to measurement accuracy) in specific impulse was found. Subsequent analysis substantiated that the specific impulse is not sensitive to changes in either fuel or oxidizer orifice diameter.

In another portion of the optimization program, the resultant momentum angle of the inner combustion zone was changed nine degrees further inward. As predicted (later) from momentum angle considerations, a decrease of specific impulse was noted (four seconds). At the same time, however, a large reduction of throat temperature was measured at high off-design mixture ratios. No measurable temperature change was observed at low or moderate mixture ratios. Returning the momentum angle to its original outward position caused a return to the higher specific impulse and the higher chamber throat temperatures at high mixture ratios shown in Figure 7. The experiment verified the importance of momentum angle upon performance. The higher performance configuration was selected since throat temperatures were still within target levels and very large safety margins existed for the columbium material.

Since the performance optimization discussed above would require still further outward rotation of the inner zone momentum angle, a further increase of wall temperature is implied. Experimental data, therefore, exist which indicate that inner momentum angle changes which are beneficial to specific impulse are, at the same time, detrimental to chamber temperatures. In terms of developmental risk, momentum angle modifications for optimization of specific impulse offers a high development risk due to the experimental evidence of an important negative effect upon wall temperatures.

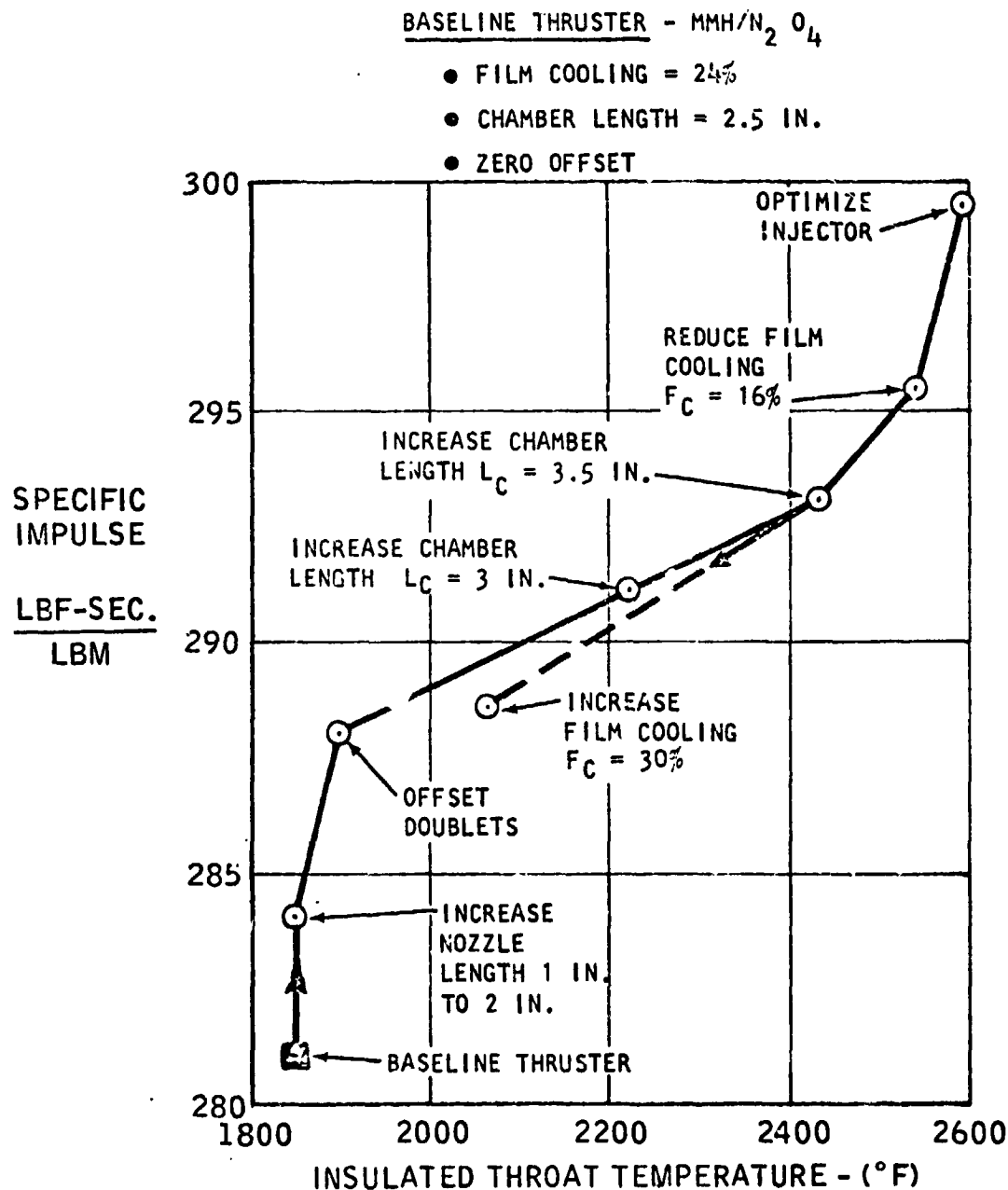
Our understanding of the reason for the contrary interaction is presently incomplete. The existing analytical film cooling model cannot account for momentum angle effect upon cooling and temperature at the present time.

Since the dominant factor in optimizing the injector performance is found to be the momentum angle (rather than contact time, Rupe number, or zone O/F ratio), a rating of "high risk" relative to development cost and time must be assigned to any changes that affect this injector momentum angle.

### MMH Thruster

Figure 27 illustrates the type of performance improvements which can be made for the MMH-fueled SS RCS thruster and indicates the effect of these improvements upon thruster throat temperature. The particular sequence of improvements were selected according to increasing developmental risk and cost. The first improvement - an increase in exhaust nozzle length - is an experimentally verified improvement which also imposes no penalty in chamber temperatures. The second least risk improvement is the use of offset doublets. Here, a small increase in chamber wall temperature occurs due to the

# SSRCS THRUSTER - PERFORMANCE AND TEMPERATURE TRADEOFFS



ORIGINAL PAGE IS  
OF POOR QUALITY

increase in core temperature. Further improvements can be made by increasing the combustion chamber length and reducing film cooling. Both of these produce significant increases in wall temperature. The performance improvements here are also based upon experimental data and, therefore, the risk is relatively small. The highest risk approach - optimizing the injector - would produce a relatively large gain in performance without much further change in throat temperature at the design point. However, as discussed earlier, it would involve changes in the injector momentum angle which were found to cause significant increase in chamber temperature at high off-design mixtures (see Figure 7).

It must be emphasized that these performance-temperature tradeoffs are presented without considering the constraints imposed by the present Shuttle requirements for safety margin, envelope, and costs. Furthermore, the tradeoffs illustrated are aimed primarily at performance improvement, with some penalty in chamber temperature margin. For instance, the film cooling could be used to decrease the wall temperatures. In this event, performance would be decreased as shown by the dashed line.

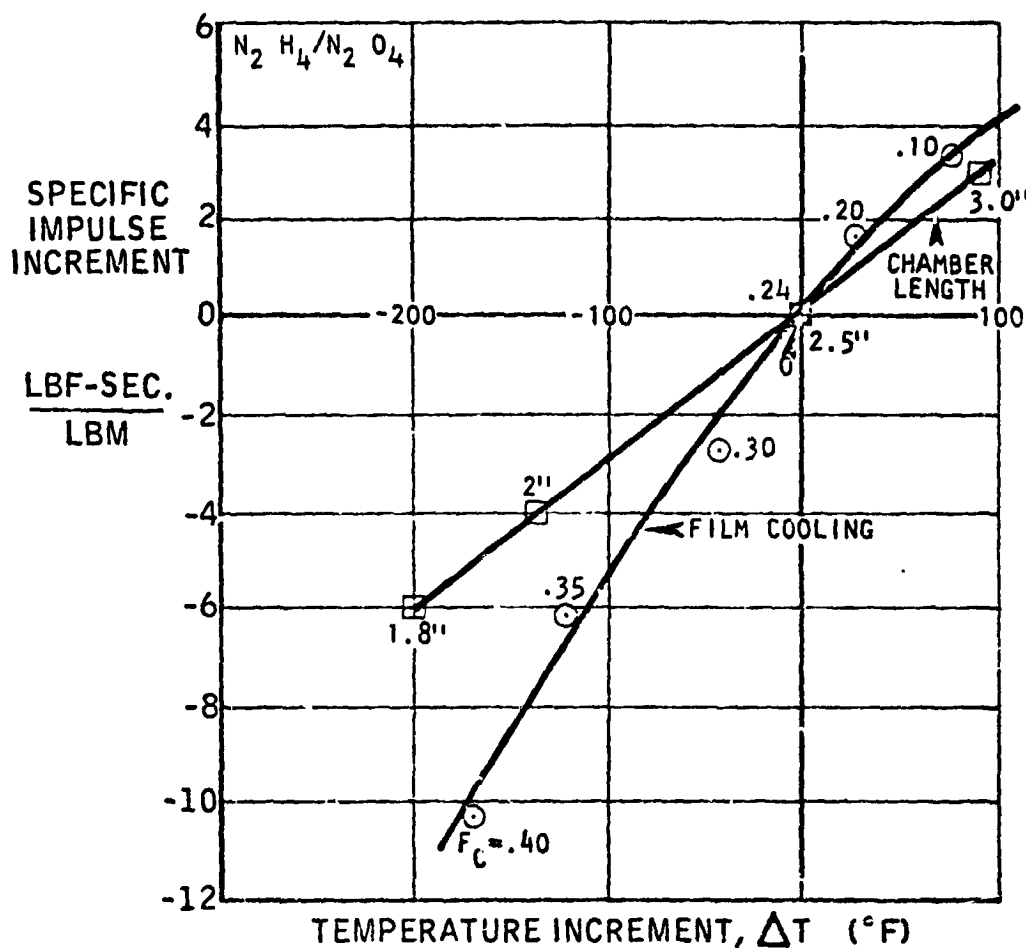
It is clear from Figure 27 that increasing the film cooling to cool a 3.5-inch chamber is a poor choice since this reduces the specific impulse more than changing the chamber length does. Instead, a small increase in chamber length (say 2.75-inch from 2.5) while keeping the 24% film cooling would be the better way of increasing performance if, for instance, the wall temperature of 2060° F was desired.

Figure 27, therefore, illustrates a few of the many combinations of changes that can be made in specific impulse and throat temperature. By appropriate combinations of the suggested modifications, the thruster can be tailored to provide arbitrarily specified values of both specific impulse and wall temperatures (within certain limits). Each specification would have different weights, costs, and risks associated with its achievement.

### Hydrazine Thruster

Since the use of hydrazine as the fuel is predicted to result in throat temperatures higher than the re-entry temperatures, the emphasis for a hypothetical Configuration B should be to reduce throat temperatures without sacrificing performance. The throat temperature can be reduced by reducing chamber length and by increasing the film cooling. Figure 28 shows the relative tradeoffs between specific impulse and throat temperature for the two approaches. These curves were derived from the analytical film cooling model and the analytical and experimental performance data. Like the MMH thruster, a small reduction of chamber length is predicted to produce a smaller loss in specific impulse for a given reduction of throat temperature than will be produced by an increase of the film cooling. This conclusion is somewhat disappointing because an increase in the diameter of the film cooling orifices was originally visualized as a less costly and less difficult modification of the MMH thruster than reducing the length of the combustion chamber. Using these and prior predictions, we can now begin to create Configuration B.

# PERFORMANCE - TEMPERATURE TRADEOFF FOR CHAMBER LENGTH AND FILM COOLING



In evaluating the developmental risk, the assumption is made that, due to the propellant similarities, the experimental data obtained from the MMH tests can be carried over to the hydrazine thruster.

Figure 29 illustrates two of the many possible modification paths that Configuration B could follow. Both start from Configuration A at  $I_{sp} = 281$  seconds and  $T = 2310^\circ\text{F}$  (the baseline Shuttle thruster). For this analysis, attention will be paid to the Shuttle dimensional constraints. Chamber or nozzle lengths are not changed unless other dimensional changes will compensate.

One path is an attempt to meet both the Shuttle specific impulse and the original Shuttle throat temperature targets ( $2100^\circ\text{F}$ ). Shortening the combustion chamber is more effective for reducing wall temperatures with less penalty in specific impulse. Reducing the chamber length from 2.5 inches to 1.8 inches brings the throat temperature down to  $2100^\circ\text{F}$  with an attendant reduction of specific impulse. The nozzle length can be increased the same amount the chamber was shortened, thereby recovering some of the lost performance. Offsetting the injector doublets raises the performance to the target specific impulse with only a small penalty in temperature. Finally, a further improvement can be made by optimization of the injector with only a small increase of temperature. This version of Configuration B now provides superior specific impulse than either Configuration A or the MMH-fueled thruster with a throat temperature less than that due to re-entry heating but higher than the original shuttle target of  $2100^\circ\text{F}$ .

The second path shown in Figure 29 is one which only considers performance improvement. Offsetting the injector doublets and optimizing the injector provides increases in specific impulse with minimal increase upon throat temperature. Throat temperatures are above target and re-entry values. The hydrazine thruster appears to be destined by the high film coolant decomposition temperatures to operate at higher temperatures than the MMH thruster. Relatively drastic thruster changes are required to effect small reduction of temperature. However, as illustrated in Figure 5, rather large temperature safety margins exist even at these temperatures.

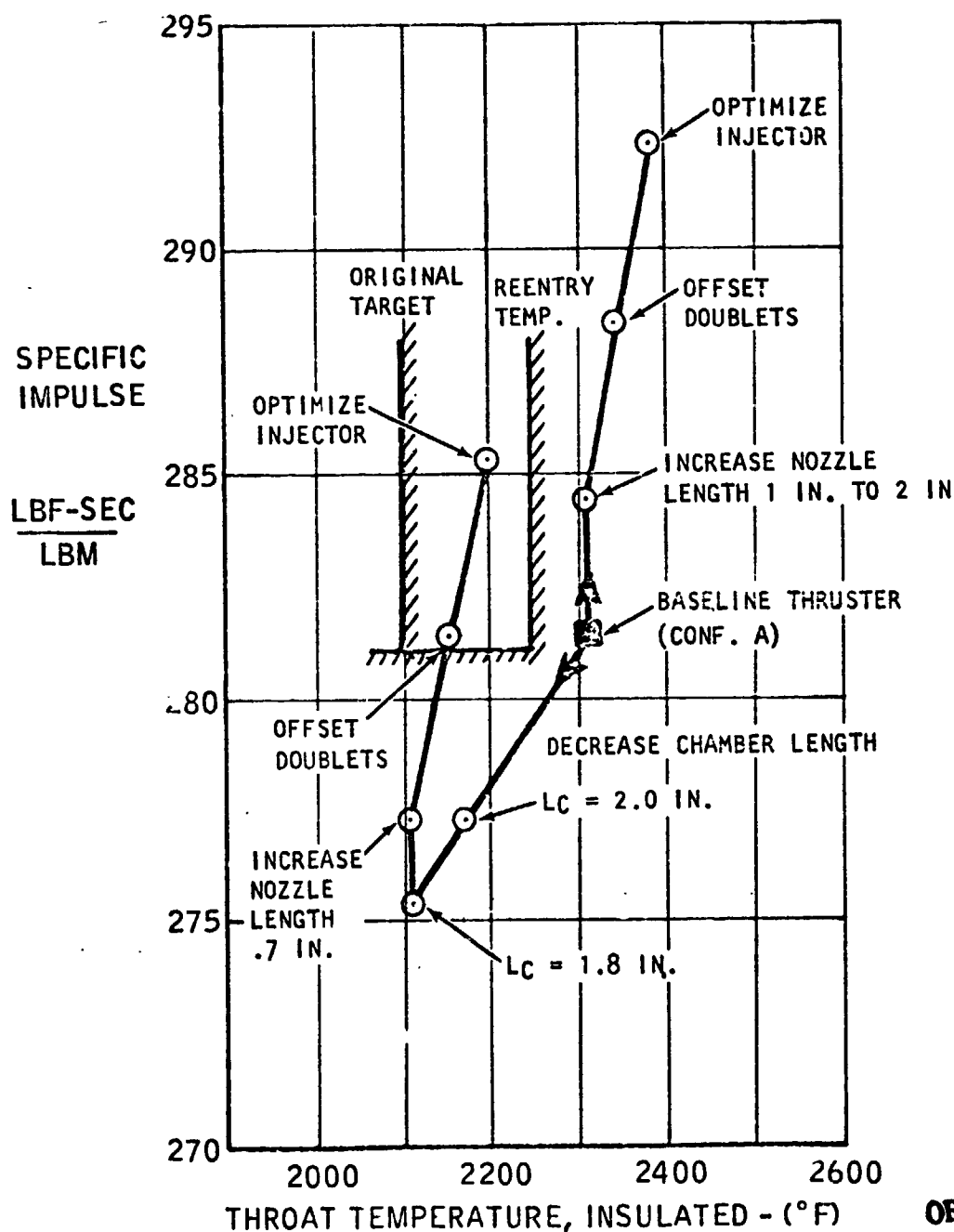
In conclusion, the objective of providing a hydrazine thruster with the same specific impulse as the MMH fueled thruster and a maximum throat temperature no greater than  $2250^\circ\text{F}$  can be achieved by a "Configuration B" thruster. It consists of the same injector as the MMH thruster but with offset doublets, a 1.8-inch chamber, and a longer nozzle to achieve the same overall installation dimensions. These proposed changes constitute "low risk" modifications based upon the experimental data with the MMH thruster. Further improvement in specific impulse, with little change in throat temperature, is possible for an "optimized" injector but at a greatly increased development risk.

# HYDRAZINE THRUSTER - CONFIGURATION B PERFORMANCE AND TEMPERATURE TRADEOFFS

BASELINE THRUSTER - CONF. A

FILM COOLING = 24%, CHAMBER LENGTH = 2.5 IN.

ZERO DOUBLET OFFSET, NOZZLE = 22:1



ORIGINAL PAGE IS  
OF POOR QUALITY



## VII. PULSE MODE OPERATION AND COMBUSTION STABILITY CONSIDERATIONS

The study has, so far, only examined steady state operation of the hydrazine thruster. Since the shuttle SSRCS rocket is used for maneuvering control of the shuttle vehicle, it is required to provide thrust pulses as short as 40 milliseconds in duration. Pulsing rockets have special problems related to the pulse mode operation and additional criteria must be satisfied to assure safe and reliable pulsing mode operation. Pulse engine operation in near space causes some unusual mass and heat transport effects which can lead to damaging explosions within the propulsion unit unless they are considered in the design phase. Four interrelated explosive events have been documented in past development programs. They have been identified as: (1) ZOTS, (2) condensed phase explosions, (3) vapor phase detonations, and (4) transducer cavity explosions. Each is generated by different combinations of the unique mass and thermal transport mechanisms inherent to pulsing thrusters. During the repeated pressurization and evacuation of the combustion chamber and injector in a low pressure environment, the pulsing engine is able to transport or store explosive materials in various portions or cavities of the thruster. All of the explosive events occur upon ignition of the rocket, but the explosive material is usually deposited from the previous pulse or pulses. A brief definition of terms is first given and then followed by a detailed discussion.

### Vapor Phase Detonations

Vapor phase detonations can occur due to the accumulation of the unburned combustible propellants during the period of time required to cause an ignition reaction between the vaporized hypergolic propellants at low ambient pressures. Vapor phase detonations are usually not damaging to the pulsing thruster because the magnitude is relatively small.

### Condensed Phase Explosions

Under certain thruster pulsing or shutdown conditions, it is possible to accumulate condensed propellant in combustion chamber of the thruster either in liquid or solid form due to condensation or freezing of fuel residues upon cold chamber walls. If the thruster is reignited with condensed propellant in it, very large and potentially damaging explosions can occur in the combustion chamber. During such an ignition, both a vapor phase detonation and an explosion of the condensed phase occur.

## Oxidizer Manifold Explosions (ZOTS)

A ZOT is essentially a condensed phase explosion which occurs within the oxidizer manifold. The transport mechanism that carries the fuel into the oxidizer manifold is more complex than for the condensed phase chamber explosion. But it, too, requires a surface cold enough to cause condensation of the fuel at the low chamber pressures that exist in near space during and after shutdown portion of the rocket pulse.

## Transducer Explosions

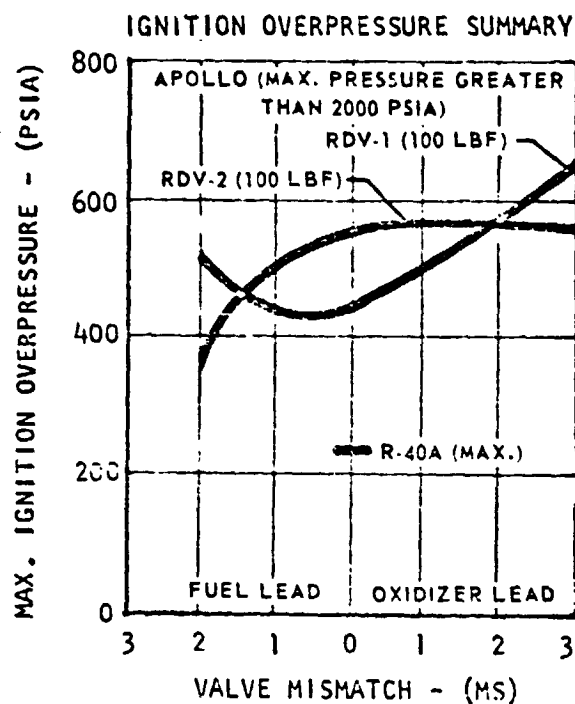
During the ignition transient, gaseous, liquid and solid forms of combustible and explosive preignition materials from the thrust chamber are pumped into the transducer cavity which had previously been at vacuum conditions. While the amount of materials entering the cavity upon each ignition is small, they condense in the cool transducer and continue to accumulate for hundreds or thousands of ignition pulses. Finally the deposits are exploded by thermal energy carried into the transducer during a long series of pulses or by a chance detonation wave caused by ignition of the rocket. The explosion can cause a malfunction of transducer sensing element.

A common feature of these explosive events is that temperature and pressure differences from one part of the thruster to another cause condensation of fuel or reaction products and provide a driving force for transporting the fuel. Another common feature is that the process is time dependent. Explosions only occur for certain pulse duty cycles and not for others. The switch from one fuel to another has important effects upon these occurrences because the freezing points, vapor pressure, and explosive characteristics of each fuel are different. Having provided some insight into the different kinds of explosive events, estimates of the effects of switching to hydrazine will be made.

## Vapor Phase Detonations

The vapor phase detonation results from the ignition of a chamber full of a detonable mixture of fuel and oxidizer vapor (including suspended liquid or solid droplets).

Before ignition, the thrust chamber is at a pressure less than the vapor pressure of both propellants. Thus, both flash into liquid, solids, and gas as they enter the chamber. The hypergolic ignition reactions occur slowly in the cold propellant vapor produced by the expansion to low pressures. By the time ignition occurs, enough propellant has entered the chamber to produce detonation pressures ranging as high as 600 psi in some thrusters. A substantial amount of documentation has been obtained on the characteristics of these vapor phase detonations. Figure 30 shows the maximum ignition overpressures measured for the vapor phase detonations in a number of Marquardt 100-lbf thrusters which operate at 100-150 psi steady state chamber pressures. These thrusters use solenoid operated valves which pass full propellant flow prior to ignition. The vapor phase detonations are



normal occurrences for pulse rockets because their fast acting valves permit large amounts of propellant to enter the combustion chamber during the ignition delay time period. No case of engine damage from this type of ignition spike has ever been observed at Marquardt. The shuttle 873-lbf thruster uses a pilot-operated (two-stage) valve and exhibits significantly lower vapor phase detonations because ignition occurs on pilot valve flow prior to the establishment of full flow from the main valve stage. The vapor phase ignition overpressure rarely exceeds design operational pressures (150 psia). Maximum ignition pressure of 250 psi (Figure 30) have been measured for MMH.

When the propellant is changed from MMH to  $N_2H_4$ , higher ignition detonation pressures are expected because hydrazine, with its lower vapor pressure and higher freezing point, produces larger amounts of liquid and solid hydrazine in the chamber prior to ignition. However, the vapor phase detonations still will not cause damage. It is the condensed phase explosions, ZOTS, and transducer explosions which may cause problems.

#### Condensed Phase Explosions

During the engine shutdown, the fuel is the last propellant to drain from its manifold from the dribble volume because its vapor pressure is lower than that of the oxidizer. A layer of fuel may freeze or remain on the chamber walls if the wall temperature is sufficiently low. As the pressure in the chamber decays to zero or to the ambient pressure, the material on the wall begins to evaporate (or sublime). Depending upon the off-time between pulses, this fuel may completely evaporate before the next pulse. This is a function of the temperature of the chamber wall, the ambient pressure, and the off-time between pulses.

The condensed phase explosion type spike has entirely different characteristics. It consists of an explosion which consumes frozen or liquid propellant on the wall of the chamber. When an explosion takes place in this frozen material, very high local pressures can be exerted on the chamber wall which is directly adjacent. These pressures can damage engines since it is analogous to exploding a plastic explosive on a wall. For this phenomenon to occur, a mechanism must exist for depositing this explosive material on the wall of the chamber. Study of this problem has revealed that the explosive material is frozen, or liquid fuel left from the preceding pulse which has subsequently been sensitized (made explosive) by the addition of oxidizer. If this frozen fuel is on the wall and an oxidizer is present in the preignition gases, the resulting compounds are explosive. The subsequent ignition of vapors in the chamber then triggers a high pressure explosion in the material on the chamber wall.

If the propellant valves are opened for the next pulse before all of the residual fuel evaporates, the fuel on the walls can explosively ignite and induce high local stresses in the chamber walls. In early Apollo 100-pound force thrusters, ignition pressures greater than 2000 psia were observed. Bursting of the brittle Molybdenum chambers would occasionally occur. This led to a program which showed that large ignition overpressures could be avoided by temperature control and engine design techniques (minimum dribble volume) that prevent accumulation of residual materials in the combustion chamber after shutdown.

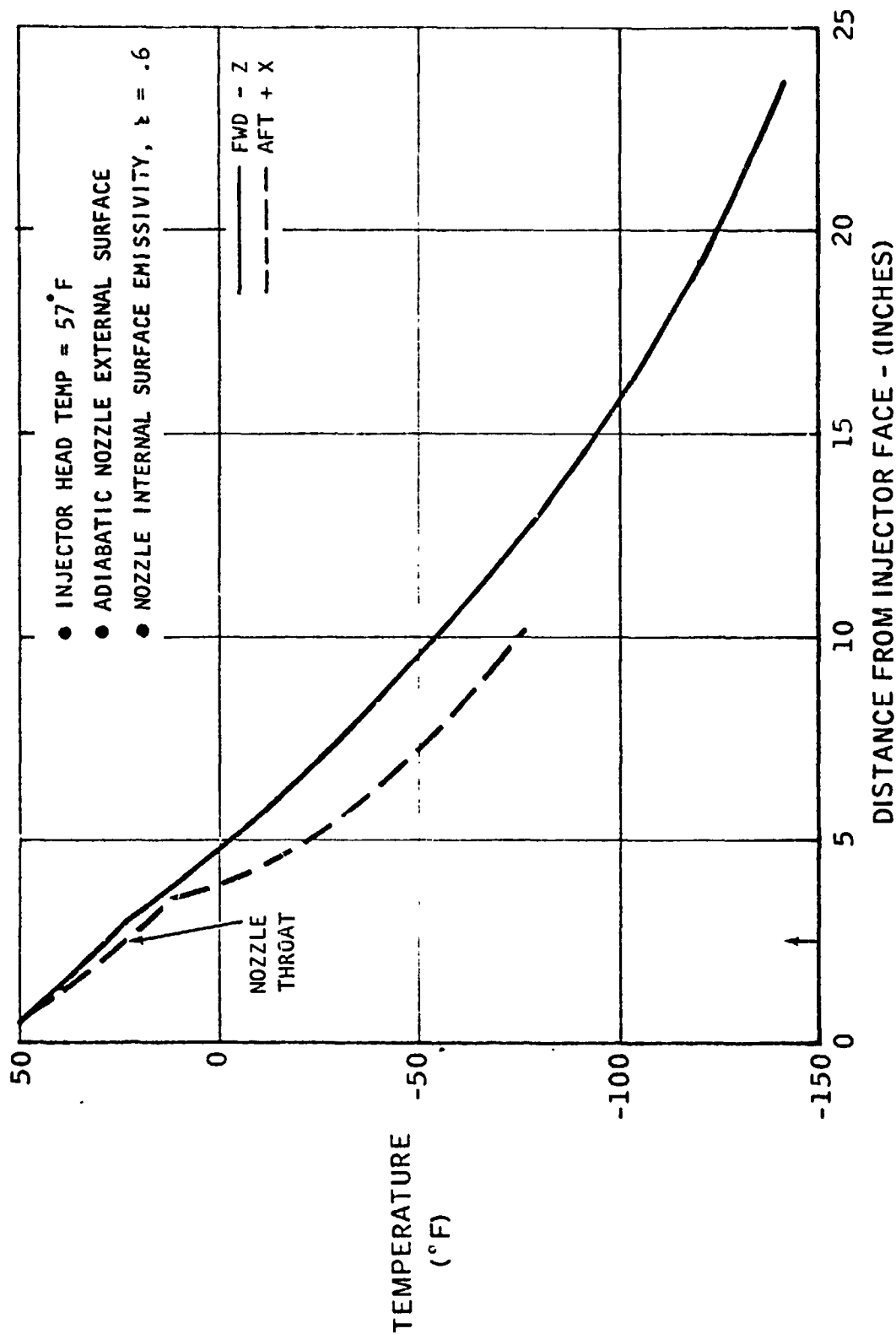
The Columbiun (C-103) used for the chamber walls is a ductile material that is designed to absorb these explosions. The injector head dribble volume is small, thereby reducing the amount of fuel which can enter the chamber after the valve closes. However, to insure long chamber life, the Shuttle thruster head and chamber are heated to encourage rapid evaporation and to avoid freezing or condensation of propellants. This prevents the condensed phase explosions from occurring.

The freezing point of hydrazine is 34.7° F compared to -62.5° F for MMH. To avoid condensed phase explosions, the temperature of the combustion chamber and head must at least be higher than the freezing temperature of the fuel. It must also be warm enough to cause rapid evaporation of the liquid fuel spilling into the chamber. Figure 31 can be examined to obtain an approximate idea for the amount of head and chamber heating required to avoid freezing of the hydrazine. It shows the temperature gradient along the inside of the insulated thruster when it is not firing and is exposed to (looking at) the cold space environment. When the heater produces an injector head temperature of 57° F, Figure 31 shows that the chamber wall temperature at the throat station can drop as low as 24° F (or 10° F below the freezing point of hydrazine). To raise that temperature to at least the freezing point requires that the head temperature be at least 67° F. If a 20° F margin is assumed necessary to provide some safety margin, the head temperature required to avoid severe condensed phase spikes due to freezing approaches 90° F.

Experimental data with MMH (Ref. 7) indicate that a failure of Apollo Molybdenum chambers occurred when nozzle bell temperature (measured at a position equivalent to Station 3 in Figure 31) was chilled to 10° F and no failures occurred when the temperature was 20° F. The bell temperature had to be 70-80° F warmer than the -63° F freezing point of the MMH to avoid an occasional large condensed phase explosion capable of shattering a Molybdenum chamber.

Test data were also obtained with A-50 (50% hydrazine, 50% UDMH). Shattering of the chamber occurred at bell temperatures of 50° F (i. e., 15° F warmer than the 35° F freeze point of the hydrazine component). No experimental data were obtained at higher temperatures with the hydrazine/UDMH fuel. If the same margin is required for hydrazine as for MMH, a bell temperature of about 104-114° F would be indicated. However, one possible interpretation of test data of Reference 7 indicates that a bell temperature of 60° F would have avoided large condensed phase explosion (i. e., 25° F warmer than the freezing point of hydrazine).

# AFT X AND FWD - Z COLD SOAK TEMPERATURE



The experimental data is not conclusive due to the use of A-50 rather than hydrazine, but it does clearly suggest that an additional temperature margin of 40-105°F is required to provide equivalent protection from condensed phase explosions.

As mentioned earlier, both the relatively smaller propellant manifold volumes and the ductile Columbian chamber material of the shuttle thruster significantly increase the safety margin for condensed phase explosions, compared with the Apollo thruster. Therefore, the thermal conditioning requirements are less for the shuttle engine.

In summary, the investigation indicates that thermal conditioning of the hydrazine thruster be at least 40°F higher than the present 50-90°F range of the MMH thruster. Head temperatures of 90-130°F are indicated to provide an equivalent safety margin.

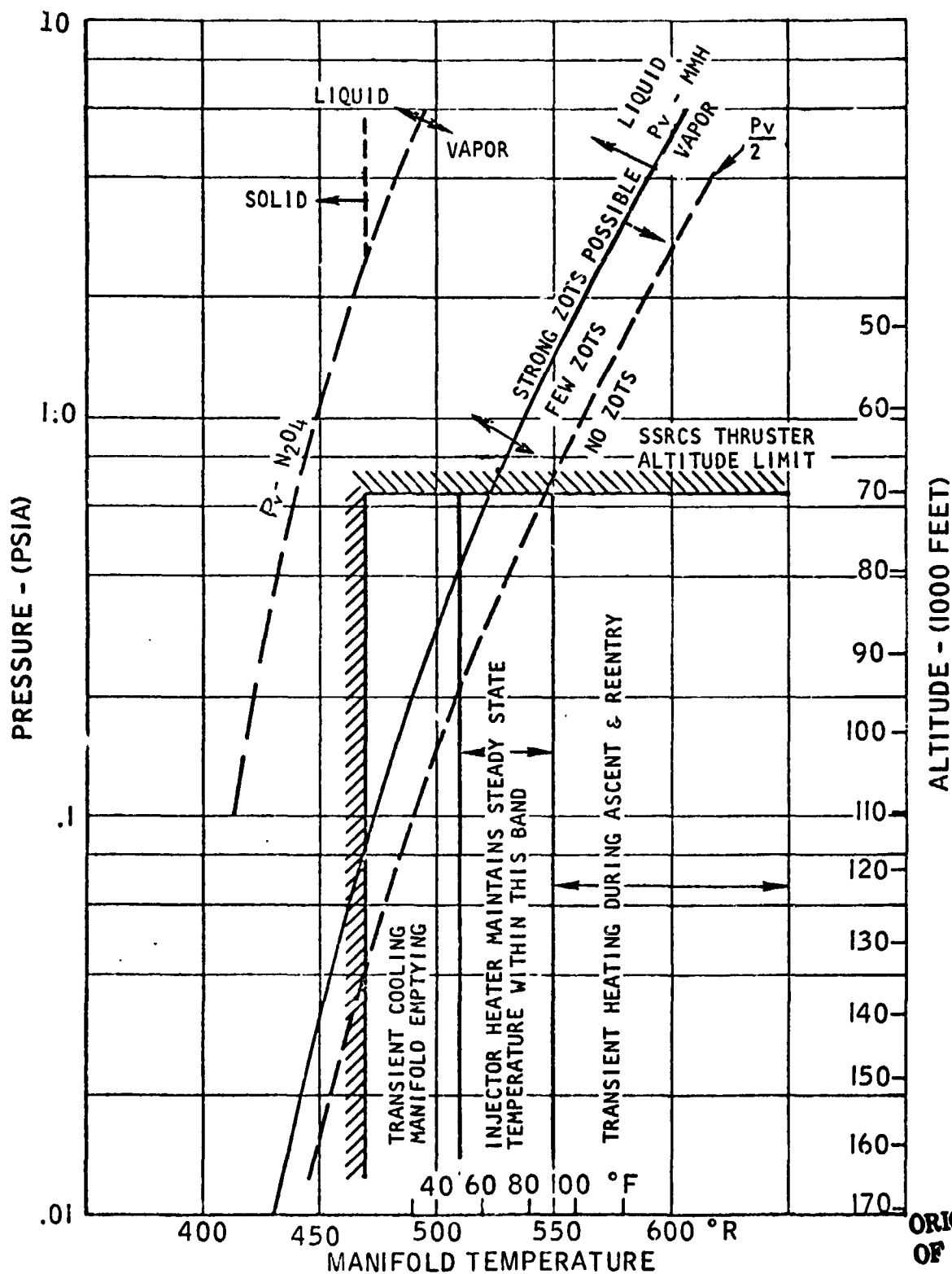
### ZOTS (Reference 8)

A ZOT is an explosion in the oxidizer manifold. After valve shutoff, the propellant manifolds empty at different rates. When the chamber pressure decays, the high vapor pressure oxidizer manifold empties first and then the low vapor pressure fuel manifold. When the oxidizer manifold is emptying, its temperature drops due to the evaporation of the nitrogen tetroxide at the low chamber pressures. Cooling of 50°F has been measured, and this chilling provides the mechanism for transporting fuel vapor into the oxidizer manifold. The fuel spilling into the warmer combustion chamber after a firing is vaporized, and this vapor enters the now empty oxidizer manifold where it condenses upon the cold surfaces. The condensation lowers the pressure, causing more vapor to enter the manifold. Condensation continues until the chamber empties or the manifold warms up enough to stop condensation. When the thruster is restarted, the reaction between the incoming oxidizer and the previously condensed fuel produces an explosion in the small volume of the oxidizer manifold. This can generate pressures as high as 20,000 psi (Apollo 100-lb thruster) and can cause damage to the Teflon seat in the valve.

The "ZOT Plot" for MMH shown in Figure 32 defines the flight regime region where ZOTs can occur. The heavy line is the vapor pressure line for MMH expressed as a function of pressure (altitude) and temperature. Strong ZOTs are possible above the vapor pressure line, and few occur below it. The shaded zone shows the region in which the thruster must operate.

The SSRCS is required to fire in the atmosphere at altitudes as low as 70,000 feet. When the atmospheric pressure in the chamber after shutdown exceeds the vapor pressure of the monomethylhydrazine, the vapor remains in the chamber for very long time-periods, and substantial amounts may condense in the chilled oxidizer manifold. Once in the oxidizer manifold, the condensed fuel does not re-evaporate easily when the ambient atmospheric pressure is greater than its vapor pressure. A ZOT occurs after the oxidizer valve opens. These explosions do not occur in space because the vaporized fuel escapes from the chamber so fast in a vacuum that little can condense in the manifold. If any did condense, it, too, would rapidly re-evaporate. The lower dashed line  $P_{\text{vapor}}/2$  represents the atmospheric pressure at which fuel vapor within the thruster reaches sonic velocity in the exhaust

# ZOT PLOT



ORIGINAL PAGE IS  
OF POOR QUALITY



nozzle. This line defines the altitude at which the evaporation efflux rate is the same as in space. The evaporation rate reaches a maximum at this condition, and the stay time of the fuel in the chamber is shortened enough to limit the amount of fuel which can condense in the oxidizer manifold.

The thruster operating temperature limits are more difficult to define. An electric heater on the injector head attempts to maintain the manifold temperature between 50°F to 90°F. However, after the thruster firing is terminated, portions of the oxidizer manifold can be chilled as much as 40°F below the minimum regulated bulk temperature of the head for certain periods of time due to the evaporation of the residual oxidizer. This transient cooling to 470°F defines a potential low temperature limit of 470°R. Examination of Figure 32 indicates that strong ZOTs are possible if the thruster is fired between 70,000 to 120,000 feet altitude.

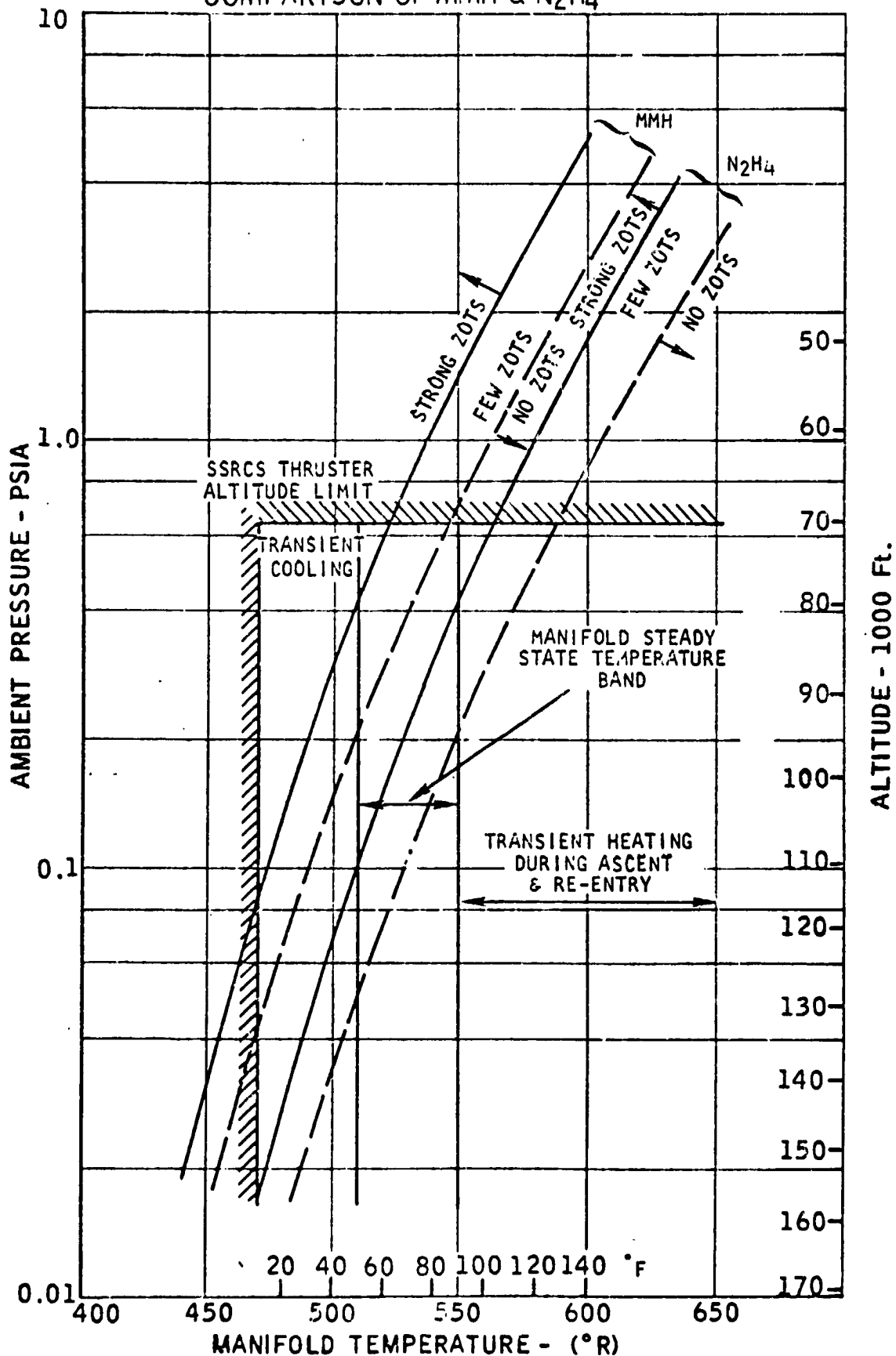
However, ZOTs are not expected to occur during the possible re-entry maneuvers due to aerodynamic re-entry heating. Re-entry heating is especially severe in the forward thrusters and substantial for the aft engines. The manifold temperature of re-entry maneuvers at 70,000 feet depend upon the amount of prior firing time. Typically, they are calculated to range from 90°F to 300°F. The cooler temperatures are a result of prior engine firings where the propellant flow serves to cool the re-entry heated thruster. At these temperatures, Figure 32 indicates that the MMH-fueled thruster will not be subject to damaging ZOTs.

Figure 33 illustrates the change in the flight regimes when the fuel is changed from MMH to hydrazine. Due to the lower vapor pressure of hydrazine, the ZOT region has been moved approximately 42 degrees to the right side of the figure. ZOTs can occur over a larger portion of the present shuttle operating region.

To provide an equivalent ZOT-free envelope capability, the hydrazine-fueled thruster needs to be kept 42 degrees warmer than the MMH thruster. This can be achieved by increasing the heater power. There are other reasons that additional heating is believe necessary. The freezing point of hydrazine (35°F) is too close to the present minimum injector head conditioning temperature of 50°F and to the shuttle vehicle propellant conditioning temperature of 40°F. The additional heater power will insure a more adequate margin against freezing the fuel in the lines and valve.

ZOTs can occur for only a limited range of pulse duty cycles. Figure 34 provides some information regarding the effects of pulse on-time, off-time and other parameters upon the magnitude and frequency of ZOTs. Tests were conducted at close to 70,000 feet altitude with propellant and manifold temperature in the region where strong ZOTs can occur. As indicated in the figure, off-times in excess of one second are required before enough fuel enters the oxidizer manifold to cause a manifold explosion. The explosion amplitude and the frequency of explosions increase as the off-time increases to 15 seconds. For off-times longer than 15 seconds, evaporation of fuel out of the manifold and back to the chamber acts to reduce the magnitude and frequency. No damage to the shuttle valves occurred with these relatively moderate ZOTs.

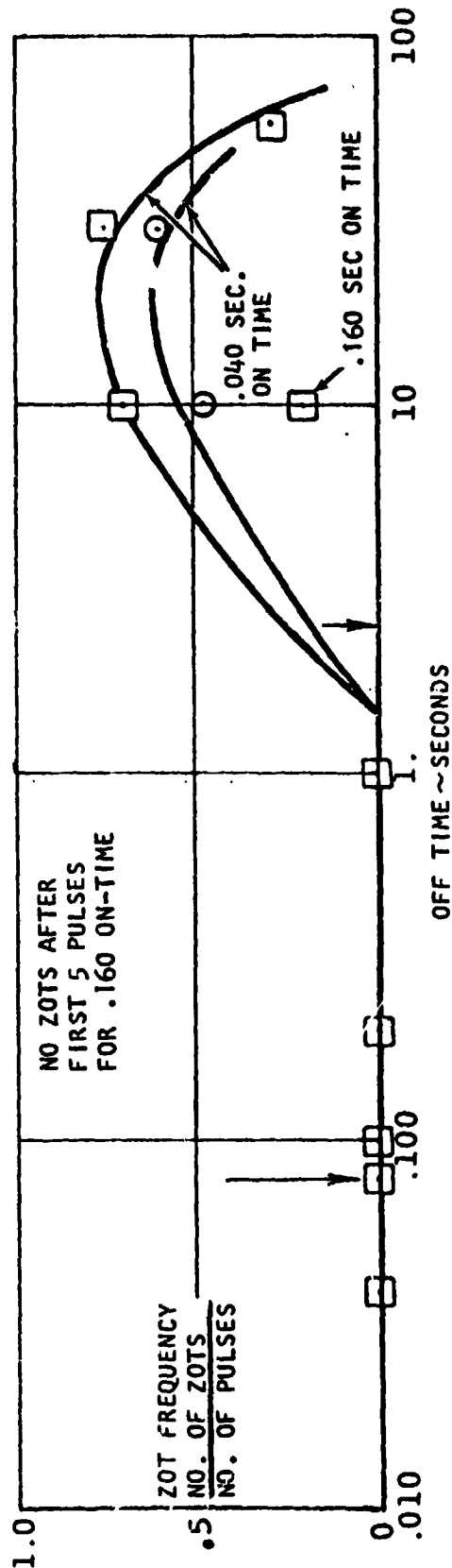
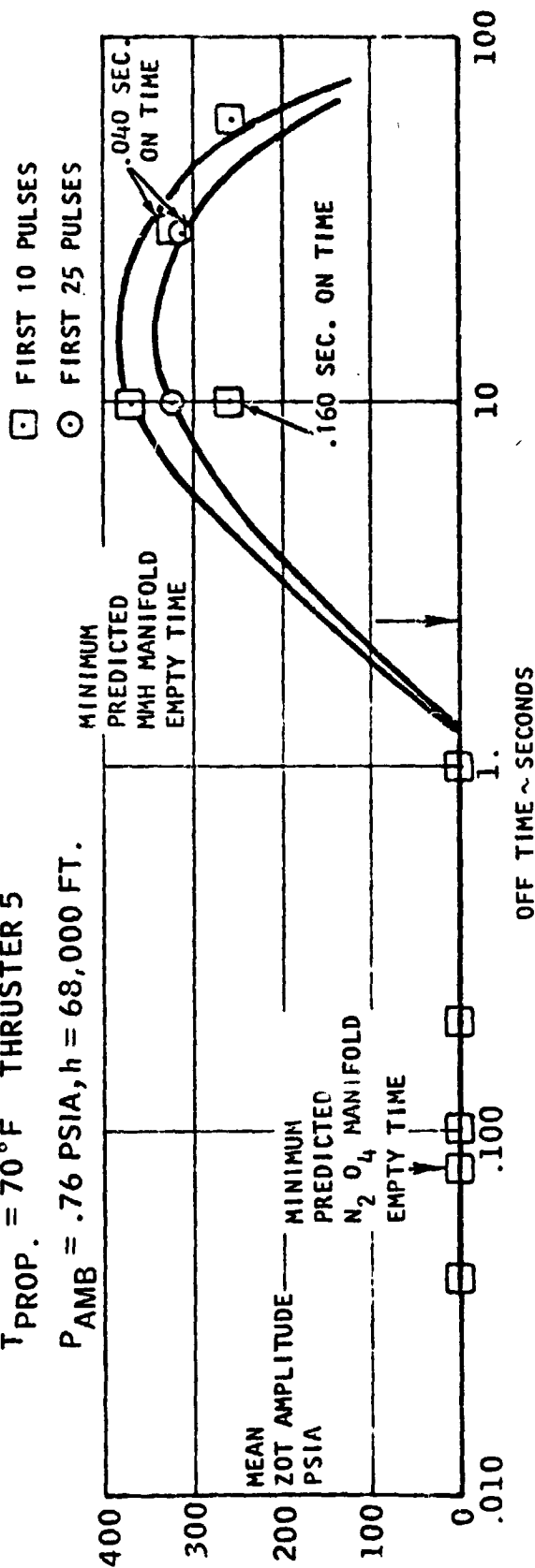
# ZOT PLOT COMPARISON OF MMH & N<sub>2</sub>H<sub>4</sub>



# FREQUENCY AND MAGNITUDE OF ZOTS EFFECT OF PULSE DUTY CYCLE

$T_{PROP.} = 70^{\circ}F$  THRUSTER 5

$P_{AMB} = .76$  PSIA,  $h = 68,000$  FT.



The important conclusion that can be drawn from the ZOT plot is that ZOTs occur over a wider range of altitudes for hydrazine than for MMH. To provide an equivalent ZOT-free region as MMH, the manifold temperature for the hydrazine thruster must be at least 40°F warmer. Since the heater steady state head temperatures are 50-90°F for MMH, this implies a head temperature range of 90-120°F for hydrazine. This temperature range is similar to that recommended from condensed phase explosion considerations.

### Transducer Cavity Explosions

Pressure transducer cavity explosions are produced by a different combination of pulsing rocket events. The transducer is connected to the rocket combustion chamber by a 2-inch long by 1/8-inch diameter tube. The transducer cavity and tube are natural traps for any fuel vapor, oxidizer vapor, and reaction products produced during the ignition transient or for liquid residues left from previous pulses.

Each time the rocket pulse is initiated in a vacuum, these materials are rammed into the cavity where they tend to condense or collect on the cool cavity walls. The residues, which are found to be explosive, continue to accumulate each time the thruster is fired. The accumulation can be detonated by an occasional large amplitude condensed phase explosion or by the thermal energy carried into the tube or transducer as the high pressure hot combustion gases rush into the previously evacuated cavity during ignition. These explosions may cause the transducer to cease functioning as a pressure sensing element, but it still maintains its integrity as a plug to prevent the escape of combustion gases.

Sufficient concern for the shuttle transducer exists that a special program to prevent transducer failure was initiated. The transducer used for the shuttle thruster has a special protective device behind the sensing diaphragm which supports the diaphragm and prevents excessive deflection and damage to the strain gauge when an explosion occurs. This is expected to greatly increase the reliability of the transducer for MMH usage.

Studies of preignition and post-combustion chemical reactions (Ref. 9) occurring at low pressures and temperatures indicate that explosive residues are formed which are capable of being detonated by pressure waves or ignited by thermal waves. The explosive residues that are suspected and identified in the nonflame reactions include the mononitrates and dinitrates, the mononitrites and dinitrites, and the azides of hydrazine or monomethylhydrazine. Also identified are hydrogen azide, nitrosyle azide, ammonium azide, and ammonium nitrate. Add to this the fact that hydrazine and monomethylhydrazine are themselves monopropellants which exothermally decompose at about 600°F and thus there are an enormous number of possible explosive mixtures formed during the preignition or post-combustion periods.

When hydrazine is used as a fuel, the explosive materials formed appear to be more shock and the thermally sensitive than for MMH. As a result, it is expected that transducer explosions would occur more frequently with the hydrazine thruster.

Experimental data are not yet available to predict the frequency of occurrence or the magnitude of the explosions for MMH, nor has a model been developed for predicting the frequency or amplitude of the explosion. Based upon the damage observed in failed transducers, the maximum pressure has been estimated to exceed 5000 psi (as compared with the chamber pressure of 150 psia).

### Combustion Instability

High frequency combustion instabilities are large amplitude acoustical resonances within the chamber which are driven and sustained by energy from the combustion process. The resulting intense oscillation of the combustion pressure and velocity is considered undesirable because heat transfer is increased by factors as high as 10 and causes rapid and catastrophic failure of the chamber walls. Damping must be provided by baffles or acoustic cavities in many high performance thrusters to dissipate this oscillation energy.

To provide sufficient energy to cause instability, some coupling between the combustion process and acoustic frequency must exist. There seems to be agreement between theory and experiment on the existence of a frequency-dependent combustion reaction time and on the effects of injection characteristics on the heat release rate which drives the oscillation. A relatively simple "sensitive time lag" theory appears to adequately predict the behavior of combustion systems provided that the sensitive time lags have been determined experimentally. Fortunately, such data exist for  $N_2O_4/N_2H_4$  combinations (Ref. 10).

The sensitive time lag theory predicts zones of stable and unstable operation as a function of a dimensionless time lag  $\tau^*$  (see Figure 35) and an interaction (or excitation) index  $N$ .  $\tau^*$  is defined as

$$\tau^* = \frac{2 \tau c}{D} \quad (1)$$

$\tau$  = experimental sensitive time lag of the combustion process

$c$  = speed of sound in combustion gases

$D$  = chamber diameter

Smith and Reardon correlated their data to define the sensitive time lag for hypergolic propellants using like-on-like doublets as follows:

$$\tau = 0.25 d_f^{1/2} M_c (P_c/P_{cr})^{-1/3} \quad (2)$$

where:

$d_f$  = fuel orifice diameter, inch

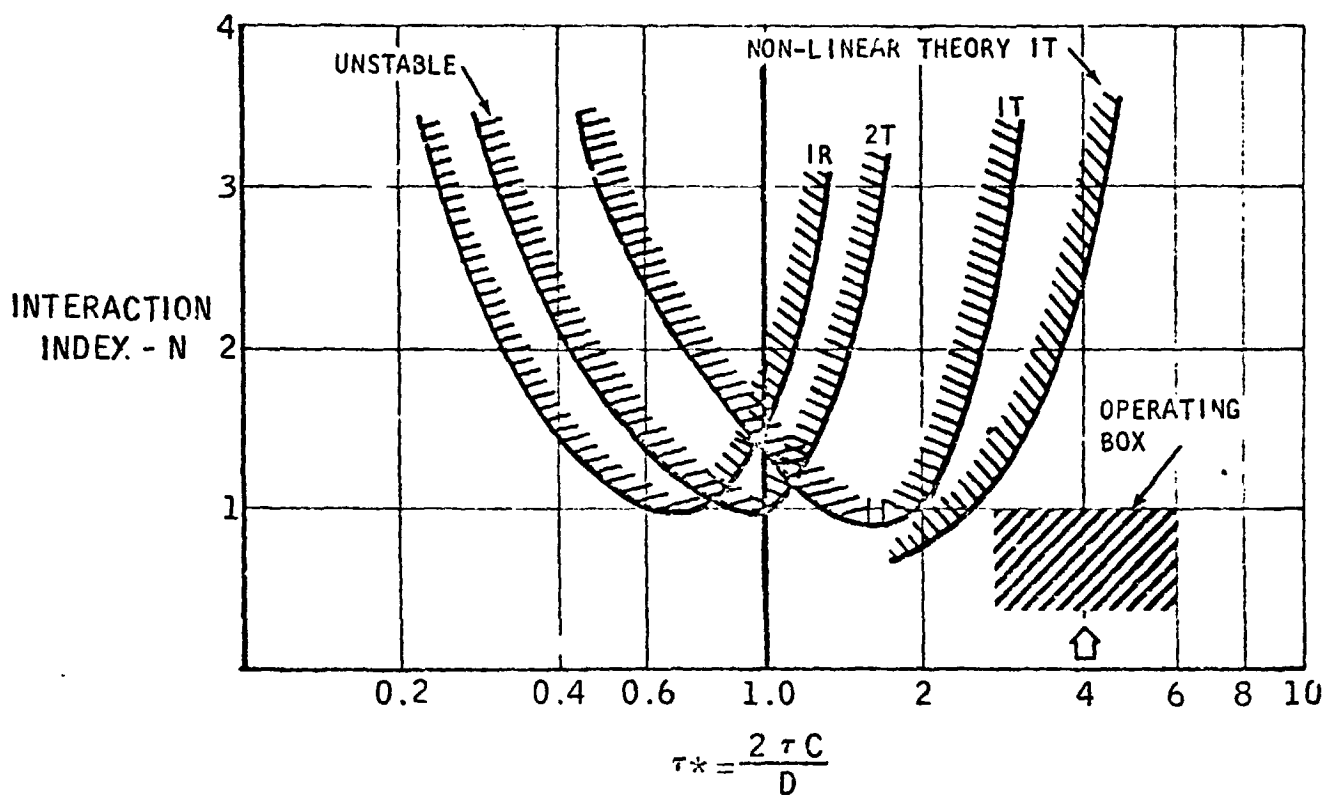
$M_c$  = chamber Mach number

$P_c$  = chamber pressure

$P_{cr}$  = critical pressure of fuel

ORIGINAL PAGE IS  
OF POOR QUALITY

# STABILITY MAP-TRANSVERSE MODES



ORIGINAL PAGE IS  
OF POOR QUALITY

Other correlation equations of the same form exist which relate to the properties of the oxidizer and/or both propellants. However, since the vaporization and mixing of the fuel is the limiting factor for these propellants, the correlation equation for the fuel was used.

From Equation (2), the sensitive time lag is 0.20 ms using the fuel as the controlling propellant. The nominal value of the dimensionless time constant  $\tau^*$  of Figure 35 becomes  $\tau^* = 4.0$ . However, there is a very large scatter in the experimental data from which the correlation equation is derived. Therefore, the stability picture is better described by the operating box shown in Figure 35. This operating box indicates the experimental band for the sensitive time constants and for the interaction index  $N$ . If the operating box overlaps one or more of the unstable zone, instability can be expected as a result of normal combustion.

The interaction index  $N$  is an indicator of the amount of excitation required to cause an instability. The operating box shown in Figure 35 shows the limits of  $N$  and  $\tau$  measured during normal combustion and indicates that stable operation can be expected. Bombs or other unusual disturbances provide higher excitation than shown by the box. For the shuttle thruster, instability can be caused by the ignition transient, bombs, or other explosive events in the combustion chamber. The operating box is close enough to the stability boundary that moderate interaction index for the explosive event could cause operation in the nonlinear mode.

Marquardt's experience with pulsing thrusters is that the ignition transient and/or other explosive events in the operation of the thruster determine the amount of stabilization devices required to avoid destructive combustion instability (first tangential mode in the shuttle thruster). The conventional "bomb" excitation recommended by CPIA for stability rating a thruster has been found by Marquardt to be inadequate compared to other special techniques which produce multiple explosions in the chamber.

Compared to the explosive events, the excitation provided by the normal combustion process is small. While experimental data on the shuttle thrusters without acoustic cavities clearly indicate that the offset doublet configuration is less stable than the zero offset doublets, no combustion instability was found for either configuration with cavities, since the acoustic cavities are designed to cope with the explosive rating test.

The excitation index of hydrazine thruster is not expected to be significantly different than for the MMH-fueled thruster. The two primary variables affecting the interaction index; namely, the heat release rate and the radial location of the heat release zones, appear experimentally to be the same magnitude as for MMH. However, explosive phenomena upon ignition or during operation could be more severe unless the additional thermal conditioning of the thruster and fuel recommended above is provided. If such conditioning is provided, the explosive excitation should be equivalent and the present cavity design should be adequate.

It is recommended that tuning of the acoustic cavities to the instability frequency be implemented for the hydrazine thruster to assure maximum damping. The resonant frequencies of the cavities and the chamber are both a function of the same combustion gas properties

(i.e., the speed of sound) and in theory no revision should be necessary. However, Marquardt has observed that the localized film cooling of the head affects the cavity temperatures and, therefore, a shift in cavity frequency will occur due to the lower cooling effectiveness of the hydrazine.

### Feed System Stability

Flow oscillations of the propellant supply system can occur due to interactions between the flow and the combustion chamber pressure. The primary parameter controlling the feed system stability is the injector pressure drop. To provide the same feed system stability margin as the MMH-fueled engine, the hydrazine-fueled thruster must have the same injector pressure drop. If the pressure drop is smaller, stability is degraded.

When operating at a mixture ratio of 1.4 and the same thrust and specific impulse, the hydrazine-fueled thruster incurs an additional injector pressure drop of 2 psi on the fuel side. Since the allowable pressure drop across both the valve and the injector is 83 psi, a small adjustment of the "trim" orifice in the valve can be easily made. This change acts to increase the stability since the pressure drop across the injector alone has increased and has been compensated by decreasing the pressure drop across the valve.

For the oxidizer side of the feed system, the pressure drop is reduced by 8-9 psi due to the lower mixture ratio. The trim orifice in the oxidizer valve can be used to increase the overall pressure drop across the valve and to meet the overall valve/injector pressure drop of 83 psi. However, since the feed system stability is more sensitive to reduction of injector pressure drop than to the valve pressure drop, the stability of the oxidizer side is reduced despite the balancing of overall pressure drop. If the same or better feed system stability is desired, an increase of the length-diameter ratio of the final orifice or a decrease of the diameter of the feed tube leading to the final orifice can be made.



## VIII. WEIGHT AND COST

### Configuration A

Configuration A is the basic MMH-fueled shuttle thruster with no or little modification. As a result of this study, a number of minor changes are recommended. "Minor" is used here to mean that the modifications do not produce a significant change of tooling and the manufacturing cost. They are to increase the heater power by a factor of two to three, to increase the oxidizer manifold pressure drop by a dimensional change in the oxidizer manifold feed tube and possibly a retuning of the acoustic cavities by changing their depth. These changes involve no change in manufacturing approach and thus will not produce a significant change in production cost.

Table I lists the thruster weight, the predicted specific impulse, and throat temperature along with similar numbers for the MMH-fueled SSRCS primary thruster. The weight presented in Table I is for the unscarfed 22:1 area ratio thruster similar to that shown in Figure 1. Many of the shuttle thrusters have nozzle extensions (scarfs) which are shaped to be flush with the external surfaces of the shuttle vehicle. Figure 8 shows the scarfed nozzle used for the forward facing "Z" thrusters. No significant increase of the heater weight from its present 0.35 pound or its product cost is anticipated. Therefore, the thruster weight and production cost for Configuration A is expected to be the same as for the MMH-fueled shuttle thruster.

### Configuration B

Configuration B incorporates additional changes that act to lower the throat temperature of the hydrazine thruster. The objective of this study was to define a hydrazine-fueled configuration which provides specific impulse and throat temperatures within present shuttle constraints. Figure 29 suggests that this can be done a number of ways and, therefore, some judgment is necessary to select a path. If minimum development risk is selected as a criteria, then only those modifications which are supported by experimental data can be considered low risk. The path which consists of reducing chamber length, increasing nozzle length, and offsetting the doublets represents the lower risk path, since experimental data (with MMH) provide confidence these changes will produce the desired results.

Optimization of the injector will raise the impulse further, but it is a high risk option, since actions and limited attempts to optimize the shuttle injector provided experimental evidence that interactions between the injector momentum angle and the film cooling effectiveness do exist. Since the analysis indicates that Configuration B goals can be met without optimizing the injector parameters, the low risk configuration was chosen for Configuration B (i.e., no optimization).

Table I also lists the weight and performance of Configuration B. The weight of a 4-inch diameter, 0.7-inch long x 0.074-inch thick piece of chamber which is to be removed almost

TABLE I

THRUSTER	I <sub>SP</sub> SECONDS	INSULATED THROAT TEMPERATURE	AFT +X WEIGHT 22:1 NOZZLE
MMH SSRCS	281	1850 °F	21.5 LBS
N <sub>2</sub> H <sub>4</sub> CONF. A.	281	2310 °F	21.5 LBS
N <sub>2</sub> H <sub>4</sub> CONF. B.	282	2150 °F	21.5 LBS

NO DIFFERENCE IN PRODUCTION COSTS BETWEEN ANY OF THE THRUSTERS FOR THE SAME NUMBER OF UNITS IN A PRODUCTION RUN.

ORIGINAL PAGE IS  
OF POOR QUALITY

exactly equals the 5.8-inch diameter x 0.7-inch long x 0.045-inch thick piece of nozzle which is added. The change in chamber and nozzle contours does not change the manufacturing cost except through some initial tooling costs for the shear-formed nozzle. A comparison of the three thrusters at their design points (from Table I) reveals no significant change in weight, or specific impulse. However, both the hydrazine thrusters are running hotter than the present MMH thruster. Configuration A exceeds the expected re-entry temperature slightly, while Configuration B provides an acceptably lower temperature.

## IX. CONCLUSIONS

Conversion of the Space Shuttle Reaction Control Thruster from the MMH fuel for which it was developed to  $N_2H_4$  appears to be feasible from the thruster viewpoint. Achievement of the same specific impulse is predicted for both Configurations A and B. However, unmodified thruster (Configuration A) is predicted to have nozzle throat temperatures of 2310°F at design mixture ratio. While this exceeds the target temperature of 2100°F, it is only slightly in excess of the 2250°F temperature produced by re-entry heating on the forward thrusters (see Table I).

To approach the 2100°F target throat temperature, the combustion chamber must be shortened, the exhaust nozzle lengthened a corresponding amount, and the injector doublets must be offset. The effects of these changes to the thruster geometry have been documented with MMH fuel, and they therefore constitute a low risk modification from a development viewpoint. Manufacturing risk is not significant, since no change in manufacturing technique or approach is involved.

The following additional changes are also believed necessary to assure trouble-free operation of both the Configurations A and B thrusters in the pulse mode:

1. Heater power should be almost tripled to condition the head to a 90-120°F temperature range.
2. The pressure drop through the oxidizer manifold should be increased 10% to avoid feed system/combustor instability.
3. The acoustic cavities should be retuned (change in depth) to maintain the same combustion stability margins as the present MMH thruster.

The film cooling analysis is new in that an attempt was made to consider the decomposition of the fuel film cooling layer. Significant questions regarding some of the assumptions for the decomposition process remain unanswered. These relate to the laminar burning velocity of the decomposition flame and the decomposition temperature of the coolant. The accuracy of predictions is certainly no better than  $\pm 100^\circ\text{F}$  since the primary variables, the decomposition temperatures, and subsequent ammonia dissociation, are not clearly defined.

However, the good agreement between predictions and the experimental data for the MMH thruster suggest that the approximations used in the analysis produce reasonable results. The temperature predictions for the hydrazine thruster also fall within the band of experimental measurements for previously evaluated thrusters whose film cooling configurations were similar to the shuttle thruster.

# REFERENCES

1. "High Temperature Oxidation Resistant Coatings" prepared by Committee on Coatings, National Materials Advisory Board, Division of Engineer, Natural Research Council, Published by National Academy of Sciences/National Academy of Engineering, 1970.
2. "Thruster Assembly, Primary Reaction Control System", Specification Document No. MC467-0028, Code Identification No. 03953, Rockwell International/Space Division Rev. D, 8/16/77.
3. Gordon and McBride, "Computer Program for Calculation of Complex Chemical Equilibrium Compositions, Rocket Performance, Incident and Reflected Shocks, and Chapman-Jouguet Detonations", NASA SP-273, March 1976.
4. Lawver, B.R., "Some Observations on the Combustion of  $N_2H_2$  Droplets", AIAA Journal, April 1966, pp. 659-662.
5. Allison, C.B., "Hybrid and Decomposition Combustion of Hydrazine Fuels," NASA CR-72977, July 1971.
6. Gerbracht, F., "Space Programs Summary 37-47 Vol. III," pps. 149-153, Jet Propulsion Laboratory.
7. Moffett, R.L., "S/M RCS Engine Structural Proof Testing Program," The Marquardt Company Report A1966, November 11, 1966.
8. Zwick, E.B. and Minton, S.J., "An Investigation of Oxidizer Manifold Explosions (ZOTS) in the Apollo SM/RCS Engine," The Marquardt Company, Report S-483, 1 February 1966.
9. Miron, Y. and Perlee, H.E., "The Hard Start Phenomena in Hypergolic Engines, Vol. III, Physical and Combustion Characteristics of Engine Residues," Pittsburgh Mining and Safety Research Center, Interim Report No. 1646, Bureau of Mines, March 22, 1974.
10. Smith, A.J., Reardon, F.H., et al, "The Sensitive Time Lag Theory and Its Application to Liquid Rocket Propellant Stability Problems," Aerojet General, AFRPL-TR-67-134, March 1968.
11. Rupe, J.H., "A Correlation Between the Dynamic Properties of a Pair of Impinging Streams and the Uniformity of Mixture Ratio Distribution in the Resulting Spray," Jet Propulsion Laboratory, CIT. Progress Report 20-205, Marcy 28, 1956.
12. Kushida, Raymond and Houseman, John, "Criteria for Separation of Impinging Streams of Hypergolic Propellants," Jet Propulsion Laboratory, Technical Memorandum 33-395, July 1968.

13. Houseman, J., "Optimum Mixing of Hypergolic Propellants in an Unlike Doublet Injector Element", JPL Technical Report 32-1487, 1970.
14. Breen, B.P., Zung, L.B., et al, "Injection and Combustion of Hypergolic Propellants" Dynamic Science, AFRPL-TR-65-48, April 1969.
15. Graham, A.R., "An Experimental and Theoretical Investigation of Film Cooling in Rocket Motors." Report F57-3, Purdue University, October 1957.
16. Kinney, G.F., Abramson, A.E. and Sloop, J.L. "Internal-Liquid-Film-Cooling Experiments with Air Stream Temperatures to 2000°F in 2 and 4-Inch Diameter Horizontal Tubes", NACA Report 1087, 1952.
17. Gates, R.A. and L'Ecuyer, M.R. "A Fundamental Investigation of the Phenomena That Characterize Liquid Film Cooling," Report TM-69-1, Purdue University, January 1969.
18. Bartz, D.R., "A Simple Equation for Rapid Estimation of Rocket Nozzle Convective Heat Transfer Coefficients," Jet Propulsion, January 1957. pp. 49-51.
19. Welsh, W.E., Jr., and Witte, A.B., "A Comparison of Analytical and Experimental Local Heat Fluxes in Liquid Propellant Rocket Thrust Chambers," Jet Propulsion Lab Technical Report 32-43, February 1961.
20. Hatch, J. and Papell, S., "Use of a Theoretical Flow Model to Correlate Data for Film Cooling or Heating an Adiabatic Wall by Tangential Injection of Gases of Different Fluid Properties," NASA TN D-130, 1959.
21. Kosser, W.A., Jr., and Peskin, R.L., "A Study of Decomposition Burning," Combustion and Flame, Vol. 10, No. 2, June 1966, pp. 152-160.
22. Antoine, A.C., "Eighth Symposium (International) on Combustion," pg 1057, Williams and Wilkins, Baltimore, 1962.
23. Gray, P., Lee, J.C., Leach, H.H., Taylor, D.C., "The Propagation and Stability of the Decomposition Flame at Hydrazine", Sixth Symposium (International) on Combustion, August 1956, p. 255, Reinhold Publishing, New York.
24. Murray, R.C. and Hall, A.R., Trans. Faraday Society, 47, p. 743, 1951.
25. Bock, L.H., Massier, P.F., Cuffel, R.F., "Flow Laminarization Phenomena and Heat Transfer in a Conical Supersonic Nozzle," Journal of Spacecraft, August 1967, pp. 1040-1047.

ORIGINAL PAGE IS  
OF POOR QUALITY

## APPENDIX A

### TANKAGE CONSIDERATIONS FOR CONSTANT TAKEOFF WEIGHT

#### I. Tankage off-load to provide same takeoff weight with hydrazine.

Takeoff propellant weight,  $W_T$ , is:

$$W_T = W_o + W_F \quad (1)$$

where

$W_o$  = weight of oxidizer

$W_F$  = weight of fuel

but

$$W_o = \rho_o V_o \text{ and } W_F = \rho_F V_F \quad (2)$$

where

$V_o$  = volume occupied by the oxidizer

$V_F$  = volume occupied by the fuel

Let  $V$  = maximum tank volume (equal volume tank)

Then the takeoff weight for the hydrazine-fueled thrusters is using (1) and (2) and assuming tanks for the MMH system filled completely.

$$W_{TM} = \rho_o V + \rho_M V \quad (3)$$

where the subscript M denotes MMH.

The takeoff weight of hydrazine-fueled thrusters is

$$W_{TH} = \rho_o V_o + \rho_H V_H \quad (4)$$

where the subscript H denotes hydrazine.

We seek to find what values of  $V_o$  and  $V_H$  for the hydrazine system will provide the same takeoff propellant weight as the MMH system (using (3) and (4)).

$$\frac{W_{T(MMH)}}{W_{T(N_2H_4)}} = \frac{(\rho_o + \rho_M) V}{\rho_o V_o + \rho_F V_F} \quad (5)$$

The mixture ratio at which the  $N_2H_4$  thruster must operate to achieve simultaneous emptying of both oxidizer and fuel tank is:

$$\left(\frac{O}{F}\right)_H = \frac{\rho_o V_o}{\rho_H V_H} \quad (6)$$

Combine Equations (6) and (1) the following two equations can be obtained to describe the required volumes of fuel and oxidizer.

$$\frac{V_H}{V} = \frac{\rho_o + \rho_M}{\left(1 + \frac{O}{F}\right)_H \rho_H} \quad (7a)$$

$$\frac{V_o}{V} = \frac{\rho_o + \rho_M}{\left(\frac{1 + O/F}{O/F}\right)_H \rho_o} \quad (7b)$$

Let us now find what percentage of the tank volume is required for the hydrazine system at its equal volumetric flow ratio. Using Equations (2) and (6),

$$O/F = \frac{W_o}{W_F} = \frac{\rho_o V_o}{\rho_F V_F} = \frac{\rho_o V_o}{\rho_H V_H}$$

For MMH, the equal volumetric flow ratio is

$$\left(\frac{O}{F}\right)_{MMH} = \frac{\rho_o}{\rho_{MMH}} = \frac{1.446}{1.008} = 1.43$$

Using Equation (7) with the hydrazine equal volumetric flow ratio (i.e.,  $O/F = 1.43$ )

$$\frac{V_H}{V} = 0.95$$

and

$$\frac{V_o}{V} = 0.95$$

Therefore, to have the same takeoff weight only 95% of the original tank volume,  $V$ , is required for the  $N_2H_4$  thruster. This results from the greater density of hydrazine compared with MMH.



- II. Find mixture ratio at which hydrazine tank is full (i.e., let  $V_H = V$ ). Solving Equation (7a) for the minimum mixture ratio,

$$\left(\frac{O}{F}\right)_{H \text{ min.}} = 1.32$$

At this mixture ratio the oxidizer tank is off-loaded by the following amount (for the same takeoff weight):

$$\frac{V_o}{V} = 0.91$$

- III. Correction of above mixture ratios for required vehicle ullage volumes.

The oxidizer tank requires a 7.5% ullage volume to allow for thermal expansion variations, while the fuel tank only requires 5%.

For tanks with equal volumes, the MMH mixture ratio which satisfies the ullage requirements and the requirement that both tanks empty at the same time is:

$$\frac{O}{F}_{MMH} = \left( \frac{O}{F}_{MMH \text{ Equal volume}} \right) \frac{(1 - 0.075)}{(1 - 0.05)}$$

$$\frac{O}{F}_{MMH} = 1.65 \times 0.973 \approx 1.6$$

Similarly, the equivalent operating mixture ratio for  $N_2H_4$  corresponding to the equal volumetric flow ratio is:

$$\frac{O}{F}_{N_2H_4} = 1.43 \times 0.973 \approx 1.4 \text{ (1.39)}$$

Finally, the corrected O/F ratio at which the hydrazine tank is at maximum permitted fuel load becomes:

$$\left(\frac{O}{F}\right)_{N_2H_4 \text{ min.}} = 1.32 \times 0.973 = 1.28$$

## APPENDIX B

### ROCKET PERFORMANCE CALCULATIONS

The One-Dimensional Equilibrium (ODE) computer program was used to predict the theoretical core gas temperatures and the reference specific impulse for the Shuttle thruster. These theoretical predictions must be corrected to account for the losses in performance due to the use of the fuel as a coolant and the less than perfect combustion that exists in the combustion chamber. An analysis program was developed for predicting those losses for the MMH fueled shuttle thruster. This program was modified to account for the different physical and chemical properties of hydrazine.

#### Combustion Zones

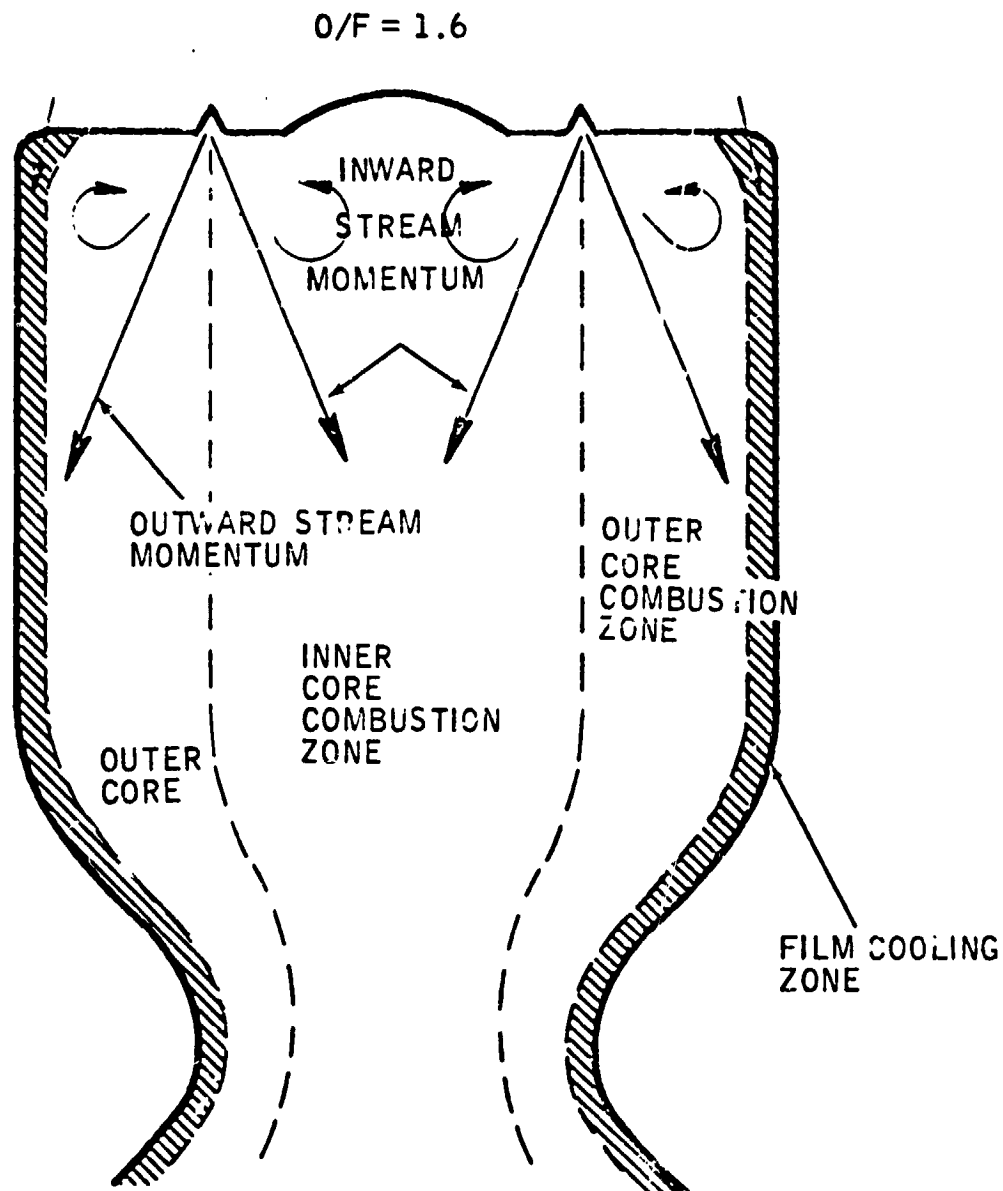
The Shuttle rocket performance is analyzed as a three-zone process. The sketch in Figure A1 illustrates the three zones. The outermost zone is the film coolant zone. Liquid fuel is deposited on the chamber walls by film coolant orifices at injection angles of  $20^\circ$  and  $45^\circ$  around the periphery of the chamber. The steeper injection angle (for half the injection orifices) was found necessary to provide additional injector face cooling because recirculation of the hot combustion gases back toward the face causes face heating.

There are two main combustion zones created from a single ring of injection orifices. The flow on the outer zone is inclined 20 degrees outward and the inner combustion zone is inclined 21 degrees inward. The nonaxial momentum angles produced by the single doublet injector orifices (i.e., oxidizer and fuel jets impinge upon each other) creates recirculation patterns in the combustor which actively feeds thermal energy back to the injection zone and improves combustion efficiency.

The net momentum angle of the propellants varies as the propellant mixture ratio is changed, and this has a strong effect upon thruster performance.

The mixture ratio in each of the two core combustion zones is different and is used as a parameter to optimize thruster performance. The outer core zone is operated fuel rich compared to the inner core. This protects the chamber wall from oxidizer. The analysis assumes that no mixing occurs between the two core combustion zones.

## THREE ZONE MODEL



However, mixing is assumed to occur between the film coolant zone and the outer core zone. This assumption recognizes that a portion of the film coolant moves back toward the face to provide face cooling and that additional loss of liquid coolant to the core flow occurs due to the liquid film instability of the coolant sheet.

### Zone Mixture Ratios

The effect of zone O/F ratio upon  $I_{sp}$  is shown in Figure B-2, which presents the decrease in specific impulse ( $\Delta I_{sp}$ ) referenced to the theoretical optimum at an O/F = 1.0. Examination of the chart indicates that operation at the equal volumetric flow mixture ratio of 1.4 results in a loss of seven  $I_{sp}$  seconds of performance compared with an O/F = 1.0.

If film cooling is used (say 25% of the fuel), the core O/F ratio becomes 1.87, and the loss in  $I_{sp}$  in the core flow approaches 22 seconds compared with an O/F = 1.0. However, the specific impulse obtained from the film coolant zone acts to partially compensate for this loss. The important observation is that the film cooling flow influences the combustion zone mixture ratio and gas temperature and specific impulse.

### Doublet Combustion Performance

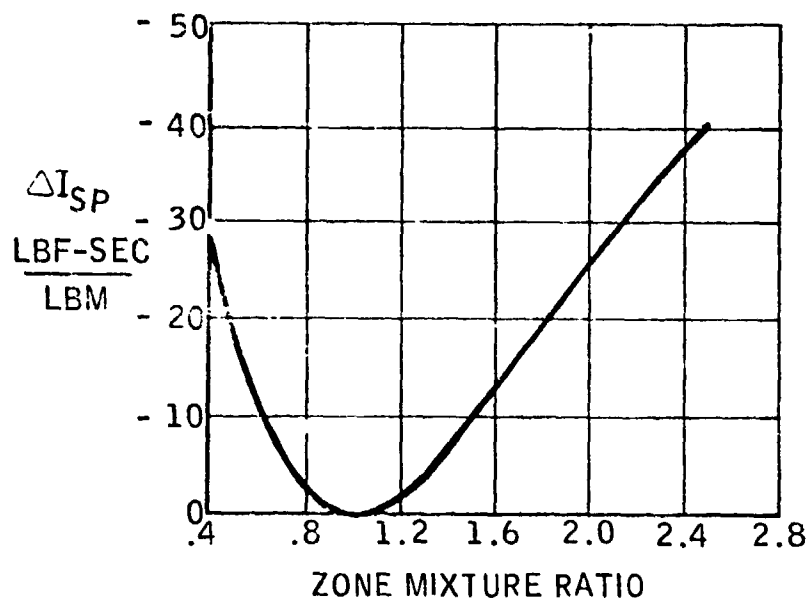
The shuttle thruster employs 84 "unlike" doublets in the single ring-dual momentum injector to achieve good mixing with a short combustion chamber ( $L^* = 10''$ ). The objective of the mixing process is to achieve a uniform mixture ratio across each combustion zone.

Rupe at JPL defined the parameters for maximizing mixture uniformity with nonreacting fluids (Ref. 11). Rupe found a limit to the degree of uniformity even at optimum mixing (Rupe number = .5). One interesting and significant facet of Rupe's investigation, aside from the difficulty of getting uniform O/F distributions, was that the impinging liquid jets penetrated each other. Instead of splashing or bouncing off each other, the impinging jets were found to cross over. Figure P-3 shows the O/F distribution measured across a research rocket engine using a single doublet injector with the oxidizer and fuel orifices oriented as shown in the top figure. The line labeled "penetrated" shows the O/F distribution at optimum Rupe number. Observe that the side of the engine opposite the oxidizer orifice is oxygen rich and the side opposite the fuel orifice is fuel rich. The O/F maldistribution is quite evident for the "optimum" penetrated flow mixing.

ORIGINAL PAGE IS  
OF POOR QUALITY

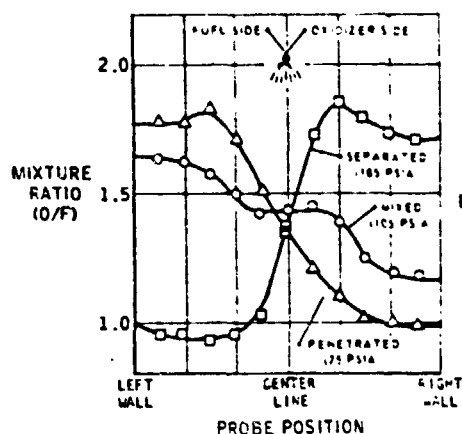
# EFFECT OF ZONE MIXTURE RATIO UPON SPECIFIC IMPULSE

## HYDRAZINE THRUSTER

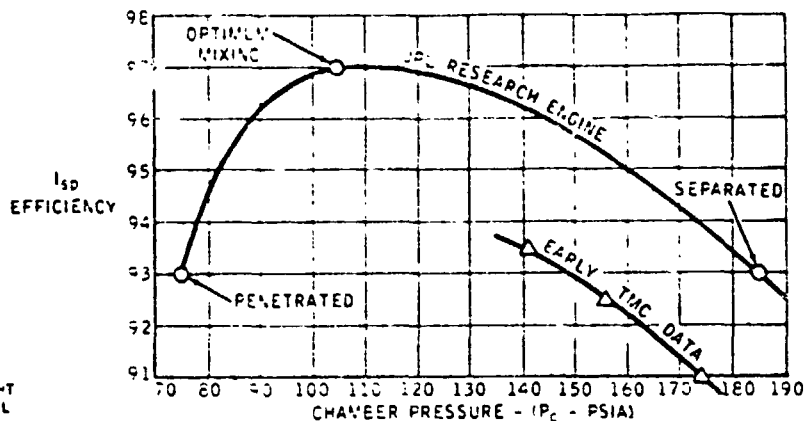


## MIXTURE UNIFORMITY PARAMETERS

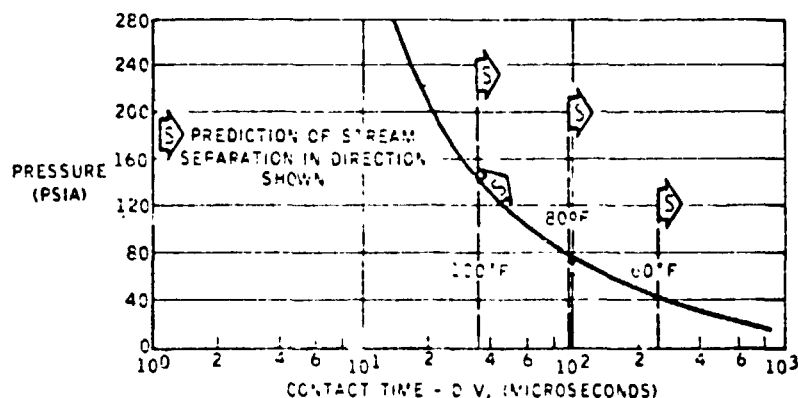
### MIXTURE RATIO PROFILES FOR VARIOUS MODES OF JET IMPINGEMENT



### EFFECT OF MIXING UPON PERFORMANCE



### DOUBLET STREAM SEPARATION MODEL (AFTER HOUSEMAN AND OTHERS)



Other investigators, also working with impinging unlike doublets, reported that under certain operating conditions the two jets bounced off each other or "separated". This separation of blow apart was attributed to chemical reactions occurring sufficiently rapidly at the impingement point to prevent mixing of the liquid jets. The O/F variation across the combustion chamber for "separated" mixing is also shown in Figure B-3 where it can be observed that profile is as maldistributed as the "penetrated" data but completely reversed.

Kushida and Houseman, at JPL (Ref. 12), formulated an analytical model to define the operating regions in which penetrated or separated flow would occur. The key element of the model was the concept of a "contact time" which they showed was related to the ratio  $D/V$  (diameter of injector orifice to velocity of the injector jet). They postulated that if two hypergolic propellants remained in the impingement zone long enough to start a chemical reaction, the reaction products would cause the jets to blow apart or separate. If the contact time ( $D/V$ ) was too small, mixing would occur before the chemical reaction and penetrated mixing would be observed. They hypothesized that either vapor phase or liquid phase reactions could cause the separation.

Houseman (Ref. 13) later conducted the experiment with the single doublet research engine, discussed above, where he verified that the mixing patterns varied from penetrated to separated mixing as functions of chamber pressure. He found that more uniform mixing than either penetrated or separated mixing could be obtained between these two regions. Figure B-3 also shows the O/F profile (labeled "mixed") obtained in the crossover region from penetration to separation. The gas generation due to chemical reaction at the impingement point was proved to be beneficial for achieving a more uniform mixture ratio.

That these changes in O/F profile are significant to performance is shown in Figure B-4 which shows that the  $C^*$  efficiency rises from 93% for penetrated mixing to 97% at the mixed flow condition and then back down to 93% for separated flow.

Kushida and Houseman had predicted that the vapor phase chemical reaction would be a function primarily of chamber pressure and the experiment validated their hypothesis. Figure B-5 shows the estimated vapor phase line for the Marquardt injector geometry using MMH/ $N_2O_4$  propellants. Operation of the injector to the left of the line would result in penetrated mixing. Separated mixing occurs to the right of the line. Optimum mixing occurs in the neighborhood of the vapor phase line.

Some controversy exists as to the nature and shape of the liquid phase reaction lines (which also cause separation). Houseman has formulated models for two different liquid phase reactions, each being a different function of pressure and temperature. Experimental data by Breen, et al, of Dynamic Sciences (Ref. 14) suggests that the liquid phase reactions are dependent primarily upon temperature. These latter data are shown in the figure as dashed lines (adjusted for our injector geometry).

The diagram of the D/V plane, therefore, describes the mixing behavior of impinging doublet injector elements. The design objective is to choose the injector D/V so as to operate in the optimum mixing region; i.e., on the vapor phase reaction line defining the transition between penetrated and separated flow.

For the performance analysis, both Rupe number and contact time (D/V) were assumed to interact independently of each other as a first approximation to describing the mixed flow region. Figure B6 shows the effect of Rupe number upon  $I_{sp}$ . Rupe number = .5 is used as the zero reference point.

The limited experimental data relating to the chemical reaction time for hydrazine based fuels with nitrogen tetroxide suggest little or no difference between hydrazine and MMH. Therefore, the contact time was assumed the same for the two fuels. Figure B7 presents some experimentally derived data from the Shuttle thruster on the effect of contact time (D/V) upon specific impulse. Optimum contact time for the MMH (and therefore the  $N_2H_4$ ) thruster is 32 microseconds at 150 psia chamber pressure.

#### Momentum Angle Effects

Recirculation of hot combustion gases back towards the injection zone is induced by tilting the resultant momentum angle relative to the centerline of the combustion chamber. Test data generally reveal an increase in both performance and injector head or face temperatures. The performance change resulting from the momentum angle is shown in Figure B8. This empirically derived curve was obtained from experiments with a number of different thrusters developed at Marquardt using single ring, single momentum injectors and having small  $L^*$  chambers (short chambers). It predicts that maximum improvement of specific impulse occurs as the momentum angle is increased to  $15^\circ$ . Thereafter, the performance improvement decreases to zero at  $30^\circ$  and is degraded beyond.

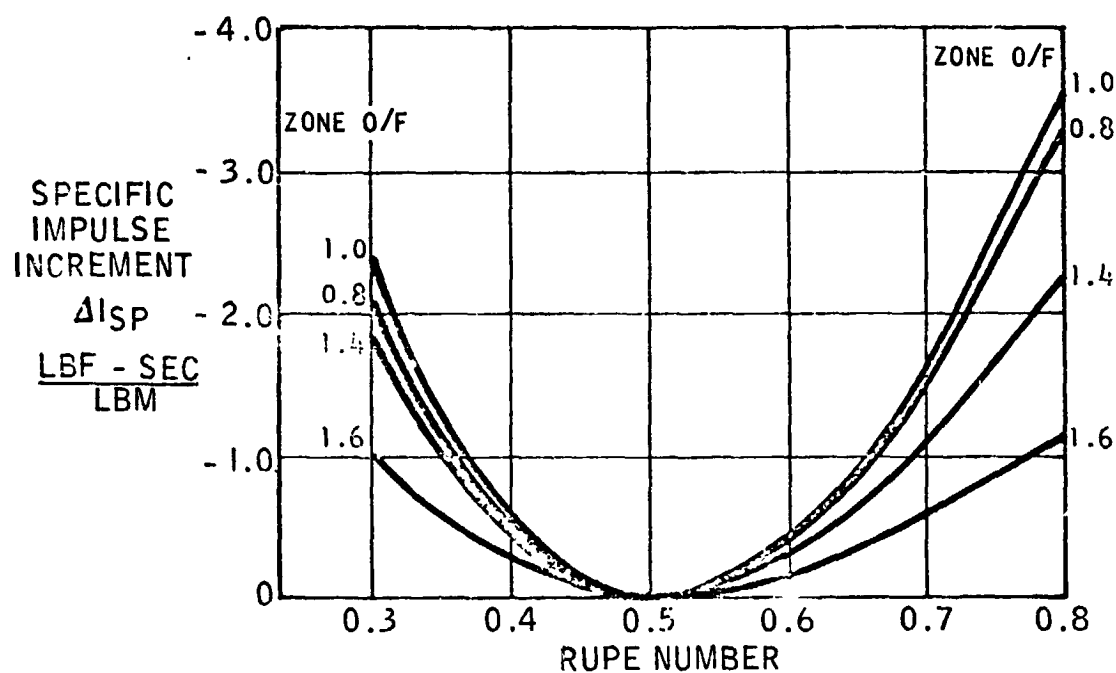
#### Rocket Performance Calculations

The functional relationships discussed previously were combined into a computer program which calculates the changes in specific impulse as the thruster design parameters are varied. The analysis procedure accounts for variations of doublet mixing efficiency as the doublet Rupe number and contact time (or blowapart) parameters are changed. It also considers the effects of the mixture ratios in each combustion zone and the effects of changes in resultant momentum angle of the two propellants in each zone. The remaining combustion efficiency terms due primarily to secondary mixing within each zone and between zones were derived empirically from experimental data of thruster performance. This was assumed to be a function of chamber length. Finally, the performance increment due to the film cooling zone is included using the assumption that the cooling zone gas temperature is a fixed value. The results of the calculations are presented in Section III of this report.



# EFFECT OF RUPE NUMBER UPON SPECIFIC IMPLUSE

HYDRAZINE/N<sub>2</sub>O<sub>4</sub>

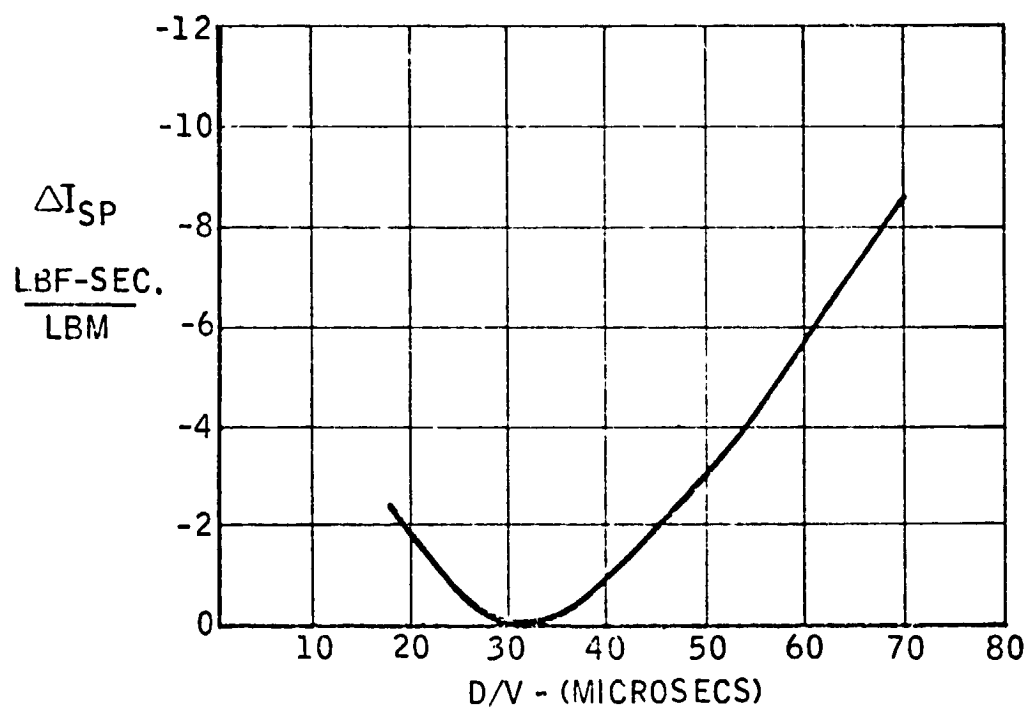


$$\text{Rupe Number} = \frac{1}{1 + \frac{\rho_o D_o V_o^2}{\rho_f D_f V_f^2}}$$

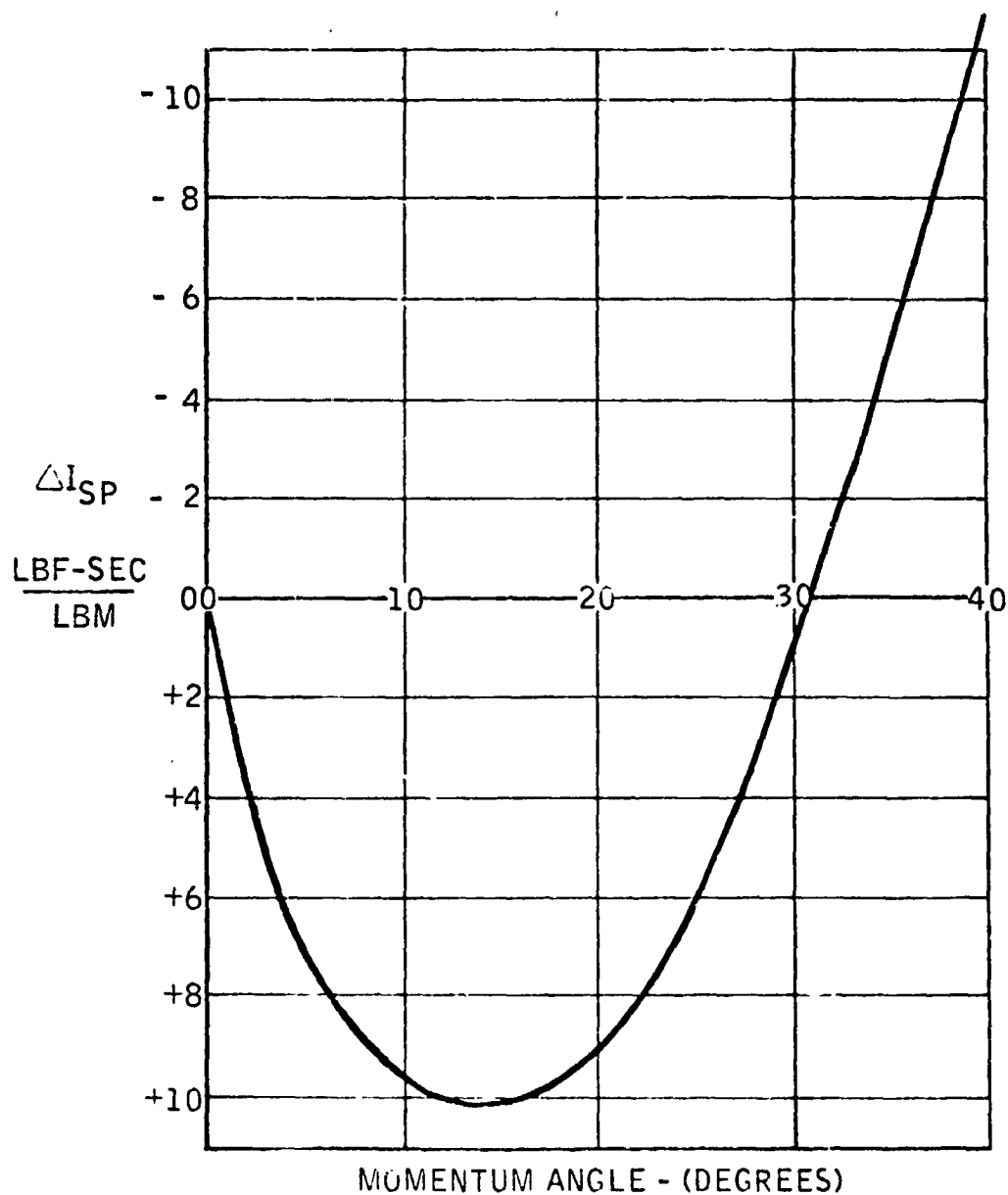
# EFFECT OF CONTACT TIME UPON SPECIFIC IMPULSE

$P_C = 160 \text{ PSI}$

$D_O/D_f = 1.29$



# EFFECT OF MOMENTUM ANGLE UPON $I_{SP}$



## APPENDIX C

### FILM COOLING ANALYSIS TECHNIQUE

The conventional film cooling analysis was extended to include the effects of monopellant decomposition of the film coolant. The following sections discuss the conventional film cooling analysis techniques used for calculating the behavior of the liquid and vapor film cooling zones. In addition, an approach was formulated to estimating film temperatures when thermal decomposition of the coolant occurs.

#### Liquid Film Cooling

The effectiveness of liquid film cooling depends upon how far the liquid film extends along the chamber wall. Prediction of the liquid length is one objective of the analysis. Liquid can be lost by a number of different mechanisms:

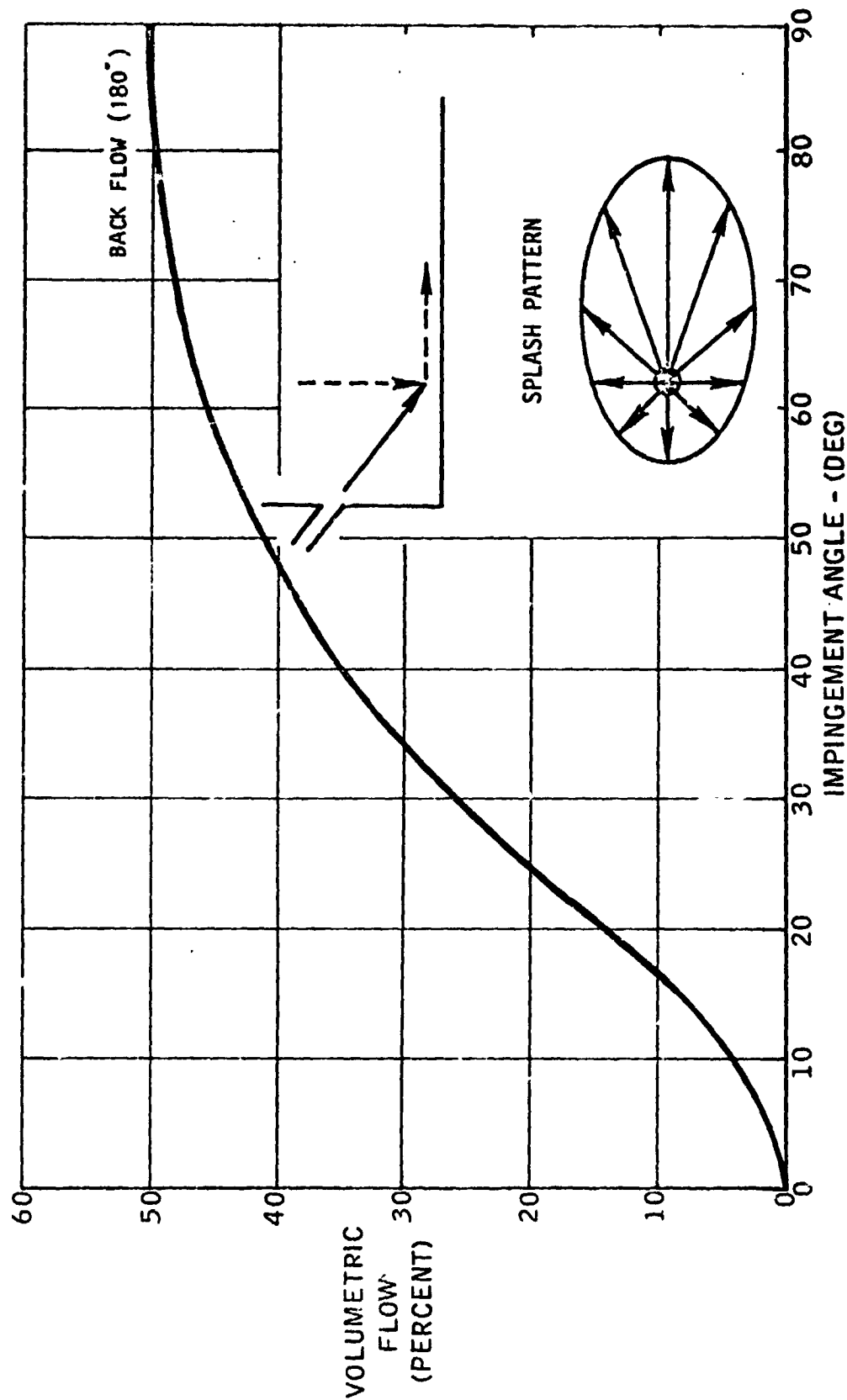
1. Splashing due to the method of injection.
2. Liquid lost due to instabilities of the flowing liquid film.
3. Evaporation of the film due to thermal influx.

Only the liquid evaporating from the film on the wall is performing its function of cooling the wall. Liquid carried away before any cooling can be achieved (i.e., Item 1) or fluid droplets which break away from the film before the heat of vaporization can be used to cool the wall (Item 2) are assumed ineffective for wall cooling.

#### Injection Losses

The film coolant is injected at 84 points around the circumference at angles of 20 degrees and 45 degrees to the chamber wall. The coolant flow, therefore, has a component parallel to the wall which carries the coolant toward the exit nozzle and another component perpendicular to the wall which splashes the liquid in a circular pattern in all directions. As a result of this splash pattern, a portion of the coolant flow moves back toward the injector face. As mentioned earlier, the 45-degree angle was chosen specifically to cause coolant flow to reach the face and reduce the heat flux due to the recirculation of combustion gases. For the analysis, all coolant moving back toward the face was assumed to be lost for cooling the chamber and the nozzle. Figure C-1 shows the percentage of the injected flow lost toward the face as a function of impingement angle. For the 20-degree impingement angle streams, only 15% of the flow moves toward the injector face and 85% acts to cool the chamber and nozzle. For the 45-degree injection angle, 34% acts to cool the face. The total percentage of the liquid film from both sets of orifices which act to cool the chamber and nozzle is 74%. Twenty-six percent is used for injector head cooling.

# SPLASH PATTERN LOSSES



### Film Instability Losses

The liquid film moving toward the nozzle loses liquid droplets due to waves which appear on the film surface. Loss of liquid from the film by entrainment in the gas increases with the thickness and flow rate of the coolant film. As the film flows along the chamber wall, evaporation at the liquid gas interface causes the thickness of the film to diminish from a maximum near the injection point to zero at the point where the film is completely evaporated. Therefore, the intensity of surface ripples decreases in the direction of the flow.

If coolant which breaks away from the film surface is carried away from the liquid film by turbulent mixing before it evaporates, its heat of vaporization will not be effective in film cooling. On the other hand, if the entrained coolant is evaporated immediately adjacent to the liquid film, its heat of evaporation will contribute to film cooling.

As experimental study of liquid entrainment and film stability in film cooling in rocket motors was made by Graham. His experiments were made with films injected tangential to the chamber wall. From measurements of the liquid film length and calculations of what the liquid film length should be in the absence of fluid entrainment. Graham calculated a stability effectiveness,  $\eta_s$ , defined as follows (Ref. 15):

$$\eta_s = \frac{W}{W_f} \quad (1)$$

where  $W$  is the effective film flow rate which adheres to the wall and  $W_f$  is the initial film flow rate at the point of injection.

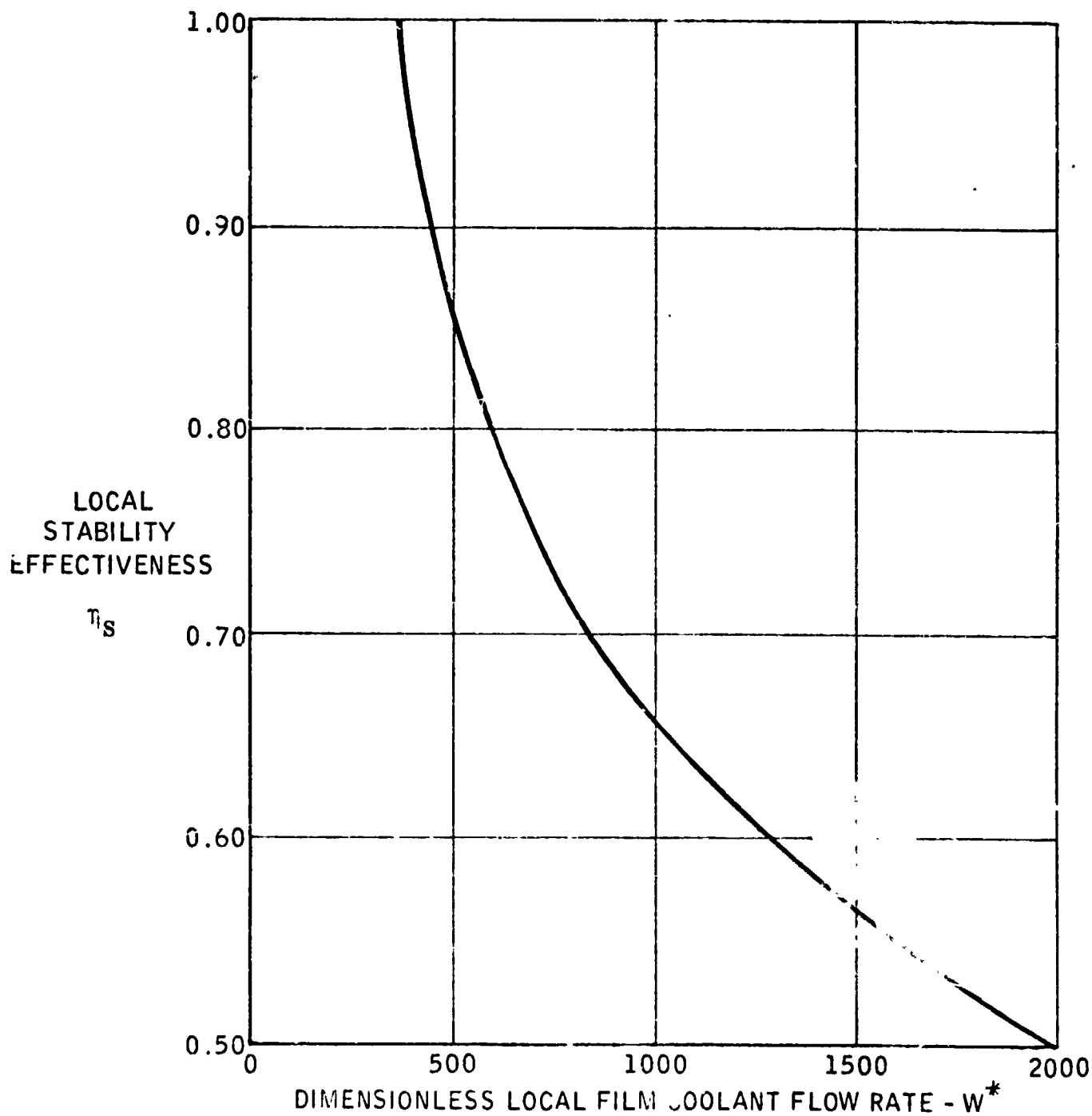
The stability effectiveness,  $\eta_s$ , was correlated by Graham with a dimensionless parameter  $W^*$  which is, in effect, a Reynolds number of the fluid film and is defined as follows:

$$W^* = \frac{W}{\pi D \mu}$$

$W^*$  is a function of distance from the injection point, since the liquid flow rate is reduced by evaporation as the film proceeds downstream. Graham's results, which relate the local stability effectiveness to the local value of  $W^*$ , are shown in Figure C2.

Graham's calculations of theoretical liquid length assumed that the heat transfer coefficient between the core and the liquid film was the same as it would be between the core and a smooth solid wall. Therefore, he attributed all of the difference between the theoretical and measured liquid length to entrainment of fluid droplets because of film instability. Graham's experiments were performed with rocket engines using WFNA and JP-4 at a chamber pressure of 500 psia and a thrust of 500 pounds.

# FILM STABILITY EFFECTIVENESS



ORIGINAL PAGE IS  
OF POOR QUALITY

Results of liquid film cooling experiments by Kinney (Ref. 16) with water films in air flow through ducts at temperatures from 600°F to 2000°F were also correlated with the dimensionless film parameter  $W^*$ . However, Kinney attributed the difference between measured and theoretical liquid lengths to enhancement of the heat transfer coefficient between the core and the film surface, possibly because of increased turbulence due to film instability and evaporation. Kinney assumed that there would be no loss of fluid by entrainment. A calculation of the liquid length using either Kinney's assumption of enhanced heat transfer and no liquid entrainment, or Graham's assumption of liquid entrainment and no enhancement of heat transfer, in most cases will give very closely the same result. In fact, Graham included Kinney's data in his correlation of  $\eta_s$  with  $W^*$ .

In more recent work, Gater and L'Ecuyer (Ref. 17) empirically derived an entrainment parameter which was not nondimensional. They argue that even though their parameter is not a dimensionless quantity, it can be shown to be equivalent to the dimensionless Weber number. However, they were not able to define the characteristic cooling film dimension that is required to convert their parameter to a Weber number. The significant difference in their correlation is that the surface tension of the liquid coolant was the correlating parameter rather than the viscosity of liquid (i.e., Reynolds Number) of the previous investigators. The confusing thing about their report is that they show good agreement between their surface tension parameter and the original data from which the viscosity parameter was derived.

Despite the disagreement on the precise parameter, all investigators agree that the film coolant is consumed much faster than that calculated by assuming that the heat transfer to it is the same as to a rigid wall. Examination of Figure C-2 indicates that liquid lengths can be reduced by a factor of 2 or more due to the surface ripples and waves of the coolant.

#### Vaporization Due to Heat Transfer

Although both liquid entrainment and heat transfer enhancement may be occurring simultaneously, it is very difficult to separate the two factors experimentally. Based upon Graham's results, it can be concluded that the rate of heat transfer between the core and the liquid film can be calculated from conventional equations for convection coefficients when using stability effectiveness. If the local core flow is turbulent, the heat transfer coefficient from the combustion gases to the liquid film coolant can be calculated using the Bartz equation (Ref. 18) as modified to include the more convenient reference enthalpy method developed by Welsh and Witte (Ref. 19).

$$h_g = \frac{0.026 \mu_f^{0.2}}{D_*^{0.2} P_{r_f}^{0.6}} \left( \frac{W_g}{A_*} \right)^{0.8} \left( \frac{A_*}{A} \right)^{0.9} \left( \frac{H_r - H_f}{T_r - T_f} \right) \sigma \quad (3)$$



where  $h$  is the enthalpy of the combustion gases,  $A$  is the cross-sectional area,  $D$  is the diameter, and the subscript  $*$  represents the nozzle throat;  $r$  is the recovery condition and  $f$  indicates average properties at the interface between the core and the liquid film.

The factor  $\sigma$  represents a correction for the variation of viscosity and density through the boundary layer and is equal to

$$\sigma = \left( \frac{T_g^{0.8}}{T_{og}^{0.12} T_f^{0.6}} \right) \quad (4)$$

where  $T_g$  is the local static temperature of the core,  $T_{og}$  is the stagnation temperature of the core and  $T_f$  is the average interface temperature.

This calculation of heat transfer to the liquid film is used only for the evaporation model with inert coolants. For the decomposition model, the evaporation rate is evaluated using the laminar flame speed of the decomposition flame.

#### Gaseous Film Cooling

A liquid film injected along the chamber wall will eventually evaporate due to heat flux from the core gas and from the wall. Downstream of the evaporation point, vapor exists along the wall which can provide a thermal barrier between the core gas and the chamber.

A number of different gaseous film cooling models have been proposed and investigated. To date, no one model has been accepted as universally applicable. The objective of gaseous film cooling analysis is the reliable prediction of film recovery temperatures in various parts of the thrust chamber. The film recovery temperature is the driving temperature for heat transfer to the chamber walls. The film temperature also affects the convective heat transfer coefficient through its influence on the viscosity, heat capacity, Prandtl number, and boundary layer characteristics of the film. Thus, a reliable gaseous film cooling model is necessary to the determination of thrust chamber temperatures.

Gaseous film cooling models are basically of two types - those which assume no core-film mixing and those based upon mixing. Marquardt has used models based on both approaches and has successfully correlated data in each case. The correct model depends upon the problem at hand.

#### Model of Hatch and Papell (subsonic flow) (Ref. 20)

Hatch and Papell derived their model for gaseous film cooling making the following assumptions.

- (a) Coolant exists as a discrete layer (no mixing).
- (b) Temperature profile in the coolant does not change rapidly.

- (c) Temperature gradient through the coolant is small.
- (d) No heat is conducted through or along the wall.
- (e) Conditions are uniform normal to the wall.
- (f) The main gas stream is fully developed turbulent flow.
- (g) The gas traverses the distance  $X'$  before heat diffuses through the gas layer to raise the wall temperature.

A simple heat flow balance on a slab of gaseous coolant leads to:

$$\frac{dT_f}{dX} = \frac{h_g L}{(WC_p)_c} (T_r - T_w) \quad (5)$$

where

- $T_f$  = film temperature
- $x$  = distance downstream
- $W$  = coolant flow rate
- $C_p$  = coolant heat capacity
- $L$  = coolant slab width
- $T_r$  = core gas recovery temperature

Integration gives

$$Ln \frac{T_r - T_f}{T_r - T_i} = - \frac{h_g LX}{(WC_p)_c} \quad (6)$$

Using test data from engine firings using both air and helium, Hatch and Papell found empirical multipliers which, when applied to Equation 6, gave correlation. The following is the final form of their expression.

$$\frac{T_r - T_f}{T_r - T_i} = \exp \left( - \frac{h_g A}{C_{pc} W_c} \right) \quad (7)$$

$$\frac{1}{\phi} = \left( \frac{\delta}{\alpha_c} \frac{U_g}{U_f} \right)^{1/8} f \left( \frac{U_g}{U_f} \right) \quad (8)$$

ORIGINAL PAGE IS  
OF POOR QUALITY

2-2

The factor  $1/\delta$  accounts for the finite thermal diffusivity of the film and the effect of velocity differences between the core and the film.

### Film Decomposition

The thermal decomposition of the coolant film will provide additional heating, since the reaction is exothermic. The decomposition of hydrazine and MMH occurs over a range of vapor temperatures. Detonation is found to occur at vapor temperatures in the neighborhood of 500°F (hydrazine) to 700°F (MMH) in inert atmosphere. At lower gas temperatures the decomposition reaction proceeds more slowly.

The surface of the film coolant layer injected along the wall must first be brought to the boiling temperature, at which time rapid vaporization occurs. At 152 psi chamber pressure, this temperature is 350°F for MMH and 395°F for hydrazine. The vapor generated is heated further and is ignited by the combustion flame of the core combustion zone. Heat released by the decomposition flame near the coolant layer is conducted back to the liquid surface where it acts to increase the rate of evaporation. The monopropellant flame reaches a stable position when the velocity of the vapor approaching the flame is equal to the laminar flame velocity for the decomposition process. In an oxidizer-rich combustion environment, the hot decomposition products can mix with the oxidizer to produce a second flame due to the bipropellant reaction.

Allison presents an analytic model for the monopropellant and the hybrid (monopropellant plus bipropellant) combustion process as well as for the bipropellant flame (without the monopropellant flame). He also presents experimental data on droplet combustion which provides good agreement with the analytical model. His analysis and the experimental data indicate that it is the monopropellant reaction alone which determines the mass burning (evaporation) rate for large drops (where the flow field approaches that of a two dimensional film). His experimental data show no change in mass burning rate from zero oxygen mass fraction (i. e., single flame monopropellant reaction) to 42% oxygen mass fraction (i. e., the two-flame hybrid reaction). He has also experimentally demonstrated that the mass burning rate for large drops was also independent of the ambient temperatures from 2510°F to 4090°F.

Other experimenters (References 21 and 22) seem to find that the laminar burning velocity for hydrazine decomposition is independent of ambient (chamber) pressure level. If this is so and if the mass burning rate is primarily a function of the laminar burning velocity, then the prediction of how rapidly the film cooling layer is consumed becomes quite simple. The mass burning rate,  $M$ , is

$$M = \rho V_L$$

where  $\rho$  is the density of the coolant vapor above the liquid surface

$V_L$  is the laminar burning velocity.

$M$  is the weight flow of coolant per unit surface area  $= \dot{W}/\pi DL$

The liquid film length then becomes

$$L = \frac{W\eta}{\pi D_l V_l}$$

$\eta$  = film cooling effectiveness

$D$  = chamber diameter.

If the laminar burning velocity is known and independent of pressure, the calculation of mass burning rate is only a function of the coolant vapor density, which is a function of chamber pressure. The decomposition model for predicting the liquid length leads to the simple result that the mass burning (or evaporation) rate is a constant at any given chamber pressure. Variation of the core combustion temperature or the oxidizer content of the core combustion gases cause no change in the mass burning rate because the mono-propellant flame establishes the primary heat flux to the film.

To serve as a starting point for the calculations, a laminar burning velocity of 117 cm/sec reported in References 23 and 24 was used for hydrazine. The laminar burning velocity for MMH was estimated by assuming the ratio between the two propellants was the same as measured by Allison ( $V_l$ , hydrazine/ $V_l$ , MMH = 3.2).

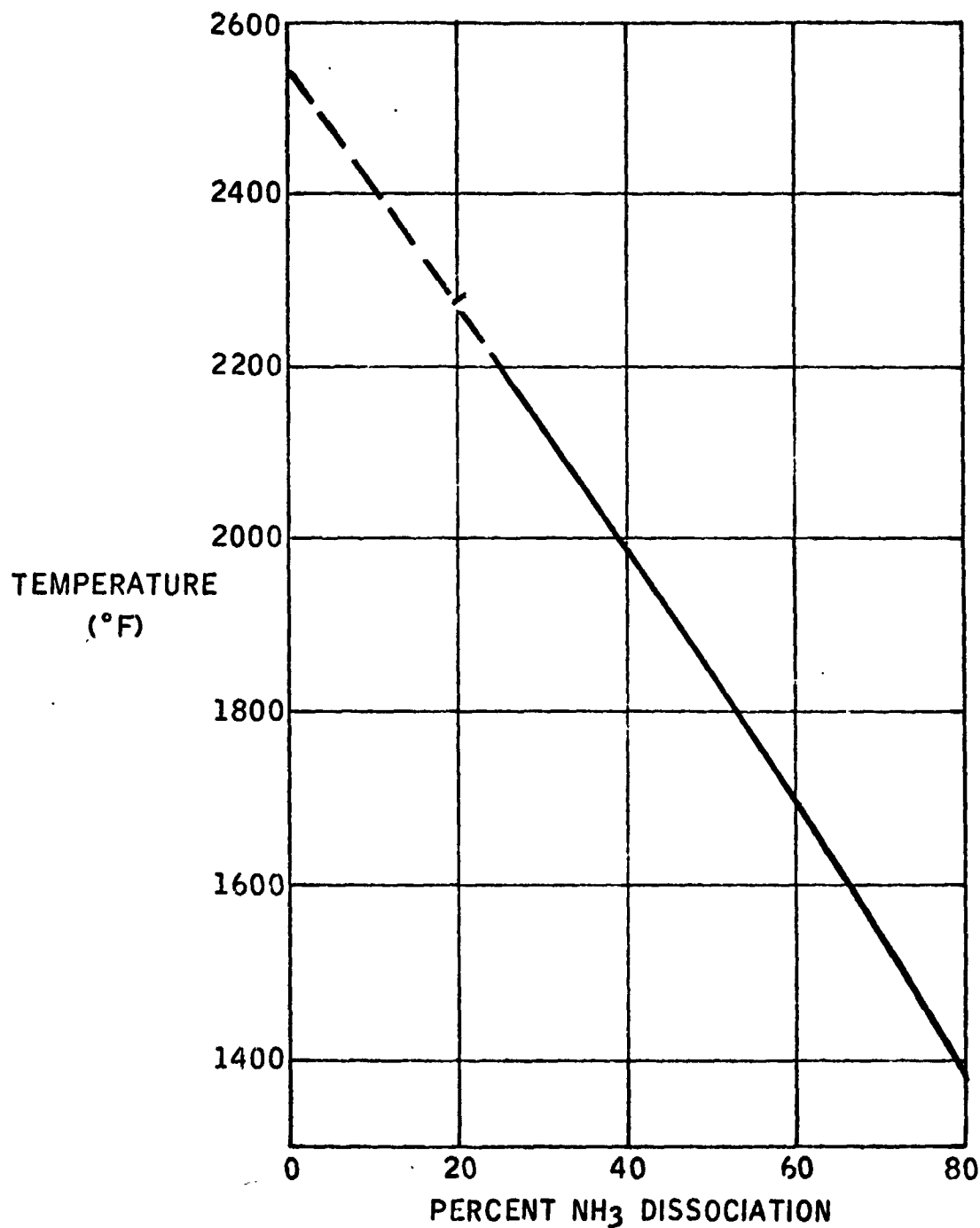
The decomposition temperature of the film coolant must also be estimated. For this analysis where the adjacent core combustion zones are usually fuel rich, the assumption is made that there are no bipropellant (oxidation) reactions with their attendant additional rise in temperature. However, the decomposition temperature of hydrazine is a variable and is known to be a function of the amount of ammonia in the decomposition products. Initially, hydrazine decomposition produces large amounts of ammonia at high temperatures. However, the ammonia begins to dissociate at these temperatures and in doing so absorbs heat thereby lowering the temperature of the decomposition products. Figure C-3 shows the predicted temperature of the decomposition reaction as a function of the percentage of ammonia that dissociates. A large range of decomposition temperatures could therefore be expected. The ammonia dissociation rate is rapid at high temperatures and as a result of the absorption of heat, hydrazine decomposition temperatures above 2200°F are a transient phenomena.

Similar data for MMH could not be found in the literature but since ammonia is also formed in decomposition, a similar variation of decomposition temperatures are expected.

To permit a preliminary evaluation of the decomposition model of film cooling, a constant "effective" decomposition temperature was assumed for both hydrazine and MMH. This avoided time consuming computations of reaction dynamics which would involve the decomposition and dissociation reaction rates. An effective decomposition temperature of 1800°F was assumed for hydrazine and a lower temperature of 1600°F was chosen for MMH.

ORIGINAL PAGE IS  
OF POOR QUALITY

# DECOMPOSITION TEMPERATURE Hydrazine



## Gas-to-Wall Heat Transfer

Convective heat transfer between the gaseous film and the chamber wall depends, among other things, upon the level of turbulence in the film. If the film is turbulent throughout the thrust chamber, the Bartz equation discussed under liquid cooling is applicable. In the case of gaseous film-to-wall convection, the properties of the gas film, not the core, are used in the Bartz equation.

In many cases it has been found that the flow is turbulent throughout the chamber. However, it is possible for regions of laminar flow to exist in critical portions of certain engines.

For years, it has been observed that heat transfer coefficients near the throat of small thrust chambers are considerably lower than would be predicted by turbulent boundary layer methods. It was believed that this was due to injector effects in the short chambers, but the latest evidence (Ref.25) indicates that it is due to the existence of a laminar boundary layer in the vicinity of the throat.

It is theorized that a turbulent boundary layer such as exists along the chamber walls can become laminar in a strong favorable (negative) pressure gradient, especially on a highly cooled wall. The occurrence of this phenomenon is believed to depend upon the magnitude of the negative pressure gradient, the extent of wall cooling, the surface roughness, the flow Reynolds number, and the degree of turbulence in the freestream. No theoretical laminarization criterion has yet been defined, but, as a rule of thumb, thrust chambers with throat Reynolds numbers less than 200,000 will exhibit laminar flow at the throat. This rule is based upon a review of available heat flux data. However, the Reynolds number for the SSRCT thruster is above this number, and no benefits from the laminarization are expected.

- Supersonic Flow Film Cooling

The supersonic gas film relationship are based upon correlations by Parthasarthy, "An Investigation of Turbulent Slot Injection at Mach 6", AIAA Journal Volume 8, No. 7, July 1970. The correlation indicates and the test data on the SSRCS engine tend to verify that the gas film temperature increases at a slower rate as it traverses along the wall in the supersonic region than would be predicted by Hatch and Papell.

- Heat Transfer Analysis

Once the heat flux to the chamber wall is estimated by the simplified heat transfer procedures just described, the temperatures along the chamber and the insulating blanket can be calculated using the Thermal Analyzer program. The chamber, coolant film, gas core and the surroundings can be divided into finite elements. The thermal capacitance of each element and the thermal resistance (or admittance) between adjoining elements are specified, and the steady state temperature distribution is found.